



Infrared Seeker Performance Metrics

A02-158: Phase I SBIR

Final Report

December 31, 2003

DISTRIBUTION STATEMENT A
Approved for Public Release
Distribution Unlimited

Invariant Corporation

20040209 088

REPORT DOCUMENTATION PAGE

Form Approved
OMB No. 0704-0188

Public reporting burden for this collection of information is estimated to average 1 hour per response, including the time for reviewing instructions, searching existing data sources, gathering and maintaining the data needed, and completing and reviewing the collection of information. Send comments regarding this burden estimate or any other aspect of this collection of information, including suggestions for reducing this burden, to Washington Headquarters Services, Directorate for Information Operations and Reports, 1215 Jefferson Davis Highway, Suite 1204, Arlington, VA 22202-4302, and the Office of Management and Budget, paperwork Reduction Project (0704-0188), Washington, DC 20503.

| | | | |
|---|--|---|---|
| 1. AGENCY USE ONLY (Leave Blank) | 2. REPORT DATE | 3. REPORT TYPE AND DATES COVERED | |
| | 31 Dec 2003 | Final: Jan 2003 - Dec 2003 | |
| 4. TITLE AND SUBTITLE | | | 5. FUNDING NUMBERS |
| Infrared Seeker Performance Metrics | | | DAAH01-03-C-R129 |
| 6. AUTHOR(S) | | | |
| David R. Anderson, Jim Moore, John Montgomery, and Mark Chambliss | | | |
| 7. PERFORMING ORGANIZATION NAME(S) AND ADDRESS(ES) | | | 8. PERFORMING ORGANIZATION REPORT NUMBER |
| Invariant Corporation 4800 Whitesburg Dr #30-353 Huntsville, AL 35802 | | | Dynetics 1000 Explorer Boulevard Huntsville, AL 35806 |
| 9. SPONSORING/MONITORING AGENCY NAME(S) AND ADDRESS(ES) | | | 10. SPONSORING/MONITORING AGENCY REPORT NUMBER |
| US Army Aviation and Missile Command ATTN: AMSAM-RD-MG-IR Redstone Arsenal, AL 35898 Lisa B. Cannon | | | |
| 11. SUPPLEMENTARY NOTES | | | |
| 12a. DISTRIBUTION/AVAILABILITY STATEMENT (see Section 5.3b of this solicitation) | | | 12b. DISTRIBUTION CODE |
| Approved for public release; distribution unlimited | | | |
| 13. ABSTRACT (Maximum 200 words) | | | |
| Report developed under SBIR contract for topic A02-158. Advances in imaging infrared (IIR) technology and demonstration of this technology as a capable means of target discrimination, automatic target recognition (ATR), and auto-tracking have led to the development of numerous IIR weapon systems. Although excellent analysis tools exist for describing the imaging sensors themselves, no adequate method or tools exist for characterizing the auto-detection and tracking performance capability of the sensors against targets in a variety of backgrounds. This is complicated by the fact that auto-detection and tracking techniques are difficult to characterize. It is impossible to generate a single generic metric that will accurately predict the performance of all imaging auto-trackers. Typically auto-trackers can be categorized based on their fundamental algorithm. With knowledge of the detection or tracking algorithm, an appropriate metric can be used to predict performance. This effort identifies the common detection algorithms and tracker routines and uses the fundamental algorithms as metrics. These metrics will be used to analyze real imagery from various IR sensors. A methodology for a performance metric will be developed that accurately predicts auto-detection and tracker performance and a validation plan will be developed comparing actual auto-detection and tracker systems to the metric results. | | | |
| As the U.S. Army moves forward in its use of IIR technology, development of a tool capable of predicting auto-detection and tracker performance is essential for optimizing algorithm development and setting seeker system parameters. | | | |
| 14. SUBJECT TERMS | | | 15. NUMBER OF PAGES |
| SBIR Report, Signature Metrics, Seeker Performance, Auto-tracker Performance, ATD Performance | | | 105 |
| | | | 16. PRICE CODE |
| 17. SECURITY CLASSIFICATION OF REPORT | 18. SECURITY CLASSIFICATION OF THIS PAGE | 19. SECURITY CLASSIFICATION OF ABSTRACT | 20. LIMITATION OF ABSTRACT |
| Unclassified | Unclassified | Unclassified | UL |

Report Number: INV-TR-03-001

SBIR A02-158 Phase I: Infrared Seeker Performance Metrics

Final Report

Prepared for:
US Army Aviation and Missile Command
ATTN: AMSAM-RD-MG-IR
Redstone Arsenal, AL 35898
Contract Number : DAAH01-03-C-R129
CDRL A001

Government Technical POC
Lisa B. Cannon

Invariant Technical POC
David R. Anderson
Invariant Corporation
4800 Whitesburg Drive #30-353
Huntsville, AL 35802
Phone: (256) 885-9794

December 31, 2003



**REPRODUCED FROM
BEST AVAILABLE COPY**

ABSTRACT

This final report summarizes the activities of Invariant Corporation in its support of the Army Aviation and Missile Command (AMCOM) under contract DAAH01-03-C-R129. The effort was a Phase I SBIR entitled A02-158, *Infrared Seeker Performance Metrics*. The report details the technical effort performed to include identification of infrared sequences and the ground-truthing of these sequences. Signature metrics were identified and developed to process statistical differences between target and clutter. Software was developed to execute the metrics and was a deliverable under this effort. A tracker and detection prediction methodology study was identified and a validation plan for this methodology is detailed. This effort was also supported by Dynetics which was a subcontractor to Invariant Corporation on this effort.

APPROVED:



David R. Anderson
President

TABLE OF CONTENTS

| | |
|---|-----------|
| <u>1. INTRODUCTION</u> | 9 |
| <u>2. TECHNICAL OBJECTIVES</u> | 9 |
| <u>3. TECHNICAL WORK</u> | 11 |
| 3.1 INFRARED IMAGE SEQUENCES | 11 |
| 3.2 METRICS | 16 |
| 3.2.1 EXISTING METRICS | 16 |
| 3.2.2 NEW METRICS | 18 |
| 3.2.3 TRACKER PERFORMANCE METRIC | 33 |
| 3.3 SIGNATURE METRIC SOFTWARE TOOL | 36 |
| 3.4 GROUND TRUTH PROCESS | 41 |
| 3.5 METHODOLOGY FOR SEEKER PERFORMANCE PREDICTIONS | 42 |
| 3.5.1 PERFORMANCE PREDICTION METHODOLOGY PROBLEM | 42 |
| 3.5.2 PERFORMANCE PREDICTION SOLUTION | 43 |
| 3.5.3 DEVELOPMENT OF BASIC NEURAL NETWORK APPROACH | 44 |
| 3.6 VALIDATION PLAN | 51 |
| 3.6.1 MDTP METRIC TOOL | 51 |
| 3.6.2 MDTP PROBABILITY OF DETECTION PREDICTION METHODOLOGY | 52 |
| 3.6.3 MDTP PROBABILITY OF TRACK PREDICTION METHODOLOGY | 52 |
| 3.6.4 MDTP MODEL VALIDATION | 55 |
| 3.6.5 VALIDATION CRITERIA | 58 |
| 3.6.6 STATISTICAL ANALYSIS | 59 |
| <u>4. TRACKER ALGORITHM</u> | 69 |
| <u>5. CONCLUSIONS</u> | 71 |

LIST OF FIGURES

| | |
|---|----|
| Figure 1. Phase I Block Diagram | 10 |
| Figure 2. Ambient Temperature Histogram..... | 12 |
| Figure 3. Relative Humidity Histogram..... | 13 |
| Figure 4. Image Sequence Time-of-Day..... | 14 |
| Figure 5. Image Sequence Season | 15 |
| Figure 6. Correlation Area | 20 |
| Figure 7. High Contrast Target..... | 22 |
| Figure 8 Correlation Surface of High Contrast Target | 22 |
| Figure 9. Low Contrast Target..... | 23 |
| Figure 10. Correlation Surface of Low Contrast Target..... | 24 |
| Figure 11. Track Correlation Metric Output for High Contrast Target..... | 25 |
| Figure 12. Track Correlation Output for Low Contrast Target | 26 |
| Figure 13. Sobel Filter Results..... | 28 |
| Figure 14. Image With Target and Background Gates Superimposed | 30 |
| Figure 15. Tracker Performance Metric..... | 34 |
| Figure 16. Track Correlation Metric Comparison to Tracker Performance | 35 |
| Figure 17. Image Metric GUI | 37 |
| Figure 18. UML Object Interaction | 41 |
| Figure 19. TAGtool Screen Capture | 42 |
| Figure 20. Linear Spatial Filter | 44 |

| | |
|--|----|
| Figure 21. General Multi-Layer Perceptron Architecture..... | 46 |
| Figure 22. Signal-Flow Highlights of Output Neuron j..... | 47 |
| Figure 23. Essential Steps for Validation of Models and Simulations..... | 54 |
| Figure 24. Validation Methodology | 55 |
| Figure 25. Graphical Comparison with Confidence Intervals..... | 59 |
| Figure 26. Validation Results and Types of Errors | 61 |
| Figure 27. CI Width versus Number of Test | 64 |
| Figure 28. CI Width versus Pd | 65 |
| Figure 29. Effect of Number of Tests on OC Curve | 68 |

1. Introduction

Advances in imaging infrared (IIR) technology and demonstrations of this technology as a capable means of target discrimination, automatic target recognition (ATR), and auto-tracking have led to the development of numerous IIR weapon systems. No doubt, as the technology continues to improve, additional Department of Defense (DoD) time and resources will be spent in an effort to improve the detection, classification, and guidance capabilities of US assets. Although excellent analysis tools exist for describing the imaging sensors themselves, there are no adequate methods or tools currently in existence for characterizing the performance capability of the sensors against targets in a variety of backgrounds. Thus, new and improved detection and tracker algorithms continue to be developed, but with no technique for predicting their potential performance enhancement.

Performance metrics and related analysis tools have been developed for man-in-the-loop applications that adequately match predicted performance with human perception test results. While similar metrics have been developed based upon auto-detection and tracker test results, a reliable method using these metrics in predicting the performance of trackers and auto-detection algorithms for a variety of targets in diverse backgrounds has not been realized. As the US Army moves forward in its use of IIR technology, development of a tool capable of predicting sensor performance is essential for optimizing algorithm development and seeker system design. From a defensive standpoint, as foreign armies implement IIR capabilities into their weapon systems, such a tool is also necessary in mitigating risk to US ground vehicles and troops.

2. Technical Objectives

The overall objective of this effort was to investigate and develop metrics and methodologies which can be used to predict the auto-detection and tracking performance of imaging infrared missile seekers that employ staring focal plane arrays, and develop a

plan to validate the performance metrics. The specific objectives of the proposed effort are in Figure 1 and are listed below.

1. Identify a set of infrared image sequences that represent a variety of background conditions, sensor resolution, and sensor sensitivity.
2. Identify existing signature metrics and formulate new ones.
3. Develop a software tool to use for calculating signature metrics.
4. Ground-truth the image sequences identified in objective 1 and calculate the signature metrics for each image sequence.
5. Develop a methodology for predicting auto-detection and tracker performance based on the signature metrics.
6. Develop a plan to validate the performance metrics.

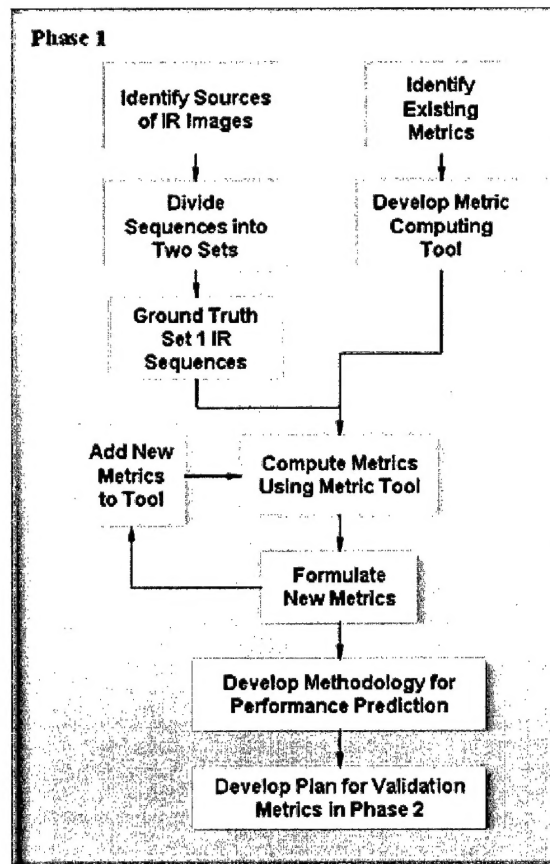


Figure 1. Phase I Block Diagram

3. Technical Work

3.1 Infrared Image Sequences

The first portion of this effort was to identify a comprehensive set of infrared image sequences for metric processing and then later in the Phase II to support the tracker and Autonomous Target Detection (ATD) prediction tool validation. The goal was to identify sequences with various backgrounds, sensor sensitivity, and resolution to ensure the future analysis results were not biased to just one sensor type or a single environmental condition. Parameters that cause variations in background, sensor resolution, and sensitivity were identified and this information was recorded for each image sequence selected. In all, 714 image sequences were identified. The sequences are collected from both tower test and captive flight tests (CFT). Each sequence contains anywhere from 300 to 8000 images. Most tower test sequences have targets at a constant range, while the CFT sequences begin at an initial range and then close on the target. The sequences were selected from several sensors that have different resolution and sensitivity. First, let's summarize the weather conditions for the images sequences selected.

For each sequence, various weather conditions were recorded while the data was collected. These parameters varied somewhat depending on the location of the test and the instrumentation that was available. The main information recorded was location, time-of-day, season, ambient air temperature, relative humidity, parametric pressure, wind speed, wind direction, dew point, and precipitation. At some sites, soil temperature, visibility, and solar radiation were also recorded. All weather related parameters are stored in a database that is a deliverable of this Phase I. To show variability, some of these parameters are plotted below. Figure 2 is a histogram of the ambient air temperature of all of the sequences. There is a large concentration around 75 to 80 degrees F, but several of the sequences were around 90 deg F and during some of the winter scenarios, there were some temperatures in the upper 30's.

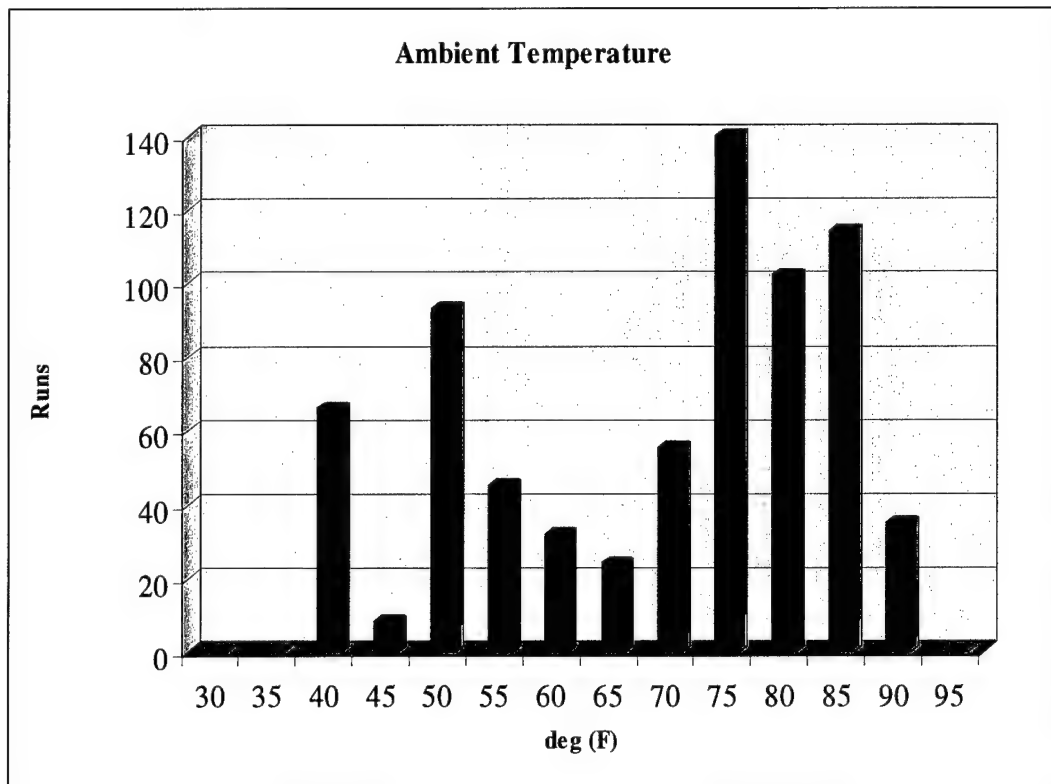


Figure 2. Ambient Temperature Histogram

Figure 3 is a histogram of the relative humidity of the selected sequences. There is a concentration of sequences with high relative humidity but there is also a large group of sequences varying between 30 and 100 percent.

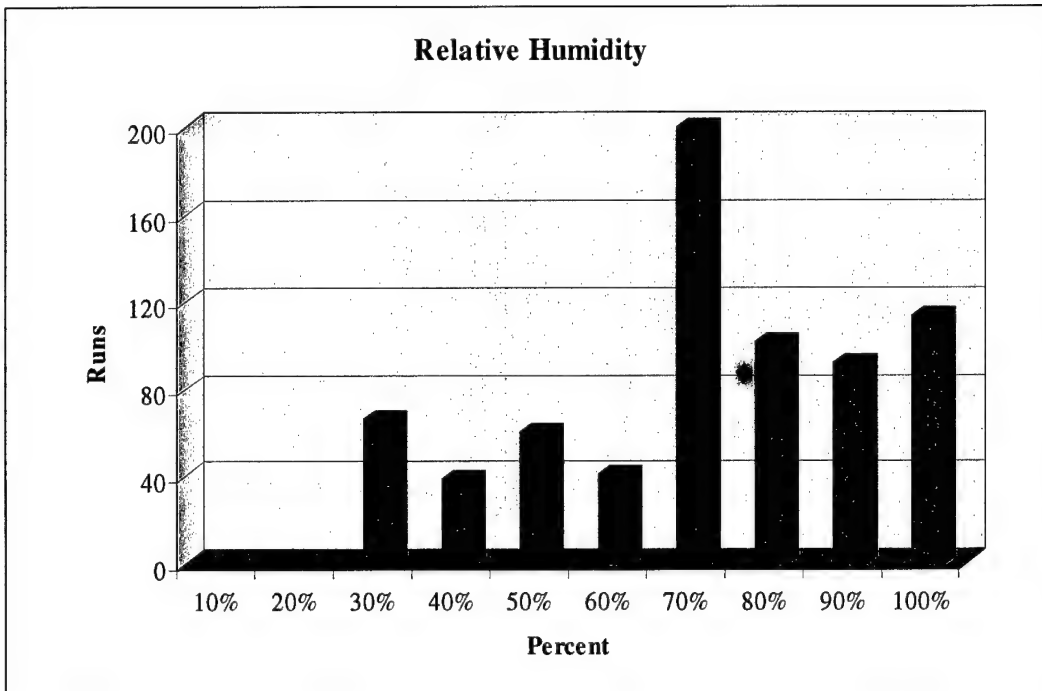


Figure 3. Relative Humidity Histogram

One of the most important aspects of an image sequence is the time-of-day in which the data was collected. Target to background signature will obviously vary greatly from the middle of the night to the heat of the day. Figure 4 shows the time in which the sequences selected were generated. Typically, most data is collected during the day, either morning or afternoon. But there is a decent percentage of this data that was collected at night.

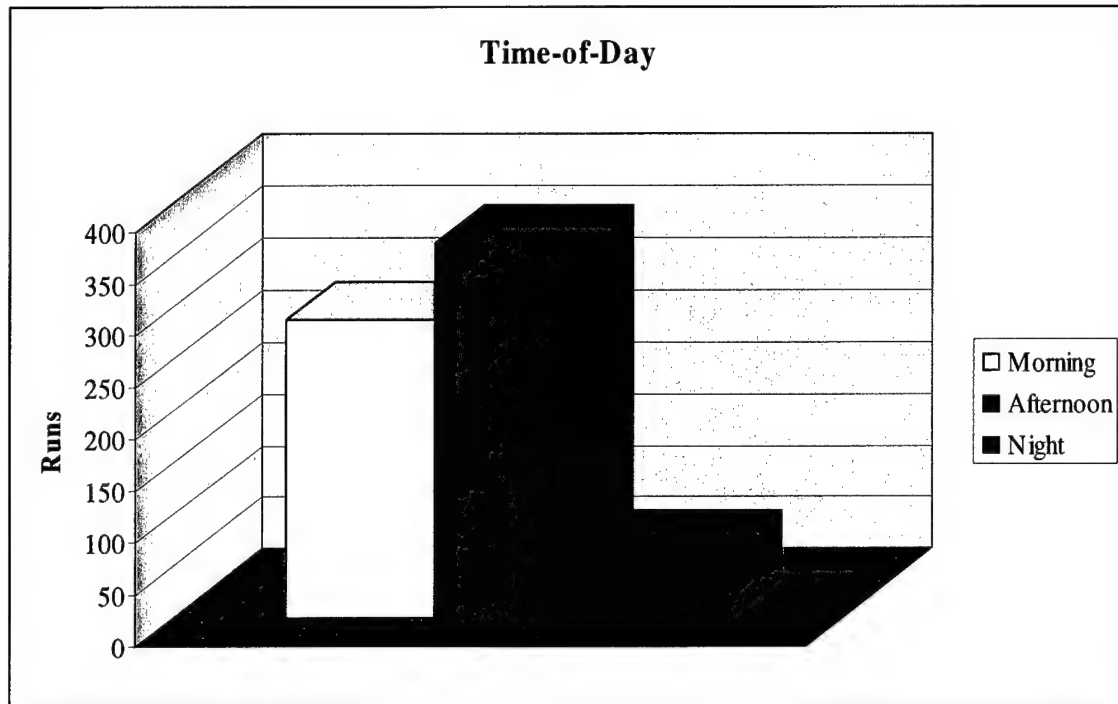


Figure 4. Image Sequence Time-of-Day

The final illustration is the season in which the data sequences were collected. Figure 5 identifies the number of runs collected during the different seasons. Unfortunately, there were no sequences collected during the summer months in the set that was identified. Nonetheless, several of the spring sequences were late in the season and had very hot summer-like conditions.

This section lists just a subset of the weather conditions recorded during data collection. Additional weather parameters were stored and are available for each sequence in Appendix A.

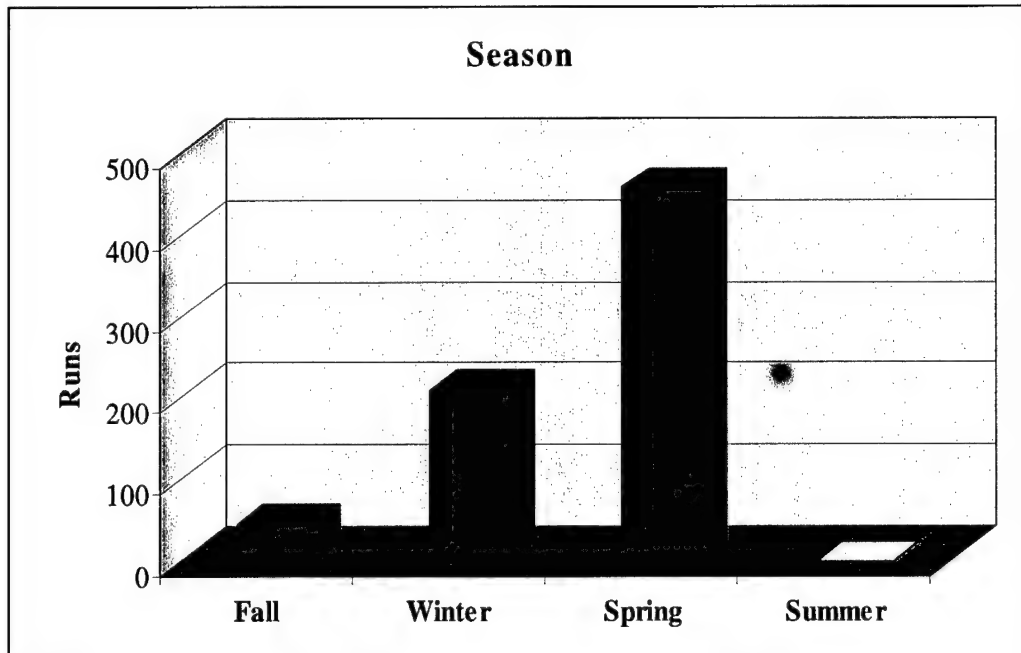


Figure 5. Image Sequence Season

Sensor sensitivity was the next important parameter to be considered when identifying the infrared sequences. This is usually measured by examining sensor fixed pattern noise and temporal noise or Noise Equivalent Delta Temperature (NEdT). For various reasons, these numbers are not always publicized. The sequences identified in this effort were generated by 4 separate sensors. The database delivered with this report identifies the sensors and gives a sensitivity performance range. NEdT for the different sensors varies from just below 50 mK to greater than 100 mK.

Finally, sensor resolution is an important consideration that provides variation in the image sequences. Resolution includes spatial pixel resolution, spectral resolution, optical resolution (blur) and grayscale resolution. The sensors used varied from 512 x 512, 384 x 512, and 256 x 256. Grayscale resolution was both 12 bits and 14 bits per pixel. The instantaneous FOV was different for each of the sensors as was the optical blur. All image sequences were collected using midwave infrared sensors. There are currently two requests for long wave infrared data, but at the completion of the Phase I, no LWIR staring focal plane array data had been obtained. But even though each of the sequences were operating in the midwave band, they all operated in a slightly different

sub-region of the 3 to 5 band. The variation in spectral band will generate variation in the resulting sequences.

All sequences in Appendix A have been ground-truthed. The proposed Phase I option is to obtain and ground-truth additional infrared sequences. Due to pending CFT data collect, good long wave infrared (LWIR) sequences should be available by that time.

3.2 Metrics

3.2.1 Existing Metrics

The existing metrics identified are traditional first order metrics that compare basic statistics between the target area and the background around the target. The three classical metrics are ΔT_{RSS} , $\Delta T_{modified}$, and SCR_{RSS} . The standard statistics used by all three are mean temperature of the target area and background, and the standard deviation in a specific area. The metrics compare the statistics calculated in a target region to the statistics calculated in the background area. The similarities of these statistics are the basis for the metrics. The classical metrics all define the target area and the background area the same. The target area in which the target statistics are calculated is defined as the bounded box around the target. It is identified during the ground-truth process. Ground-truthing will be discussed in detail later in this report. An area around the target gate is evaluated for background statistics. Typically, the background area is the ratio of 3 times the target height and 2.5 times the target width. The classical metrics are described in the following sections.

3.2.1.1 Delta Temperature Root Sum Squared (ΔT_{RSS})

This metric takes the delta temperature between the mean pixels in the target area and the mean pixels in the background area. It also calculates the standard deviation of the pixels in the target area (σ_T). These two terms are individually squared, summed and then the square root of the sum formulates the ΔT_{RSS} metric in Equation 1.

$$\Delta T_{RSS} = \sqrt{(\Delta T)^2 + \sigma_T^2}$$

Equation 1

3.2.1.2 Delta Temperature Modified ($\Delta T_{modified}$)

This metric is very similar to the ΔT_{RSS} metric. It calculates target and background statistics in the same regions of interest. The only difference is background clutter standard deviation is also calculated in the background area. It is subtracted from the target sigma before being squared and then added to the square of the delta temperature term. The addition of background clutter sigma is very important since background clutter will have a significant impact on tracker and ATA performance. Equation 2 describes the $\Delta T_{modified}$ calculation.

$$\Delta T_{modified} = \sqrt{(\Delta T)^2 + (\sigma_T - \sigma_C)^2}$$

Equation 2

3.2.1.3 Signal to Clutter Ratio (SCR_{RSS})

This metric has a strong dependence on the sigma of the clutter around the target. It is the classical signal to clutter ratio, but uses ΔT_{RSS} for the signal term instead of simply ΔT . This is important since even in the absence of target mean difference from the background, target sigma alone is a significant contributor to the ability to track or detect targets. Equation 3 describes the SCR_{RSS} calculation.

$$SCR_{RSS} = \frac{\Delta T_{RSS}}{\sigma_C}$$

Equation 3

Classical metrics have been used for years, but to date still do not do an adequate job of predicting tracker performance. Trackers respond to spatial structure and

similarities between the target and the background. These metrics do not allow for spatial frequency contribution and are purely first order statistics. They also process on a single frame of data. This is inconsistent with the auto-tracker process of using multiple frames of data to generate a history of the target information. Unless otherwise incorporated into time average filter or other custom process, temporal information is negated with these metrics.

3.2.2 New Metrics

The signal to clutter metrics described above are effective for a low level estimation of IR seeker performance. But often these metrics are not a good measure to describe the impact of the target-background signature has on the tracking process. More complicated image metrics are required to support this analysis. Tracker and ATD algorithm metrics can be developed that match more closely the image processing that is performed by the trackers being evaluated. Most imaging auto-tracker and ATD algorithms implemented in systems today are either company proprietary or classified. For this reason, no specific algorithms will be described. Instead, generalizations can be made with the knowledge of existing tracker and ATD implementations in open literature.

Trackers are typically categorized based on the type of image processing performed. They all have one thing in common. They attempt to maintain track gates around the target of interest, and they attempt to maintain an aimpoint on some portion of the target. The first type of tracker is a hot spot tracker. This is the simplest tracker type. The algorithm processes the image, and finds the hottest pixel intensity. In some cases, the image is pre-processed with a boxcar averaging filter, to eliminate noise. But in either case, the hottest pixel in the scene or processed scene is classified as target. This pixel is tracked and the aimpoint is placed on the hot spot.

The second type tracker is statistical based. Target and background means and sigmas are calculated. The tracker will evaluate the similarities between the statistics and

then classify pixels in the scene as target and background based on the calculation. Bayes' law is often used to perform the classification.

The third type of tracker is a feature-based tracker. Typically, the image is pre-filtered using some technique. There are several filters to choice from, but the Sobel edge enhancement filter seems to be a popular choice. It does a very good job of enhancing edges in the image, and can be implemented using 2 3x3 convolution masks. This makes real-time execution possible in a wide variety of hardware platforms. Using the processed image, features are extracted using some segmentation criteria. A database of features is generated and maintained that describes characteristics of each of the features. This often includes feature position, magnitude, direction, size and velocity. The features are classified as target or background based on criteria that vary from tracker to tracker. These features are used to determine the track gate size and aimpoint.

The final tracker is a correlation-based tracker. This type of tracker uses target template information, often generated by the gunner at lock-on, and maintains the track gate on the target. A correlation technique between the target template and the sensor image is performed to calculate the offset of the target in the scene from its previous location. There are several methods of performing the image correlation but given the same template and image correlation area, they will all generate similar results.

ATD algorithms typically use a target template and search the entire image to identify features that match the template. The image is often preprocessed to extract edges or high frequency components. Many ATD algorithms use a process similar to the correlation-based tracker, but search for a good correlation in the entire image instead of a local region around the previous track location.

The goal of this effort was to identify at least one new metric that closely matches the fundamental track and ATD algorithms described above.

3.2.2.1 Track Correlation Metric

The track correlation metric (TCM) correlates between the current target template containing previous target information and a correlation search region. The search region is defined by a box around the target plus a correlation search area. Figure 6 shows an example of the search area outlined with the green box. The blue box outlines the area that defines the target template.

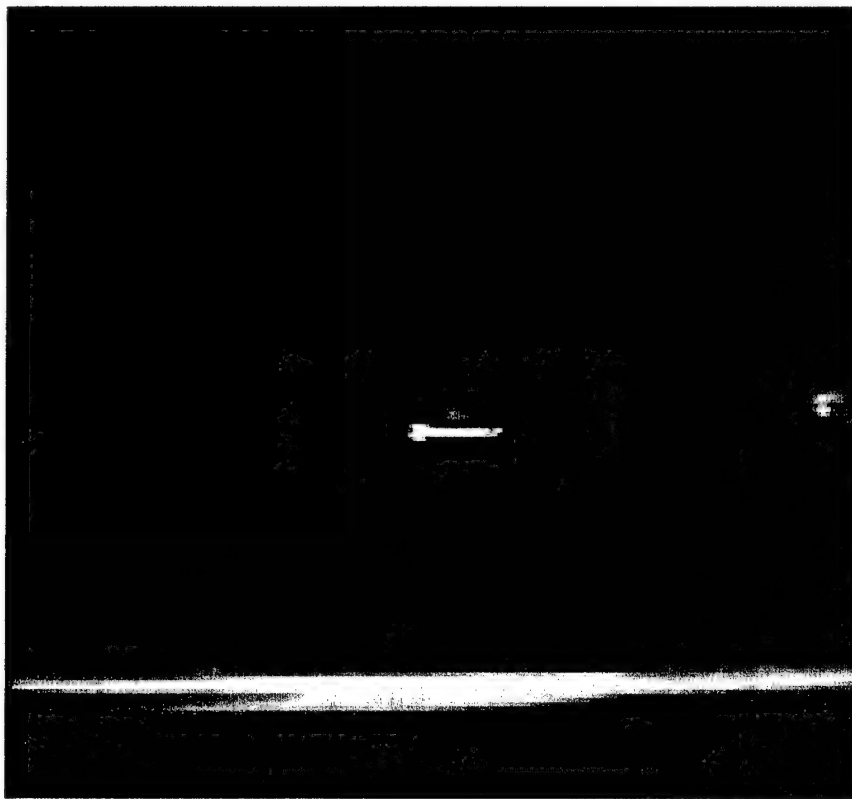


Figure 6. Correlation Area

The target template is a 2 dimensional image that has j rows and i columns. The correlation search area has n rows and m cols. n is 3 times the size of j and i is 3 times the size of m . The first step in this metric is to perform a normalized correlation between the correlation search area from (n, m) to $(n+j, m+i)$ where n and m are initially zero and

the target template. To normalize the output, the mean and sigma value must first be calculated for the correlation search area. The mean is defined as μ_c and the sigma is σ_c . Then the mean and sigma is calculated for the target template. These are defined as μ_t and σ_t respectively. The normalized cross correlation is defined by Equation 4. The result is output to a matrix called the correlation surface. This surface is populated with results as you change the starting points n and m to change the location of the correlation in the correlation search area.

$$corr_{n,m} = \frac{\sum_j (x_j - \mu_t) \times (y_{j+n,i+m} - \mu_c)}{\sigma_t \times \sigma_c} \quad \text{Equation 4}$$

Below are two examples of the resulting correlation surface. Figure 7 is the output of an InSb MWIR sensor. The target is hot with respect to the background and is outlined by the blue box. When performing a normalized cross-correlation with this input the result should be a correlation surface with a sharp peak. The target area is not well correlated with surrounding clutter, so the correlation surface values should be small off the correlation peak. Figure 8 shows the correlation surface result after processing the high contrast image. As expected, values around the peak in the surface quickly go to zero, and there are no secondary peaks anywhere in the surface.

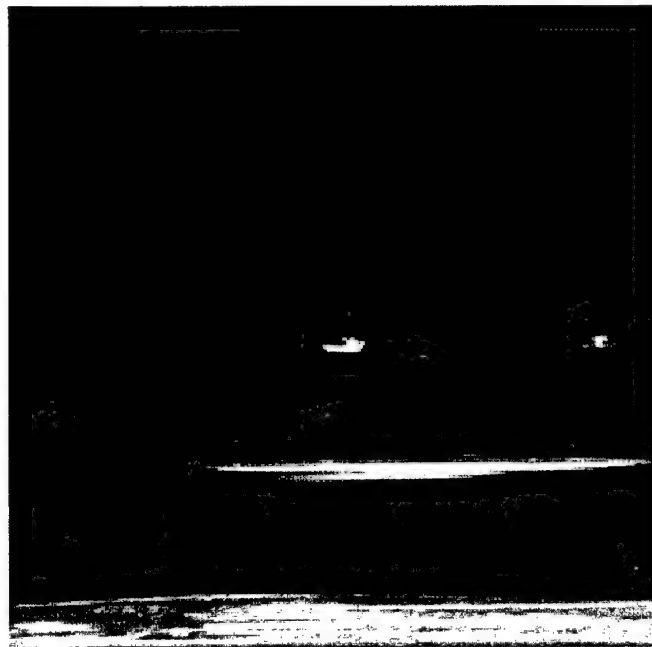


Figure 7. High Contrast Target

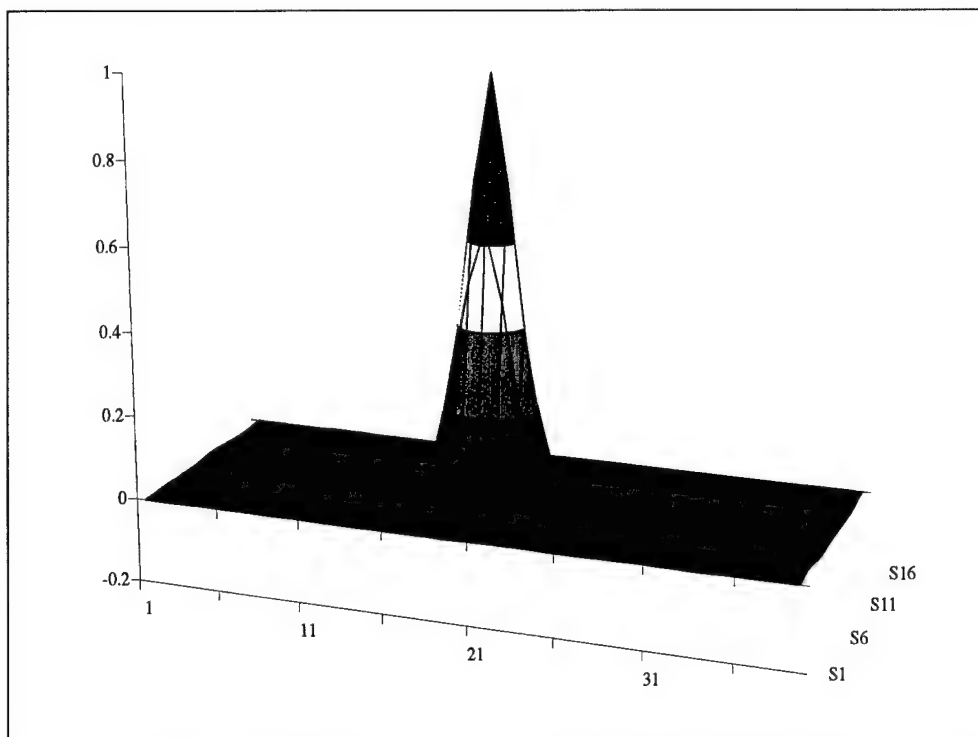


Figure 8 Correlation Surface of High Contrast Target

The next example is a low contrast target on somewhat correlated clutter. Figure 9 shows the IR image with the target outlined in blue. After performing the normalized cross-correlation, Figure 10 shows the resulting correlation surface. As expected, the surface has the peak in the center resulting from the correlation between the target template, and the target itself. But the slope from the peak is less than the previous example, and then the values ramp back up away from the peak. This indicates clutter that is correlated to the target.

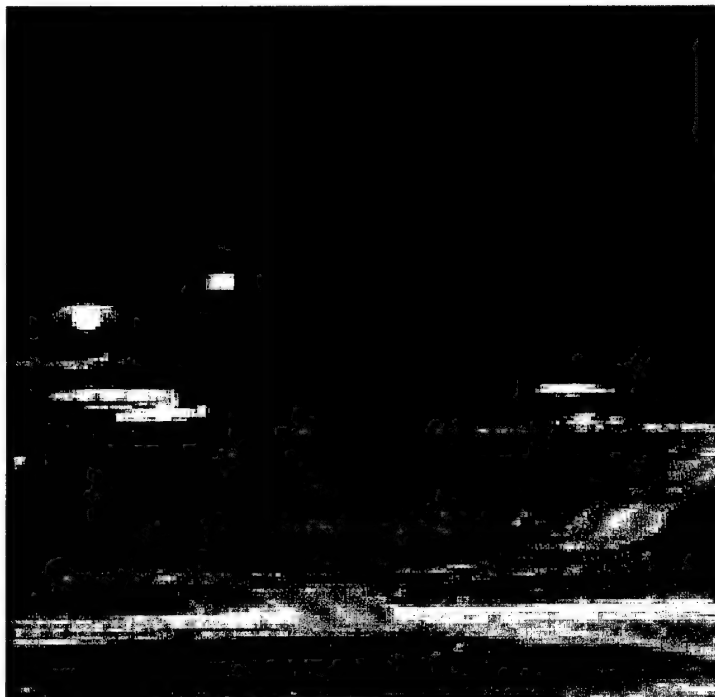


Figure 9. Low Contrast Target

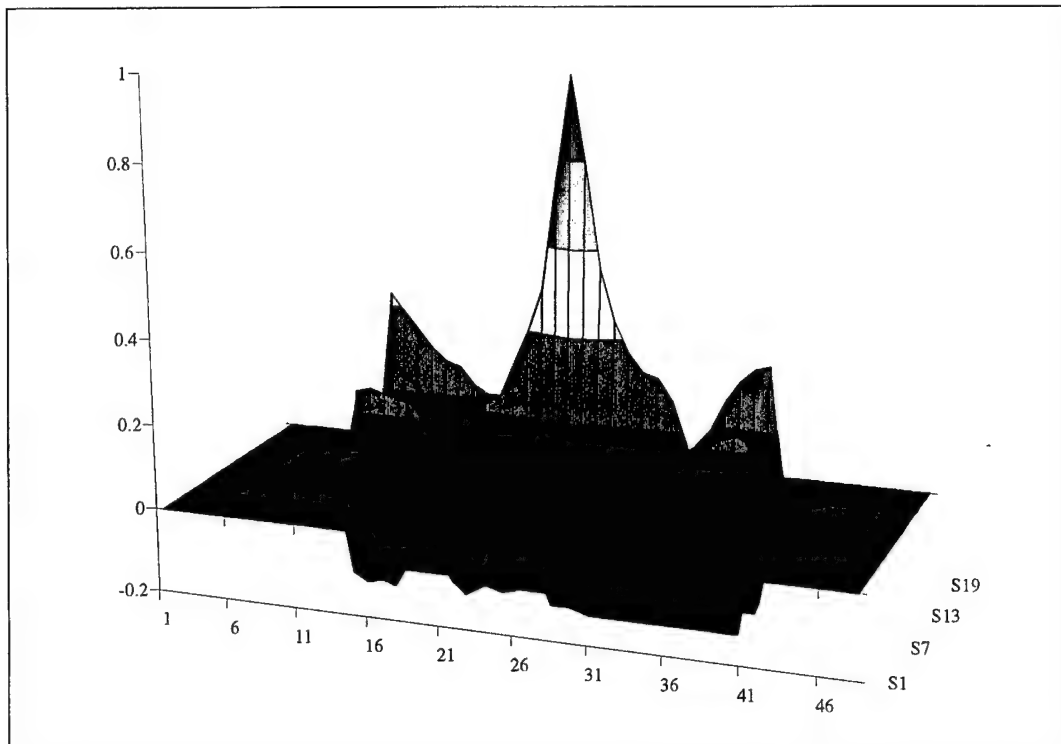


Figure 10. Correlation Surface of Low Contrast Target

The trick now is to use the information from the correlation surface to generate a metric value that is the result of the target being correlated to the background. Since the surface is normalized, you will always have a peak value of the target template correlating with the target in the correlation search area. There are also values immediately around the peak that are a result of the target correlating with itself. Since the real interest is to determine how alike the target is to background, the values of interest are where the clutter correlated to the target template. Remember that the target template is a historical snapshot of the actual target, hence the perfect correlation.

So to generate the metric value, the correlation surface away from the peak is examined. If there is a value anywhere in the correlation surface that has a large value that means it is highly correlated with the background. Lower values in the correlation surface indicate poor correlation. This is opposite from what is expected from a single metric value, since a 1 should indicate a high likelihood of distinguishing target from background, and a zero indicates the target and background are highly correlated.

Therefore, the largest value in the correlation surface that is outside the peak region is subtracted from 1.0. The result is the final metric value.

$$\text{Track Correlation Metric (TCM)} = 1.0 - \text{correlation peak}_{(\text{outside center region})} \quad \text{Equation 5}$$

Figure 11 is an example of the TCM output. The target is high contrast just off a road as indicated by the red arrow. The metric value is around 0.8 for the entire sequence indicating there is a high probability of a successful track on this image sequence.

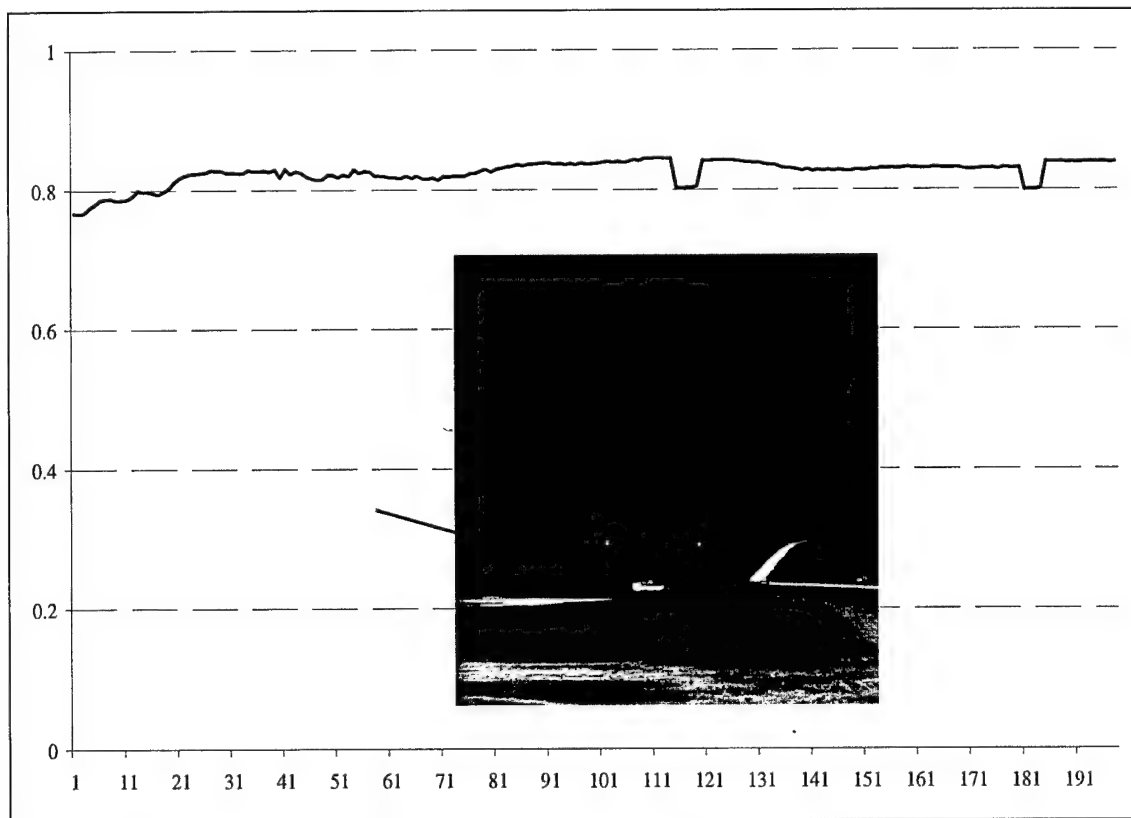


Figure 11. Track Correlation Metric Output for High Contrast Target

Figure 12 is another example of the TCM output. The target is low contrast and identified by the red arrow. The metric value is around 0.4 to 0.6 for the entire sequence indicating there is a medium to low probability of a successful track on this image sequence.

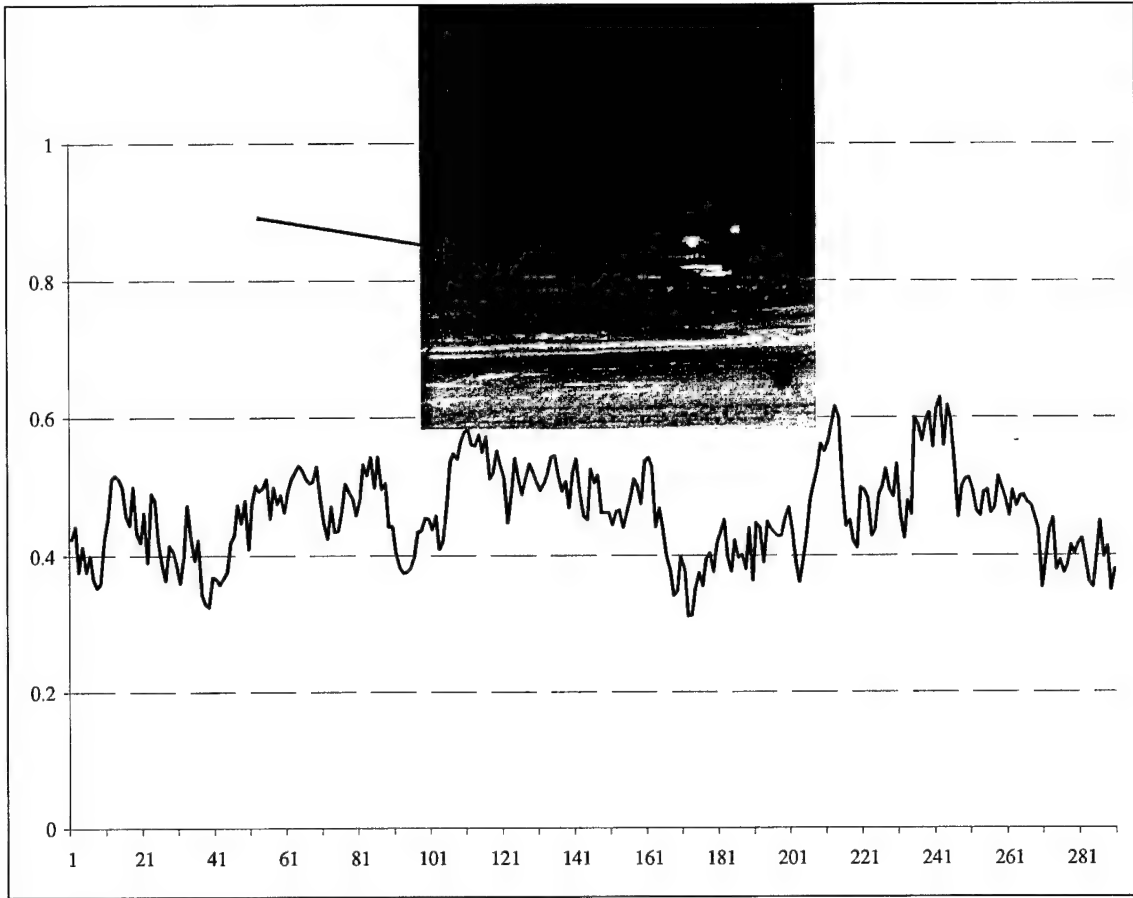


Figure 12. Track Correlation Output for Low Contrast Target

The tracker correlation metric uses a target reference that is filtered over time. Since auto-trackers react to temporal changes in the target area, it was important that the metric is sensitive to temporal changes as well. This is true because they use historical target and background information for discrimination and classification. For this analysis of the tracker correlation metric, the target template was a stored representation of the target area from previous frames. If there is a significant change in signature from one frame to the next, the metric should perform well when predicting the effect on tracker performance. Since this metric uses the fundamental algorithms used by a correlation-based tracker, the metric value should do a fairly good job of predicting the performance at that class of tracker.

3.2.2.2 Sobel Metric

Another metric under consideration for track analysis is based on the Sobel edge enhancement mask¹. It is used to evaluate the ability to pull edges out of a particular scene. Equation 6 represents the horizontal Sobel mask and Equation 7 is the vertical mask applied to the raw input image in an area around the target gate. These images are combined to form a magnitude image calculated in Equation 8. Currently, the target area of the edge image is compared to a background area to generate a signal to clutter ratio. This ratio is an indication of how well the filtered edges on the target compare to the edge features in the background clutter around the target. Future work will include a more exhaustive analysis of the persistence of the edge information. This will form the ability to predict how well a feature based tracker can maintain consistent edge features over the duration of track. The filtered images in Figure 13 illustrate the edge enhancement effects of the Sobel mask.

$$\begin{bmatrix} -1 & -2 & -1 \\ 0 & 0 & 0 \\ 1 & 2 & 1 \end{bmatrix} \quad \text{Equation 6}$$

Horizontal Sobel Mask

$$\begin{bmatrix} -1 & 0 & 1 \\ -2 & 0 & 2 \\ -1 & 0 & 1 \end{bmatrix} \quad \text{Equation 7}$$

Vertical Sobel Mask

$$magnitude_{xy} = \sqrt{Gx^2 + Gy^2} \quad \text{Equation 8}$$

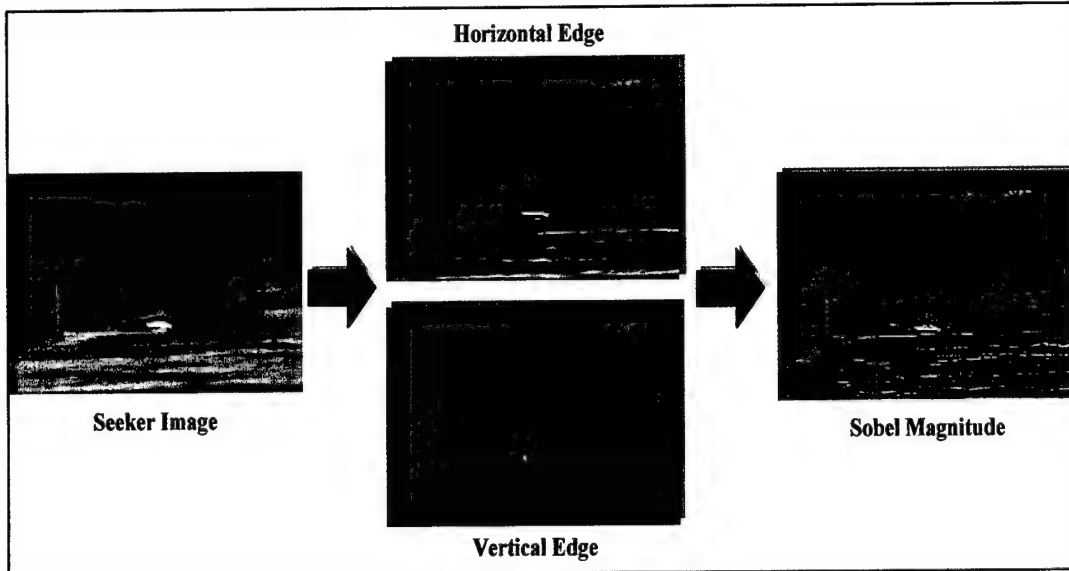


Figure 13. Sobel Filter Results

3.2.2.3 Bayesian Based Signature Metric

The Bayesian metric describes the separability of the target and background based on their statistical signatures (i.e. it is a relative metric). The metric assumes a ground-truth process has identified the target. The output of the metric is a value between 0 and 1. Values near 1 represent targets that are very separable from the background and values near 0 represent targets that are very similar to the background.

The Bayesian metric classifies pixels based on their similarity to statistical models for the target and background. The metric gate (MG) of the Bayesian metric has two components, the target pixel gate (TPG) and the background pixel gate (BPG). The TPG is centered on the target and matched to the size of the target. The BPG is also centered on the target but has larger than the size of the TPG (typical value of 3 times the TPG dimensions). The BPG excludes the area designated by the TPG. The target statistical model is formed based on the pixels inside the TPG. The background model uses only pixels inside the BPG. The mean, standard deviation, and correlation coefficient are calculated for the TPG and BPG to determine the bivariate normal distributions for the target and background pixels. Calculation of the correlation coefficient requires the user

to specify the offsets between the current pixel and its statistical pair. This offset is configurable (typical values are an offset of 1 in both the horizontal and vertical directions). These statistics can be established on a single frame or recursively updated over several frames to provide a means of memory and adaptation in the statistical model. Once the statistical models are established, each pixel within the MG can be classified according to its probability of belonging to either the background or target class based on Bayes' law. The metric is then calculated by the average success of correctly classifying target pixels as belonging to the target class and background pixels as belonging to the background class.

The Bayesian metric classifies pixels within a region as belonging to one of two groups, target or background, based on Bayes' law. The two groups are assumed to follow bivariate normal distributions with characteristic parameters being the mean, standard deviation, and correlation coefficient.

The MG is centered on the designated target position via the ground truth information and the mean, standard deviation, and correlation coefficient are calculated for both the target and the background areas. On the current or subsequent frames (user configurable), the likelihood of each pixel belonging to either the target or background class is calculated.

The TPG and BPG are each assumed to have pixel pairs that can be described with the bivariate normal distribution function. A spatial relationship defined by the horizontal and vertical offsets (XOFF and YOFF) is used to pair pixels together. The same offsets are used for the target and the background areas. It is important that the offsets not exceed one-half the target size so the majority of target pixels are paired with other target pixels. XOFF and YOFF are parameters specified by the user.

To determine the target and background statistical parameters, rectangular gates TPG and BPG are used (*Figure 14*). The user specifies the size and initial location of the TPG and BPG. The centers of the two gates are located at the same position in the image. The pixels in the TPG are excluded from the BPG calculations; therefore, the BPG must be larger than the TPG. Within the gates, pixel pairs are formed and the statistics

computed. The statistics calculated are the mean pixel value, standard deviation, and correlation coefficient.

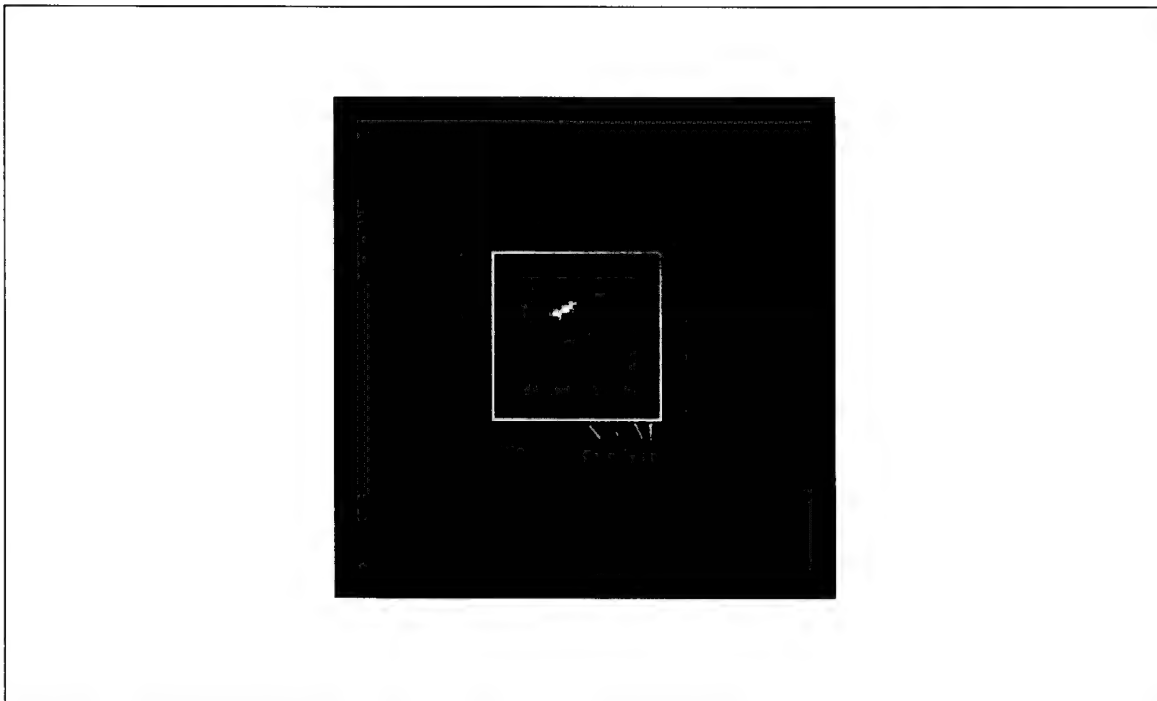


Figure 14. Image With Target and Background Gates Superimposed

Each pixel is classified by determining its target likelihood, L_t , in terms of the prior probabilities for the target and background, $P(G_t)$ and $P(G_b)$, and the conditional probability distribution functions for the target and background, $P(v_1v_2 | G_t)$ and $P(v_1v_2 | G_b)$, as shown in Equation 9. The v_1 term is the value of the current pixel being evaluated. The v_2 term is the value of the statistical pair to v_1 located XOFF and YOFF from the location of v_1 . The G_t term is the group of target pixels designated by the TPG and G_b is the background pixels inside the BPG excluding the TPG.

$$L_t = P(G_t | v_1v_2) = \frac{P(v_1v_2 | G_t)P(G_t)}{P(v_1v_2 | G_t)P(G_t) + P(v_1v_2 | G_b)P(G_b)} \quad \text{Equation 9}$$

The prior target probability $P(G_t)$ is the ratio of the number of target pixels to the total number of pixels within the MG as shown in Equation 10. The background term $P(G_b)$ is the ratio of the number of background pixels (MG-TPG), to the total number of pixels in the MG as shown in Equation 11. The values of $P(G_t)$ and $P(G_b)$ represent the probabilities of a pixel belonging to the target or background group without knowledge of its value.

$$P(G_t) = \frac{nxm}{NxM} \quad \text{Equation 10}$$

$$P(G_b) = \frac{NxM - nxm}{NxM} \quad \text{Equation 11}$$

Equation 12 and Equation 13 are the bivariate normal probability distribution functions for the target and background respectively and represent the probability of observing the values v_1 and v_2 given that the pixels belong to a specific group. For a given pixel, the same spatial relationship is used to compute the target likelihood as was used to compute the distribution functions. Therefore, if the pixel and its pair have values near that of the target mean, the target likelihood is increased. Further, if the relationship between the pixel pair values is similar to that defined by the target correlation coefficient, the target likelihood would also be increased.

$$P(v_1v_2 | G_t) = \frac{1}{2\pi\sigma_t^2\sqrt{1-\rho_t^2}} \exp\left[-\frac{1}{2\pi\sigma_t^2(1-\rho_t^2)}((v_1 - \mu_t)^2 - 2\rho_t(v_1 - \mu_t)(v_2 - \mu_t) + (v_2 - \mu_t)^2)\right] \quad \text{Equation 12}$$

$$P(v_1v_2 | G_b) = \frac{1}{2\pi\sigma_b^2\sqrt{1-\rho_b^2}} \exp\left[-\frac{1}{2\pi\sigma_b^2(1-\rho_b^2)}((v_1 - \mu_b)^2 - 2\rho_b(v_1 - \mu_b)(v_2 - \mu_b) + (v_2 - \mu_b)^2)\right] \quad \text{Equation 13}$$

Based on Bayes' rule and the fact that there are only two groups, pixels with a target likelihood value greater than 50% are classified as belonging to G_1 . Using this rule, each pixel in the MG is associated with one of the two classes.

The Bayesian metric (P_{Bay}) is the average success of correctly classifying target and background pixels. The success of correctly classifying target pixels is the ratio of correctly classified target pixels within the TPG (N_{CT}) to the total number of pixels in the TPG (N_{TPG}). The success of correctly classifying background pixels is the ratio of correctly classified background pixels in the BPG (N_{CB}) to the total number of pixels in the BPG (N_{BPG}) as shown in Equation 14.

$$P_{Bay} = \frac{N_{CT} \cdot N_{TPG} + N_{CB} \cdot N_{BPG}}{2} \quad \text{Equation 14}$$

The Bayesian metric has a value of 1 when all target pixels and background pixels are correctly classified and has a value of 0 when all pixels are incorrectly classified. If all target pixels are correctly classified and all background pixels are incorrectly classified, the metric has a value of $\frac{1}{2}$.

In summary, the Bayesian metric is a means for quantifying the separability of target and background statistics. There are several parameters in the metric that are configurable such as the distance to the pixel pair (XOFF and YOFF) and the means of establishing the statistical model (e.g. models based on current frame or recursively updated). After exercising the metric against a large data set the configurable parameters should be studied in order to provide optimum performance.

3.2.2.4 Signal to Clutter Measure

The Signal to Clutter Measure (SCM)² is a metric that predicts the probability of detecting a target in an infrared scene. It was developed by Margaret A. Phillips and Richard F. Sims of the AMCOM Research, Development and Engineering Center. This

metric takes the target signature information, as defined during the ground-truth process, and performs a correlation with the entire image. This is greatly different then metrics that compare target area statistics to local statistics around the target area. The process for performing the correlation is very similar to the TCM correlation process. It uses a snap-shot of the target area on a given frame, and performs a normalized cross correlation with the entire scene. Correlation peaks outside the target area are examined. If there are peaks inside the clutter area, then there are clutter features that could cause an ATD algorithm to get confused and mis-classify a portion of the background as target. If there are few or no correlation peaks in the clutter area, then the target signature is not correlated to the clutter and there should be a higher probability of a successful detection. The metric also examines the variance in the complete correlation surface. If there is variation in the correlation surface, this too would lower the probability of a successful detection.

The output of the SCM is a floating point number between 0 and 1 which is consistent with the desired output since it is normalized. A 1.0 would indicate a good probability of detecting the target while a 0.0 indicates a very poor probability of target detection.

3.2.3 Tracker Performance Metric

In order to grade tracker and ATA performance, a tracker performance metric (TPM) is used that compares the ground truth gate to the gate generated by the seeker algorithms. The TPM used for this analysis independently compares the ground truth gate width and height to the tracker width and height. To perform this comparison, a normal distribution is generated using the center of the gate as the mean, and the gate size as the sigma of the distribution. The overlapping area of the two distributions is calculated. Equation 15 describes the TPM calculation where $f_{trk}(x)$ and $f_{trk}(y)$ are the normal distribution functions for the track gate x and y dimensions, and $f_{gt}(x)$ and $f_{gt}(y)$ are the normal distributions for the ground truth gate x and y dimensions.

$$tpm = \sum_x \sqrt{f_{trk}(x) \times f_{gt}(x)} \cdot \sum_y \sqrt{f_{trk}(y) \times f_{gt}(y)}$$

Equation 15

Since the area under each curve is 1.0, perfect overlap would result in a value of 1.0. Any mis-match would result in a lower performance number. A normal distribution is used to weight the center of the gates stronger than the gate edges. The normal distribution will give more emphasis on the location of the center of the gate to ground truth, and less on gate size. Shown in Figure 15 are plots of two hypothetical distributions. The track gate width is smaller than the ground truth gate width but the gate height is very similar. The TPM is used to grade system performance that will ultimately be compared to the output of the metric tool. This information will be input into the neural network and used to draw a correlation between the actual performance of the tracking system and the metric values.

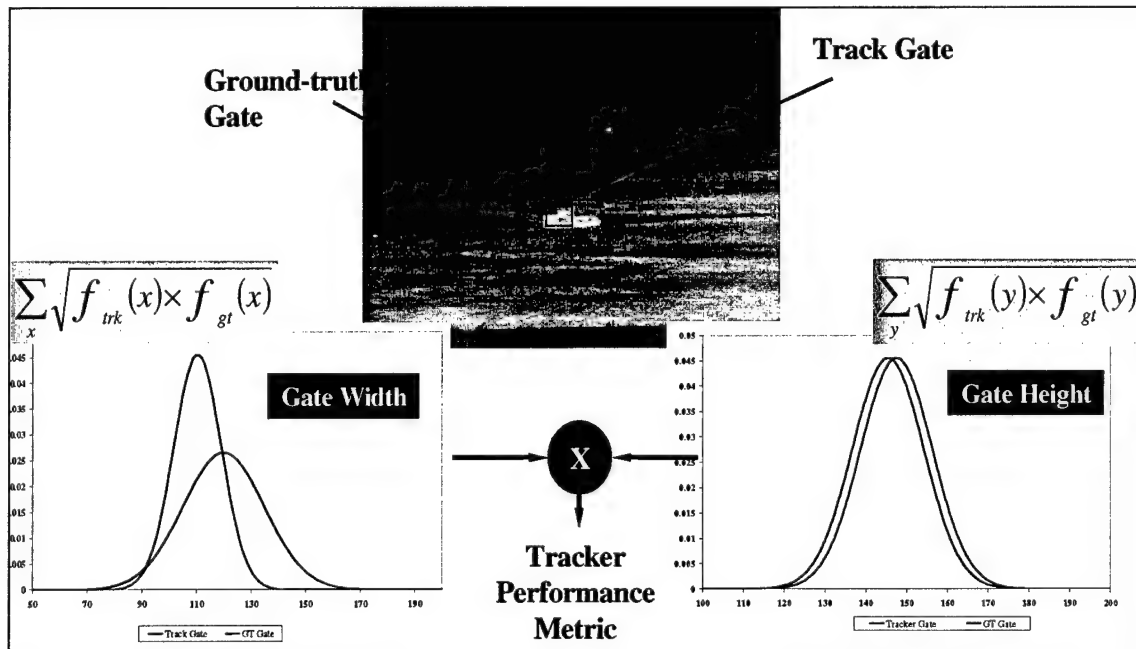


Figure 15. Tracker Performance Metric

Since the metric values are a measure of how well a tracking system will perform given a certain target to background situation, the metric values should have some relationship with the actual values as measured by the TPM. Or potentially a combination of metric values with associated costs values will be used to predict system performance. In an example case, the track correlation metric was used to compare against actual tracker performance for a specific infrared sequence. These sequences were processed using the track correlation metric and the tracker evaluated using the TPM. The track correlation metric data was compared to the actual system performance to determine if there truly is some relationship between this metric and actual tracker performance. Figure 16 shows this comparison. It is not expected that these plots would match exactly, but you can see a good correlation between the actual tracker performance and the metric output.

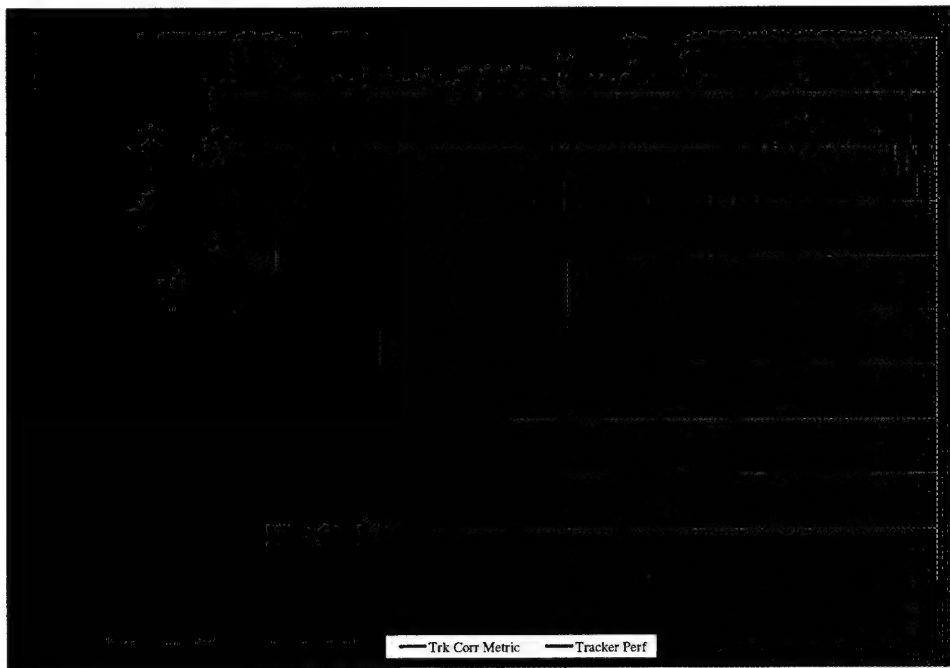


Figure 16. Track Correlation Metric Comparison to Tracker Performance

Performance on the autonomous target acquisition algorithm is more straightforward. The output of the ATA is either an X, Y aimpoint somewhere in the scene, or an estimated gate size and location. In the case where the ATA calculates a gate size, the TPM mentioned above will be used to calculate the performance of the

system. A metric value of 1.0 indicates perfect gate placement relative to ground truth while a metric value of 0.0 indicates no overlap of the normal distributions. If the ATA outputs an aimpoint only, then the performance will be limited to a 1 or zero, depending on whether the ATA placed the aimpoint successfully inside the ground truth gates or not.

3.3 Signature Metric Software Tool

The product developed under this effort is the Metric Analysis Tool. It reads standard image sequence formats, as well as raw and/or binary formats. It is written in C++, and a standard metric object framework was established to facilitate the addition of metric routines in a plug-and-play type environment. It has the ability to calculate the metrics and output results in various forms including plots to the screen and in ASCII output files. In Phase II, it will interface with the performance prediction code developed under that effort. The metric tool has VCR-type commands such as play, frame step, rewind, and stop, to allow viewing of the image sequences as they are processed. The tool contains the ability to select a large number of image sequence to process, and be able to select the metrics that will be executed. It can also be run from the command line with no GUI interaction for overnight or batch processing. It was developed using platform-independent libraries compatible with Windows, Linux, and SGI platforms.

The Metric Software Framework will provide an open-source, modular, scalable architecture for software development of additional metrics and interfaces to performance metric algorithms.

The GUI version presents the user with an interface allowing for the creation, editing, and execution of image sequences analysis. The image sequences and the metrics to be calculated on these sequences are presented to the user in a list view format. There are also three data view windows contained in the main program window. These contain a VCR type viewer to enable viewing of the image sequence, a window displaying the metric values calculated for each frame in the sequence, and a graphical representation of the metrics calculated. There are two dockable sub windows involved

in the presentation of the analysis configuration, the Project View and the Property View. An example of the GUI can be seen in Figure 17.

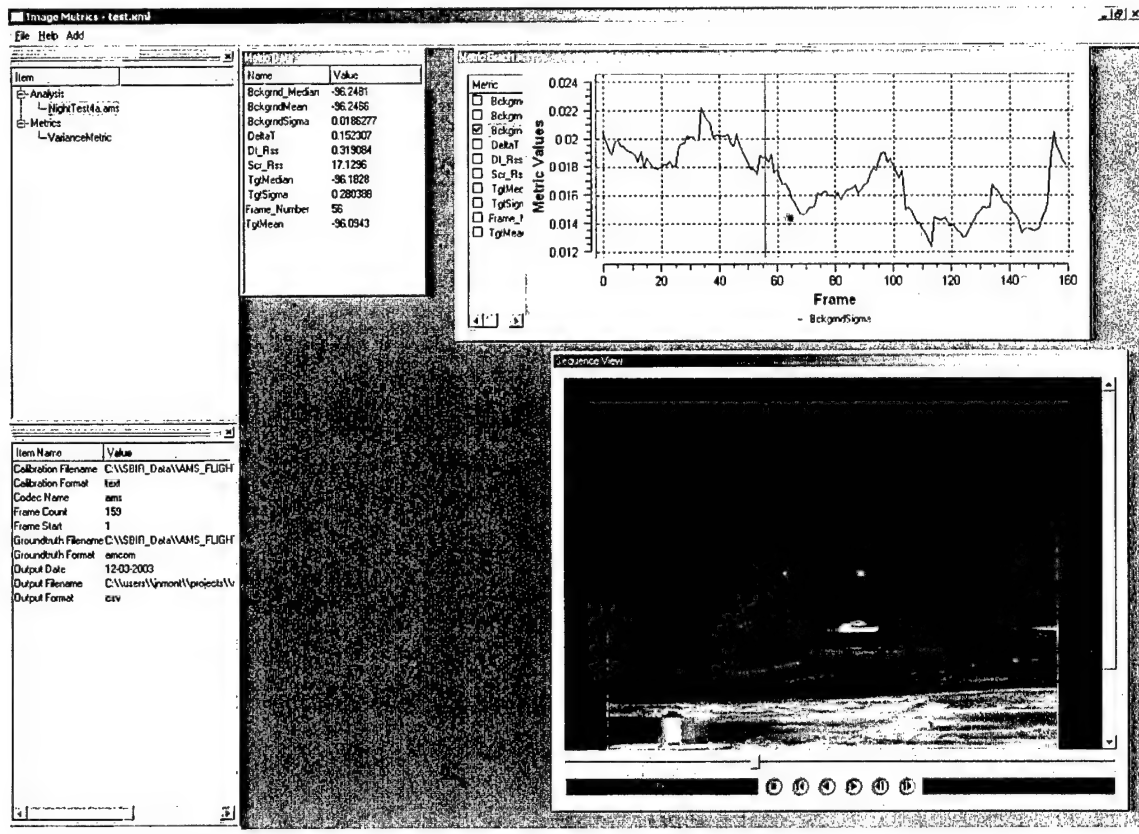


Figure 17. Image Metric GUI

The Project View window shows a hierarchical list containing the image sequence file names; these are contained under the parent item named “Analysis”. The second parent entry in this list, “Metrics”, contains the names of the metrics to be performed. Image sequences and metrics can be added and removed from the list view independently. Clicking on an individual entry in the Analysis list will cause the detail of this image sequence to be displayed in the Property View Window. This action will also display the image sequence, if it exists, in the VCR window. If the analysis has been run previously and the output file exists, the metric data will be presented as well.

The Property View window displays the individual fields describing the size and location of the image sequence file. Also presented here are the required video file decoder, date of the run, output file name, output format, ground truth filename and ground truth file format.

A menu bar in the main program window provides options for adding metrics to be calculated, the sequence to process, or a batch mode wherein the user specifies a directory and all of the sequence files in the directory will be added to the analysis. This batch mode also fills in the required information pertaining to the sequence, such as ground truth file, image size etc.

The GUI also provides feedback to the user during analysis execution. This feedback is provided in the form of a progress bar showing percent completion of the analysis for the loaded file. If the file contains multiple sequences, a new bar is displayed as each sequence calculation is performed. The GUI is multi threaded, so the interface remains usable while the calculations are being performed.

The console version of the analysis program is a separate application. This version of the tool requires the parameters to be specified either on the command line individually, or alternatively, a configuration file generated by the GUI can be used. This tool provides no inspection mechanism, but the output file can be examined in the GUI tool, or using a text or spreadsheet application.

The configuration file generated by the GUI application is stored in the Extensible Markup Language (XML). Any text editor may be used to edit this file directly, however this is not recommended. Also, the file may be viewed directly using a web browser. While not the ideal method of manipulating the file, this ability can be useful when troubleshooting a configuration file.

The metric tool software is deliverable as either a binary install or as source code with configuration files. The binary install is currently only available for Microsoft Windows, version 2000 and above. The source code install will allow the tool be built

for either the Windows or Unix operating systems. New metrics may be built and used regardless of the type of install performed.

Multi-platform build support is supplied through the use of Trolltech's qmake utility. This utility, along with the configuration files it uses, will be supplied with the installation. The qmake utility generates a system appropriate make file. This make file can then be used to build the executable on the target platform. Detailed build instructions are supplied in the users manual. These instructions provide information about the environment variables required for a successful compilation.

The GUI interfaces were built using QT by Trolltech Corporation. This is a multi-platform GUI application development environment. More information on QT can be found by visiting Trolltech's web site at <http://www.trolltech.com>. This web site also contains detailed documentation on the qmake utility.

The tool also makes use of Invariant Corporations Itools and Codec libraries. These libraries provide support for the Meta Class structure used in the metrics, the image sequence decoding, and various utility data structures used. Itools, Codec and the metric tool in general also make liberal use of the Standard Template Library.

The source code install includes a set of template files demonstrating how an end user can extend the functionality of the metric tool by creating their own metric calculations. This is a fairly straightforward process, and is laid out in a cookbook type description in the metric tool user's guide.

Several environment variables are required for proper execution of the tool. These variables and their values are described in the users manual.

The metric tool software is composed of two major components and several supporting components. The two main components are the GUI object and the Analysis object. The supporting components are the video codecs, the analysis codec, and the metrics.

The GUI component encapsulates all of the operations necessary for displaying the GUI. This is equivalent to the “main” program in the console application. The GUI also contains image codecs, the viewer, and also the graph object.

The Analysis component is the “heart” of the metric tool. This object encapsulates all of the items necessary to provide the metric objects the data they need to perform their calculation(s). The Analysis object also manages calling the metric objects and asking them to perform their calculations. The Analysis object contains a list of sub objects called sequences. These sequences contain all of the information associated with the image sequences. The required codec, the frame range, the ground truth file, the output file for the metric values, and the various formats of these items are all kept within the sequence. The Analysis object also contains a list of the metric calculations to be performed.

The tool has been designed using object-oriented methodologies and implemented C++. Each of the objects described above correspond to a class in C++. The metrics are implemented by taking advantage of the polymorphic characteristics of C++ allowing the addition of new metrics without recompiling the entire application. The software design Unified Modeling Language (UML) object interaction diagram can be seen in Figure 18.

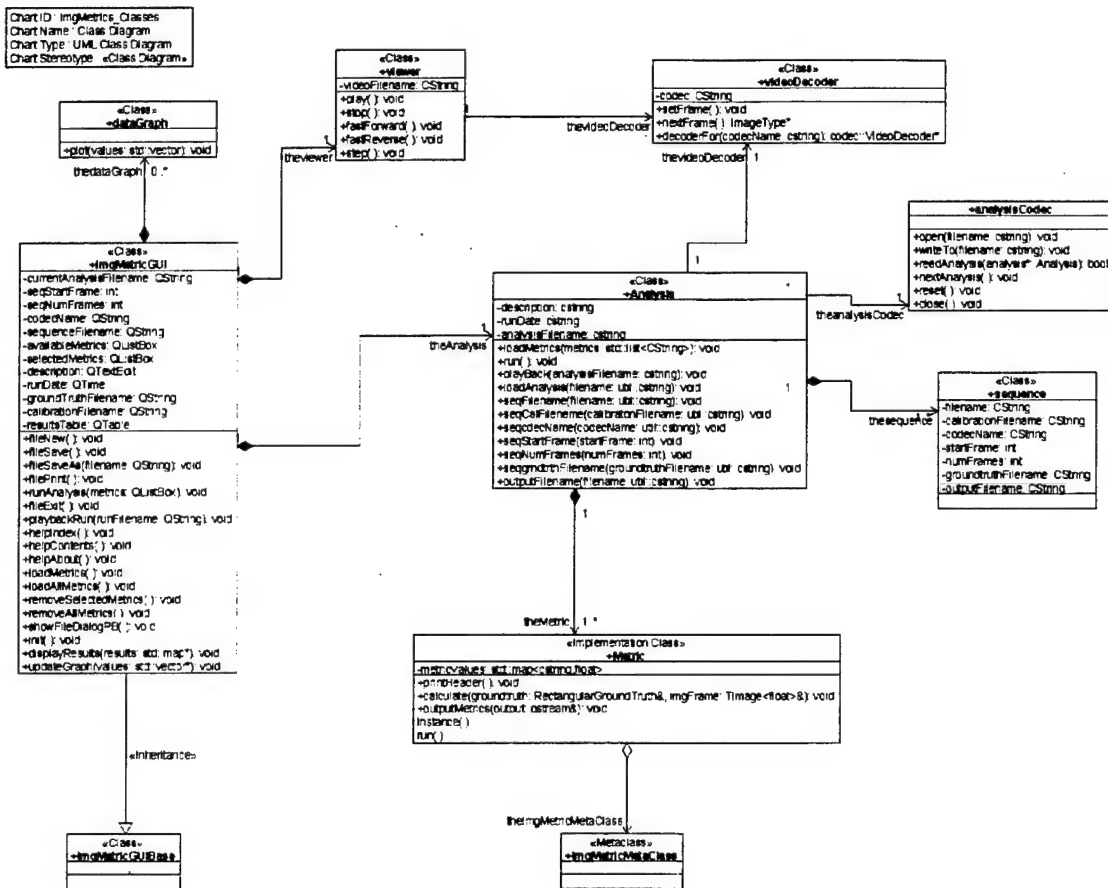


Figure 18. UML Object Interaction

Development was performed using Microsoft Visual C++ .Net, version 2002.

3.4 Ground Truth Process

To process the image sequences using the identified metrics, ground-truth information of where the target is in the image had to be obtained or generated. This was accomplished using the Tracker Analysis and Groundtruth Tool (TAGtool)³. The TAGtool runs under Windows and is a graphical software package (see screen capture shown in Figure 19) that was developed by Dynetics for AMCOM as a means of quickly and accurately ground-truthing infrared image sequences. To further reduce the time

required to process sequences, a correlation capability was used that allowed the user to ground-truth every tenth frame. The auto-correlator used the user-generated information to determine the ground-truth data for intermediate frames. All image sequences identified under this effort were ground-truthed with this process.

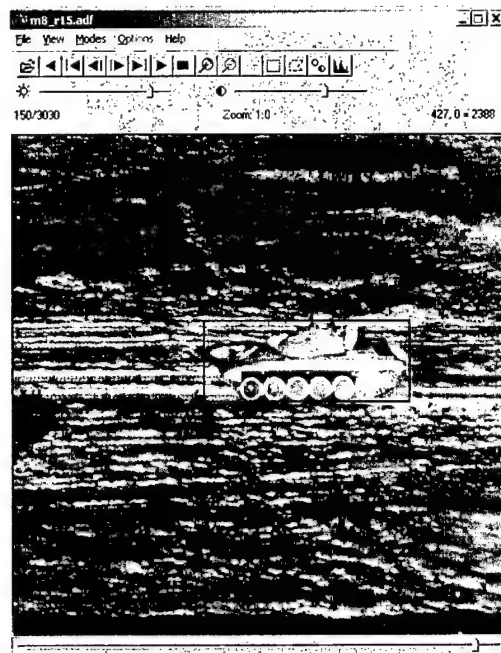


Figure 19. TAGtool Screen Capture

3.5 Methodology for Seeker Performance Predictions

3.5.1 Performance Prediction Methodology Problem

Presently, a comprehensive framework for quantitative analysis of missile seeker designs does not exist. Although parameters/metrics such as 3D Noise Statistics have been used to make relative comparisons at the component and system level, the utility of existing metrics are often system specific and depend on the operational functionality of the sensor.

Classic performance predictions by FLIR 92 and NVTHERM have started with empirical information such as Johnson's criteria from 1950's and examined system performance as a function of system design and degradations including blur and noise. These Man-in-the-Loop (MITL) performance models have been continuously modified and updated to reflect state-of-the-art in sensors coupled with human operators. The maturity of the current NVTHERM models allows for *relative* comparisons of MITL systems with range errors of $\pm 20\%$ for probabilities of detection, recognition and identification.

For Tracking and Target Acquisition Tasks, characterizing seeker performance based on system design and degradations is difficult at best. Algorithms used for these tasks often use different paradigms and information to process incoming images. As a result, particular image metrics are often not indicative of relative or absolute system performance for particular task such as Target Acquisition. The goal becomes to develop a process for finding and combining metrics capable of predicting task performance. In light of various features and image processing techniques available to accomplish a given task, useful metrics may vary by task and seeker design.

3.5.2 Performance Prediction Solution

In order for a metric or combination of metrics to be capable of estimating task performance, the metrics must be mapped to some performance measure. In the case of a single metric (say Delta T), standard curve fitting might be used to map a particular metric to a probability of detection performance. However, a combination of metrics may be more robust in estimating the actual performance. The key is having criteria for mapping. For a tracking task, the performance might be measured by the overlap of a target ground truth box and a system track gate. The desired end result would yield performance estimation for a particular scenario given a particular system and/or a set of degradations.

A classical Neural Network approach provides a good framework for determining a mapping from a set of metrics to a desired performance measure. Input to the network

may be a set of metrics and/or features available to the system evaluator. A mapping is generated based on the performance measure used to grade a particular seeker task.

3.5.3 Development of Basic Neural Network Approach

To begin, a weighted sum of the image metrics might be used to produce an output as described by Equation 16 and visualized by Figure 20.

$$y = \sum_i w_i x_i \quad \text{Equation 16}$$

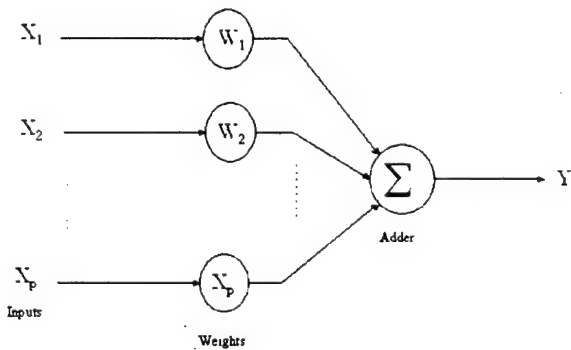


Figure 20. Linear Spatial Filter

Here the mapping between a set of input vectors (image metrics) and desired outputs (performance measure) is known empirically for selected data. The task is to determine the weight vectors that map input vectors to appropriate output.

An error signal may be defined as the difference between the weighted sum y and a desired output d generated from a specific performance measure (i.e. Track Quality).

$$e = d - y \quad \text{Equation 17}$$

Minimizing the cost function defined in Equation 18 provides a basis for minimizing the mapping error between a set of image metrics and a performance measure (Track Quality). Here E is used to represent the statistical Expectation operator.

$$J = \frac{1}{2} E[e^2] \quad \text{Equation 18}$$

Minimizing Equation 18 with respect to the weights in Equation 16 leads to the well known Weiner-Hopf equations for determining the weights w_i . The Method of Steepest Descent is often implemented rather than solving the Weiner-Hopf equations directly for the unknown weight vector.

$$\sum_{j=1}^p w_j E[x_j x_k] = E[d x_k], \quad k = 1, 2, \dots, p \quad \text{Equation 19}$$

Weiner-Hopf Equations

The Method of Steepest Descent determines weights via an iterative scheme illustrated in Equation 20 until changes are no longer significant. Here, $n+1$ represents the updated value of a particular weight and n represents the previous iteration.

$$w_k(n+1) = w_k(n) + \eta \left[E[d k_k] - \sum_{j=1}^p w_j E[x_j x_k] \right], \quad k = 1, 2, \dots, p \quad \text{Equation 20}$$

However, the Expectation operator E in equations 17 and 18 indicates the statistical autocorrelation and cross-correlation between the input vectors and the desired output is required. In many cases these correlation functions are not known. The least-mean-square (LMS) algorithm addresses this limitation by implementing instantaneous estimates of the correlation functions. The net result leads to a modification of Equation 20 as follows.

$$w_k(n+1) = w_k(n) + \eta [d(n) - y(n)], \quad k = 1, 2, \dots, p$$

$$\text{where,} \quad \text{Equation 21}$$

$$y(n) = \sum_j w(n)_j x(n)_j$$

Again, this is an iterative technique that continues until changes in the weight vector are no longer significant.

So far these approaches are applicable to linear filtering problems. For potential non-linear mappings of the image metrics to a performance measure, the LMS algorithm may be generalized via the backpropagation algorithm for Multi-layer Perceptrons. Figure 21 illustrates the general architecture of a neural network with a single hidden layer.

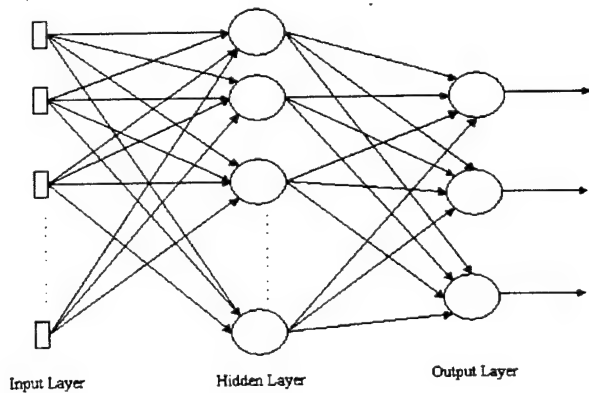


Figure 21. General Multi-Layer Perceptron Architecture

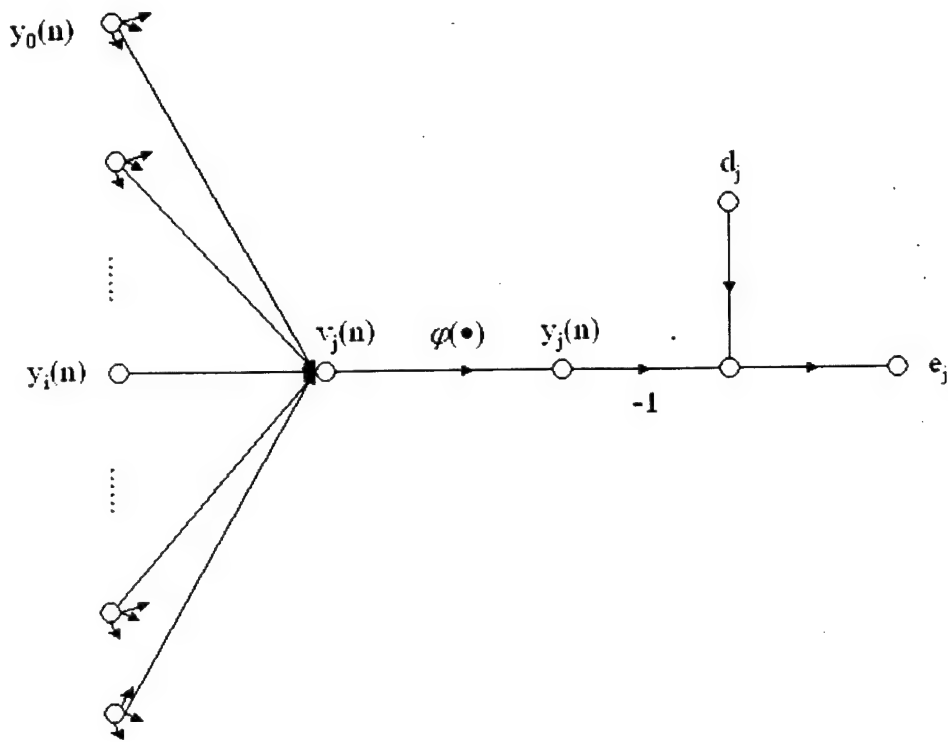


Figure 22. Signal-Flow Highlights of Output Neuron j.

The following relationships are illustrated by the signal flow graph in Figure 22 for a neuron in the output layer. Development of the back propagation algorithm begins by defining an error signal for any neuron in a similar manner as for the LMS algorithm.

$$e_j(n) = d_j - y_j(n)$$

Equation 22

where

$e_j(n)$ = error signal at neuron j;

$y_j(n)$ = observed output at neuron j;

$d_j(n)$ = desired output at neuron j;

n = current input pattern

The cost function is now defined as

$$J = \frac{1}{2} E[e_j(n)^2] \quad \text{Equation 23}$$

and e_j represents the instantaneous error received after each input.

The total input at neuron j is expressed as

$$v_j(n) = \sum_i w_{ji}(n) y_i(n) \quad \text{Equation 24}$$

The output at neuron j is a function of $v_j(n)$,

$$y_j = \varphi(v_j(n)) \quad \text{Equation 25}$$

where $\varphi(x)$ is the activation function of the neuron.

Applying a similar methodology as in the LMS approach, the weight updates are proportional to the instantaneous gradient.

$$\frac{\partial J}{\partial w_{ji}} = \frac{\partial J}{\partial e_j(n)} \frac{\partial e_j(n)}{\partial y_j(n)} \frac{\partial y_j(n)}{\partial v_j(n)} \frac{\partial v_j(n)}{\partial w_{ji}(n)} = -e_j(n) \varphi'(v_j(n)) y_j(n) \quad \text{Equation 26}$$

As before, the update rule is

$$w_{ji}(n+1) = w_{ji}(n) + \Delta w_{ji} \quad \text{Equation 27}$$

where

$$\Delta w_{ji}(n) = -\eta \left[\frac{\partial J}{\partial w_{ji}(n)} \right] = \eta \delta_j(n) y_j(n)$$

and

$$\delta_j(n) = e_j(n) \varphi'[v_j(n)]$$

An important element for calculating the update is the derivative of the activation function $\varphi'[x]$. The sigmoid function used by Rosenblatt is a smooth approximation of the step function.

$$\varphi[x] = \frac{1}{1 + \exp[-x]} \quad \text{Equation 28}$$

The sigmoid function is continuous for all values of x and ensures a well behaved derivative for the preceding equations.

$\delta_j(n)$ is defined as the local gradient. If neuron j is in a hidden layer, calculation of $e_j(n)$ is not straightforward. From Equation 25,

$$e_j = -\frac{\partial J(n)}{\partial e_j(n)} \frac{\partial e_j(n)}{\partial y_j(n)} = -\frac{\partial J(n)}{\partial y_j(n)} \quad \text{Equation 29}$$

For clarity, J is defined at the output layer as

$$J = \frac{1}{2} \sum_k [e_k(n)]^2 \quad \text{Equation 30}$$

with the subscript k denoting an output layer as opposed to the input layer j . From Equation 28, the goal is to determine the gradient of the cost function with respect to the hidden neuron y_j .

$$\frac{\partial J(n)}{\partial y_j(n)} = \sum_k e_k(n) \frac{\partial e_k(n)}{\partial y_j(n)} = \sum_k e_k(n) \frac{\partial e_k(n)}{\partial v_k(n)} \frac{\partial v_k(n)}{\partial y_j(n)} \quad \text{Equation 31}$$

where

$$e_k = d_k - \varphi[v_k(n)]$$

and

$$v_k(n) = \sum w_{kj}(n) y_j(n).$$

Simplifying, the gradient becomes

$$\frac{\partial J(n)}{\partial y_j(n)} = \sum_k e_k(n) \varphi'[v_k(n)] w_{kj}(n) \quad \text{Equation 32}$$

Substituting back into Equation 31,

$$\Delta w_{ji} = \eta \delta_j(n) y_i(n) \quad \text{Equation 33}$$

where

$$\delta_j(n) = \varphi'[v_j(n)] \sum \delta_k(n) w_{kj}(n)$$

and

$$\delta_k(n) = [e_k(n)] \varphi'[v_k(n)].$$

Synaptic updates depend on whether the neuron is in the output layer or a hidden layer. Output neurons use Equation 31, which is similar to the update rule used for the

LMS approach. Hidden neurons use Equation 32 where the local gradient depends on synaptic activity in the output layer as well as synaptic activity for the hidden neuron.

The end result is an extension of the update rule for the LMS algorithm. For LMS, weighted inputs are summed at a single node or neuron. For the Multi-Layer perceptron, the error is ‘propagated back’ through the network to provide instantaneous estimates of correlation functions. The increased computation complexity provides robust performance for mappings that are not linear.

3.6 Validation Plan

This section presents the requirements and process for validation of the Metric Detection/Track Prediction model (MDTP). MDTP is a generic analytical IR detection and track performance prediction model described in this report and proposed as part of the Phase II follow-on. MDTP validation will be accomplished by comparing the model's metric based detection and track predictions to field test results utilizing tactical and generic tracking algorithms and validated analytical detection models. A comprehensive set of IR imagery, previously collected, has been identified under this effort that encompasses various sensor/seeker systems engaging an array of targets under various environmental conditions. This section describes the methodology for utilizing this data set and outlines the necessary steps for completion of the validation process.

The result of the validation process will be a metric based detection and track prediction model, with supporting documentation, which can be confidently used as a tool for prediction of infrared (IR) seeker/sensor system detection and track performance for a variety of one-on-one engagement scenarios. This process should provide insight into the validation process and trade-offs associated with model fidelity versus complexity for the test scenarios under study.

3.6.1 MDTP Metric Tool

MDTP will utilize the collection of metrics identified in this report. It will use the metric software tool developed under this effort to calculate the metric values on new

infrared sequences. The flexibility of this framework allows the ability to quickly add new metrics if deemed necessary under the future effort. The neural network algorithms and performance prediction algorithms will be coded and integrated into the current framework. The tool will maintain the ability of running in the GUI or in a non-GUI batch configuration. The GUI will have an experiment planner that allows the user to select a large set of images for overnight or batch processing, and will continue to use platform-independent libraries compatible with Windows, Linux, and SGI platforms.

3.6.2 MDTP Probability of Detection Prediction Methodology

Developing a detection prediction model requires output from a representative algorithm, the metric calculations, and ground-truth information. For training purposes, the desired output of the network is set according to algorithm performance. For each set of metrics generated for an image, a performance value must be generated for driving the desired output of the neural network. For example, the output of the network may consist of nodes representing target detections, clutter decisions, and false alarm predictions. Once the weights of the network are determined, the output values of each node are used to predict how the detection algorithm will perform on a given image. Over an ensemble of test images, the neural network outputs can be used to calculate probability of detection and/or false alarm rates.

A subset of images from the data sources described in the next section will be used to train the neural network. Once the network is trained for a desired sensor, metric inputs to the network can be used to predict system performance.

3.6.3 MDTP Probability of Track Prediction Methodology

Tracker performance predictions will be carried out in a similar manner as for detection. A generic tracker algorithm will be applied to various image sequences with success and failure determined by the methodology described in the validation section. Image metrics will be used as training inputs to a neural network while the success/failure results will provide desired network outputs and feedback for determining synaptic weights between each neuron. Once, training is complete, the network will generate outputs based on metric input. The network output will project the success or failure of a

tracker for a particular sequence. Probability of Track can then be calculated by observing results over an ensemble of metric inputs generated by a set of image sequences.

3.6.3.1 Model Validation Methodology

Validation is defined in DoD Instruction 5000.61 as “The process of determining the degree to which a model is an accurate representation of the real world from the perspective of the intended uses of the model.” The Recommended Practices Guide (RPG) provided by the Defense Modeling and Simulation Office (DMSO) describes the essential steps for validating models and simulations as shown in Figure 23. Understanding the user’s objective and characterizing the requirements are the foundation of the validation process because they will determine the accuracy threshold for declaring the results valid. This threshold will be determined in Phase I, and the validation process will be executed in Phase II. The results of tactical tracking algorithms against imaging data collected during captive flight and ground testing will serve as the available referents. Simulation may be used to fill deficiencies in a set of validation data. Signature metrics calculated from the same set of image data will be used to predict the performance of the trackers. The accuracy of the predictions will be determined by comparing the predicted and actual tracker performance. If the accuracy exhibits the required creditability of the predictions, they will be deemed valid.

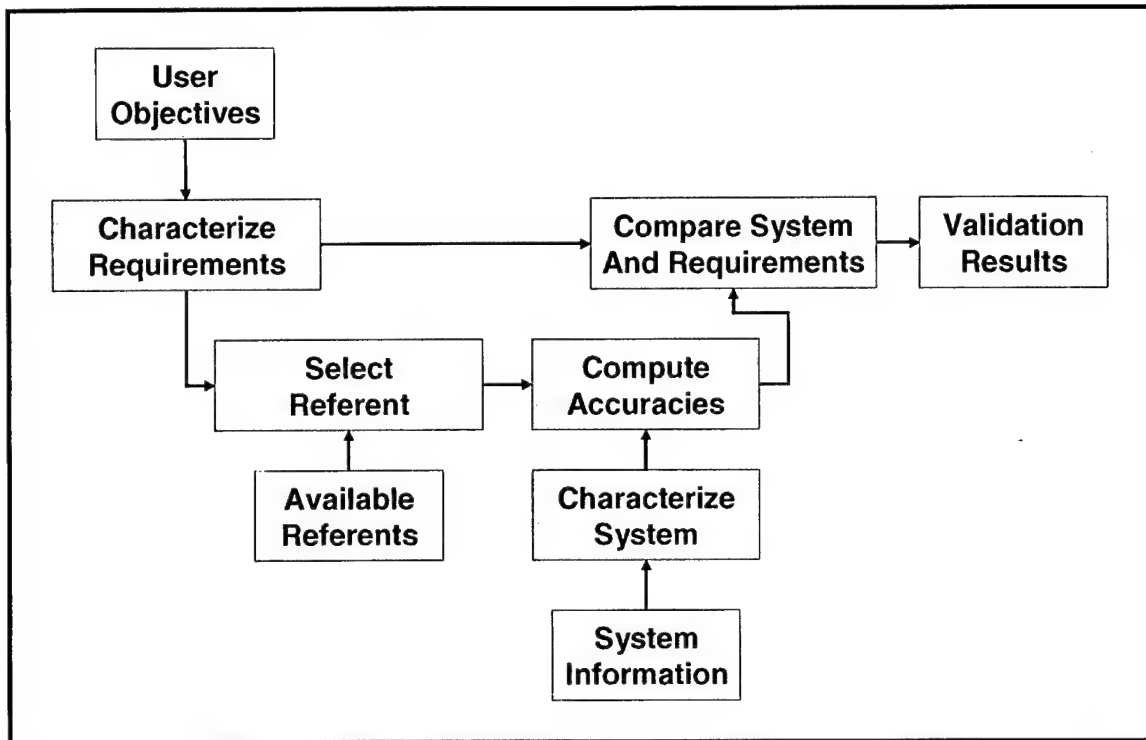


Figure 23. Essential Steps for Validation of Models and Simulations

MDTP will provide an approximation to the stochastic processes of target detection and tracking. Therefore, validation of MDTP will require a comparison between the deterministic results from the model and the discrete results from the test. The results from a single test event will have little use in the validation process; however, a collection of test results can be used to calculate the probability that the target was detected or tracked for the given test conditions (i.e., m detections out of n trials). This calculated test probability will be compared to the predicted performance from MDTP for the same test conditions. Ideally, a collection of test cases in which all conditions remain constant would be used to calculate the performance probabilities; however, this is not practical. Some variation in the test conditions of the test cases will have to be allowed. Restrictions in the variability of the test conditions for a set of test results, the smaller the test set will be. A trade-off between test condition variation and test set size (number of test results) will be conducted using sensitivity analysis. The allowed variation within a test set, the desired number of results within a test set, correlation within a test set and other validation issues are addressed in this section.

This validation methodology is described in detail in the following subsections. A validation notebook will be used to document the steps taken and used for the validation final report. Figure 24 depicts the methodology used to validate MDTP.

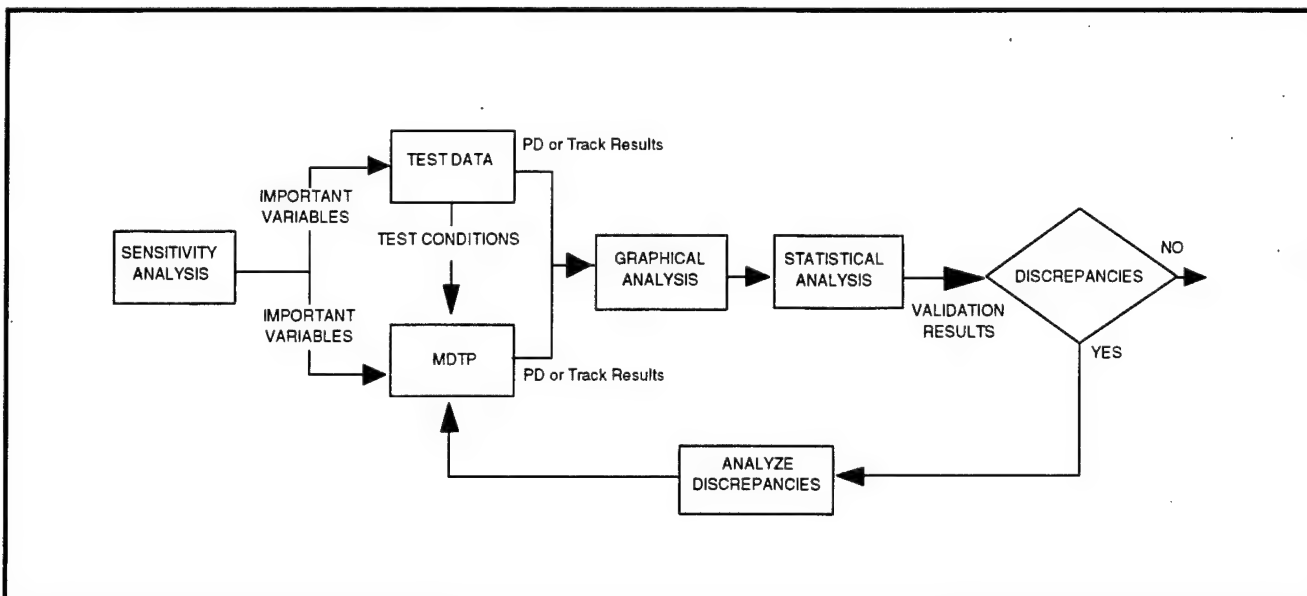


Figure 24. Validation Methodology

3.6.4 MDTP Model Validation

Utilizing a portion (approximately half) of the imagery from the database, a distinct set of metrics will be identified that will provide a methodology to predict the probability of detection and the probability of track for a given scenario, sensor characteristics, and environmental conditions. This first set of data will be used to develop and confirm the approach for developing the MDTP model. The second portion of the imagery database will be sequestered for use during the validation effort. Modifications to MDTP may be made prior to validation, based on the results of the metric analysis. Any modifications should be completed, and a baseline version of MDTP should be finalized prior to beginning the validation process.

The validation effort will utilize the sequestered data, first to evaluate the performance of generic and tactical track algorithms for comparison to the MDTP model.

This effort will require a scoring, or assessment for each tracker/image sequence combination for the success or non-success of the event. A scoring methodology has been previously developed for tracker assessment and approved by AMCOM. This methodology begins by attempting a track at the farthest range through endgame (approx. 250m). Each frame is scored "in Track" if an overlap condition exists between the ground-truth box and the track gate box. If 90% of the frames within a sequence are tracked then the track event can be declared successful, if the last frame of data is not only in track, but the center of the track gate is located within the boundary of the ground-truth box. If the tactical or multi-algorithm tracker fails then the slant range to target is decremented by 250m and another trial is attempted using the same imagery sequence. This methodology can have the affect of correlating failed cases, especially if the cause is determined to be clutter near the endgame of the sequence. Therefore, for single algorithm trackers or constant slant range imagery data (typically generic) an attempt to de-correlate the trial data is accomplished by performing track attempts on 200 frame segments of the sequence, resulting in each trial being somewhat independent from the result of the previous trial. After a specific tracker has been run on a section of the data set, bounded by specified conditions under study, the overall tracker success is determined. This success will then be compared to the performance of the MDTP model prediction for the same data set to determine whether the model correlates well with the test results.

The detection performance validation of autonomous detection algorithms, as compared to MDTP, will be handled similarly as the track algorithms. Selected single frame data sets will be used for both MDTP and ATR assessments and performance predictions will be compared for validation.

Validation is a measure of comparison between the MDTP predicted performance and the actual performance achieved during testing of various track and ATD algorithms and perception based detection models for the imagery database. The basic validation process consists of obtaining data from pertinent sources, reducing and categorizing it where necessary, and compiling it in a table format for comparison purposes on a mission set basis. These mission sets will contain enough data points to be statically significant,

therefore the number of data sets and track algorithms tested should be optimally categorized to create this significance. The key comparisons to be made are Pd, and Pt for a given set of measured metrics.

3.6.4.1 Sensitivity Analysis

A sensitivity analysis will be used to reduce the dimensionality of the validation process. If each input into MDTP were treated as a variable, then the validation would be based on many discrete points with little or no replication. Sensitivity analysis can be used to reduce the number of input variables by making several of them constant throughout the validation process. This creates the replication required to achieve validation. As an example, it is anticipated that due to the short range for the IR sensor, the atmospheric transmission will remain nearly constant over a given slant range.

It is desirable that the image sequence metrics be the only variations between trials. These metrics are used to determine the Pd and Pt, which are primarily derived from the intensity variations between target and clutter background; however, if a limited number of significant variables are introduced, the validation still can be performed.

The sensitivity analysis will be conducted over the selected data set as part of the validation process. Clearly, if MDTP is relatively insensitive to a particular parameter, it is unnecessary to measure or segment that parameter to a high degree of precision. Therefore, the sensitivity analysis can be used to refine accuracy requirements for the processing of the imagery database.

To conduct the sensitivity analysis, a series of pre-designed MDTP cases will be run. The selection of these cases will be based on orthogonal arrays to reduce the number of runs required. Once the initial MDTP run set has been defined and the most significant variables identified, a full factorial set of MDTP cases will be designed and run to characterize sensitivity to the most significant variables.

3.6.4.2 CALCULATING P_d FROM Test Data

The test data will be analyzed to determine the associated metrics, as well as the test conditions. In the simplest cases, the P_d or P_t will be determined based on m detections/successful tracks out of n trials:

$$P_d = P_t = m/n$$

It is also necessary to develop an MDTP P_d and P_t to validate against the imagery data. The conditions and metric data will be fed into MDTP to develop these values. The scoring for the test data will be on a per-look or per-track basis, since the process assumes the target is completely within the field of view of the sensor for each image analyzed.

3.6.5 Validation Criteria

3.6.5.1 Graphical Analysis

The track and ATD algorithms will be plotted alongside the MDTP results. This will allow for direct comparison between the two data sets. This is a simplified Turing test⁴. In an actual Turing test, the two sets of data would be displayed with no distinctive markings. If an expert cannot tell the difference between data from the actual algorithms and from the simulation, then the simulation passes the validation test. For this analysis, plots as shown in Figure 25 will be examined to determine if MDTP is close enough to actual test results. The crucial element in this comparison is that MDTP is not required to explicitly reproduce real-world results. It is only necessary for MDTP to reproduce results that are close enough that decisions made based on these results would be the same as those made based on actual algorithm results.

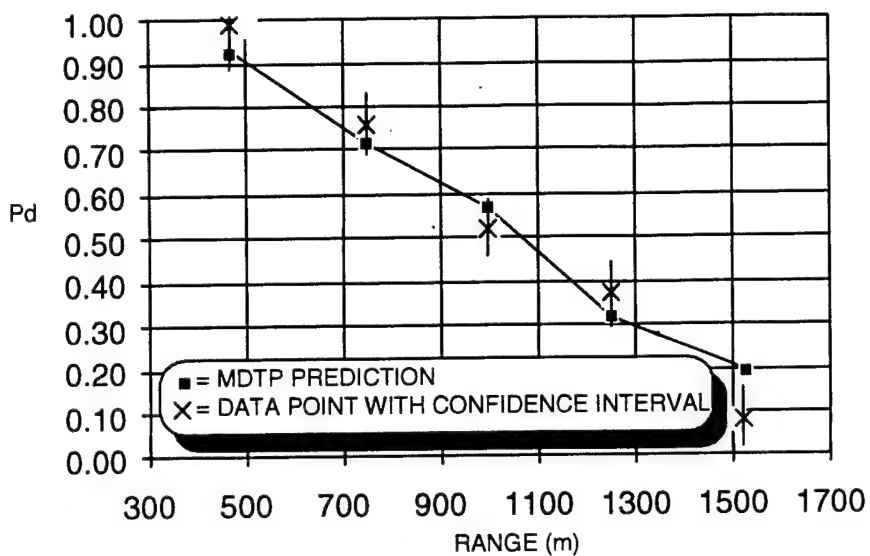


Figure 25. Graphical Comparison with Confidence Intervals

3.6.6 Statistical Analysis

There are several statistical techniques that could be used to validate MDTP. The primary statistical technique is to develop a confidence interval (CI) around each performance prediction. This technique is described in the following sections.

3.6.6.1 Comparison to MDTP Results

An initial approach to comparing test results to MDTP results would be to use hypothesis testing. The hypothesis to be tested would be:

$$H_0: P_{d,\text{TEST}} = P_{d,\text{MDTP}}$$

$$H_1: P_{d,\text{TEST}} \neq P_{d,\text{MDTP}}$$

A level of significance would be chosen, and all of the tests would be run. An equivalent approach is to use CIs. This is equivalent because at the same level of significance, if a prediction falls outside of the CI, then it also fails the hypothesis test.

CIs have the advantage of allowing a more understandable form of presentation (as depicted in Figure 25).

The CI represents the probability that the true performance prediction (P_d , P_t) is within the confidence limits with a certain probability:

$$P(LowerLimit \leq P_d \leq UpperLimit) = 1 - \alpha$$

where α denotes the level of significance.

The MDTP results will be compared to the calculated CIs, either graphically (as in Figure 25) or in tabular form. The determination of model validity is based upon whether the MDTP result falls within the CI. As an example, Figure 26 shows the possible results and the determination of whether the MDTP result is valid for each case. This figure also shows the possible sources of error. Note that it is impossible to know whether any of these errors have occurred without knowing the true P_d . However, it is possible to know the probability of committing each type of error. The method of calculating these probabilities is given in the following sections.

3.6.6.2 Type I Error

In the equation above, the level of significance, α is the probability of making a Type I error. A Type I error occurs when the hypothesis (H_0) is true, but is rejected by the sample. Therefore a Type I error occurs when the CI should include the true P_d , but does not. For this validation, a Type I error is depicted in Figure 26.

It is expected that not all MDTP results will fall within the CIs. Even if there were exact correspondence between MDTP and the test data, it would be expected that a certain number would fall outside the CIs. This number is based on the probability of making a Type I error. The probability of making an error given multiple, n_{CI} , tests (CIs), is given by:

$$P_{error} = 1 - (1 - \alpha)^{n_{CI}}$$

where the level of significance, α , is the same for each CI. Since the number of errors is binomially distributed, the expected number of errors in n_{CI} tests is αn_{CI} . Therefore, if 100 95% CIs are developed, ($\alpha = 0.05$), then with perfect correspondence between MDTP and the real tests, 5 of the MDTP results would be expected to be outside of the CIs.

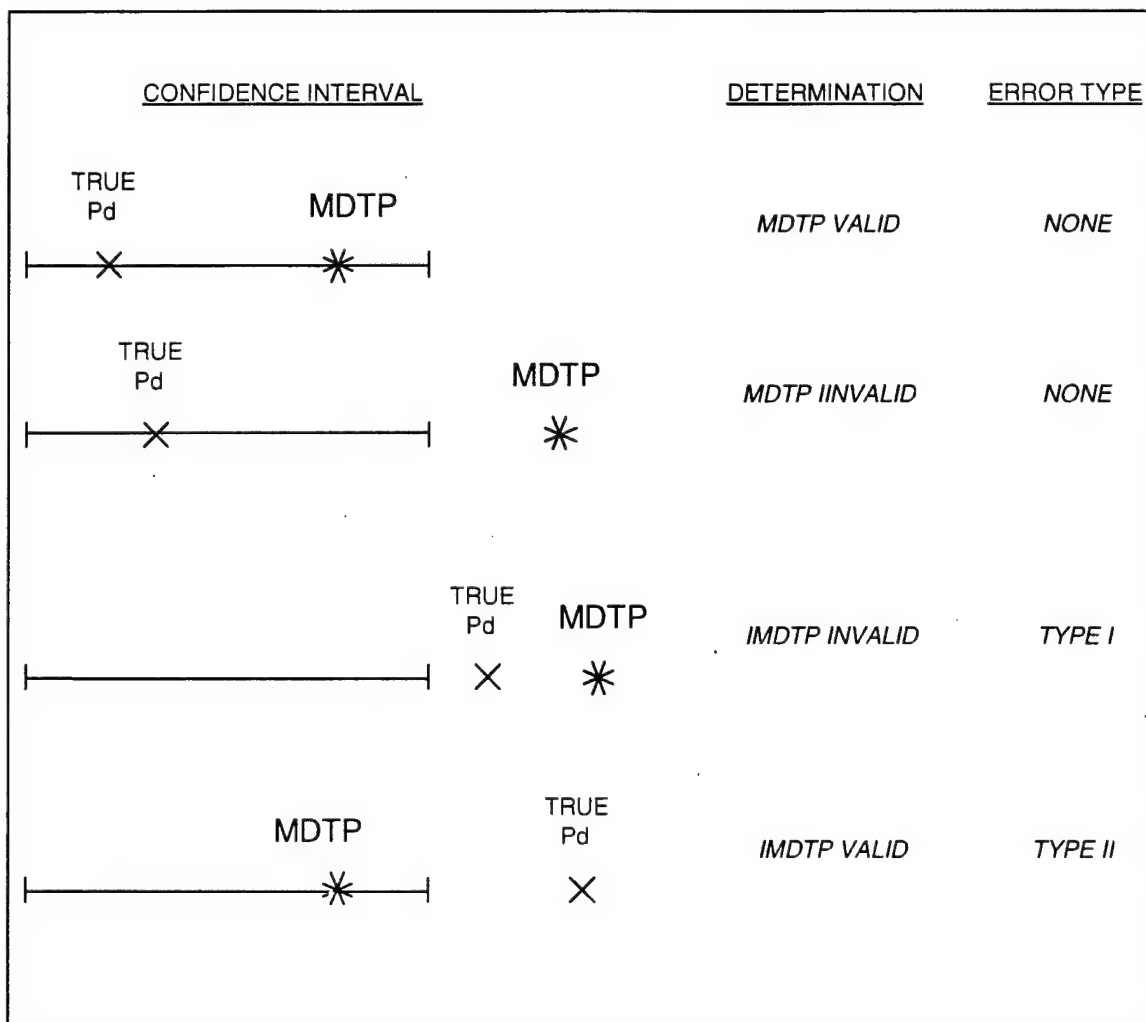


Figure 26. Validation Results and Types of Errors

3.6.6.3 CI Development

This subsection describes how to develop the CIs required for validation. The use of the standard CI for the mean is not accurate, since it is a probability (or proportion) that must be analyzed. Therefore, the CI to be developed is a CI around a proportion. For large sample sizes, this can be approximated using the normal approximation to the binomial distribution⁵:

$$\frac{m}{n} - Z_{\alpha/2} \sqrt{\frac{m(1-\frac{m}{n})}{n}} < Pd < \frac{m}{n} + Z_{\alpha/2} \sqrt{\frac{m(1-\frac{m}{n})}{n}}$$

where m is the number of detections in n trials, and $Z_{\alpha/2}$ is the value of the standard normal distribution that has a cumulative probability of $\alpha/2$. A rule of thumb for determining a sufficient sample size is given by Hicks⁶ as $nPd \geq 4$. For example, if the Pd was determined to be 0.5, then the sample size, n , should be at least 8.

The exact CI for smaller n can be calculated using the binomial distribution. From Beyer⁵, given that the lower limit of the CI is represented by θ_a and the upper limit is represented by θ_b , the lower limit is calculated such that:

$$\alpha/2 = \sum_{x=x'}^n \binom{n}{x} \theta_a^x (1-\theta_a)^{n-x}$$

where α is the level of significance, x is the number of detections, and n is the sample size. A simplified form of the equation above is given by:

$$\alpha/2 = 1 - \sum_{x=0}^{x'-1} \binom{n}{x} \theta_a^x (1-\theta_a)^{n-x}$$

The upper limit of the CI, θ_b , is calculated such that:

$$\alpha/2 = \sum_{x=0}^{x'} \binom{n}{x} \theta_b^x (1-\theta_b)^{n-x}$$

The ideal method of calculating the upper and lower limits, θ_a and θ_b , would be to solve the above equations for these two variables. This, however, is not a straightforward proposition. Fortunately, a simpler solution will produce the same results. This simpler solution is to iteratively modify θ_a and θ_b until the resulting cumulative binomial probabilities are equal to $\frac{1}{2}$. Although there are tables that can provide these solutions⁵, with the advent of spreadsheets with powerful statistical analysis functions, more precision is available through the use of an Excel spreadsheet. Using the BINOMDIST function, which returns cumulative values of the binomial distribution, a spreadsheet has been developed that implements Equations 7-10 and 7-11. Using the Solver, Excel will iteratively modify values in cells (specifically θ_a and θ_b) until the target value for $\frac{1}{2}$ has been reached. The precision can be set to almost any required level.

As an example of this methodology, consider 8 detections in 30 trials and an alpha of 0.05. This yields a P_d of 0.26666667. This example is taken directly from Beyer⁵. The CI given in Beyer (based on the tables) is:

$$P(0.123 \leq P_d \leq 0.459) = 0.95$$

while the interval calculated using the binomial methodology and an Excel spreadsheet results in:

$$P(0.12279481 \leq P_d \leq 0.45889365) = 0.95$$

and the CI calculated using the normal approximation results in:

$$P(0.108 \leq P_d \leq 0.158) = 0.95$$

The CI calculation clearly provides more precision than is possible by interpreting the tables in Beyer and is much more accurate than the normal approximation. It is relatively straightforward to implement; therefore, it will be used to calculate the CIs for this validation.

Note that solving the binomial equations works only for m out of n successes while m is in the range 1 to $n-1$. For the endpoints, 0 and n , a slightly different version must be used. For 0 out of n , there is no probability associated with the lower limit; therefore, only an upper limit can be calculated. This upper limit must be based on α instead of $\alpha/2$ to ensure a consistent CI. For n out of n , the lower limit must be calculated similarly based on $\tilde{\alpha}$.

It is instructive to examine how the number of test results affects the width of the CIs. Figure 27 depicts the CIs calculated using the binomial methodology for the example above. The bar labeled "30" represents the CI for 8 detections out of 30 tests. The "90" bar represents 24 detections out of 90 tests, and the "300" bar represents 80 detections out of 300 tests. In general, the more test cases used to develop the proportion (P_d , P_t), the smaller the CI.

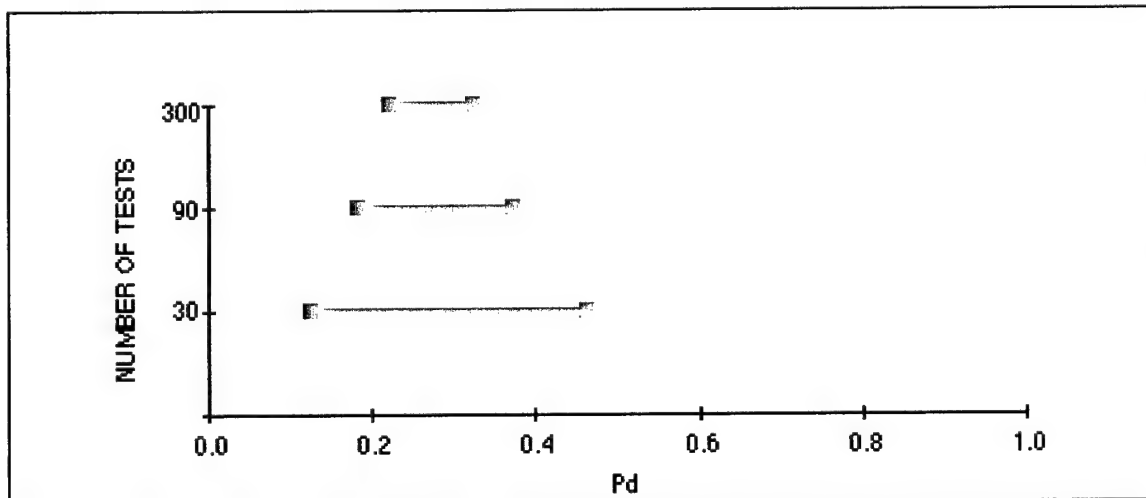


Figure 27. CI Width versus Number of Test

Another factor that affects the width of the CI is the resultant P_d for the test case. As the proportion approaches 0.5, the CI becomes wider. The smallest CIs occur as the proportion approaches low or high values (such as 0.1 or 0.9). This effect is illustrated in Figure 27. This figure shows the width of the CI determined for test results from 1/30 to 29/30, 1/90 to 89/90, and 1/300 to 299/300.

Both the number of tests, and the tested P_d have an effect on the CI width. Another important effect is on the Type II error, as will be shown below.

3.6.6.4 Type II Errors

The CI is based on the Type I error. This is the probability of rejecting a true hypothesis. A second source of errors that will be considered are Type II errors. The probability of occurrence of a Type II error is represented by β . β is the probability of accepting a false hypothesis; therefore, it is the probability that the MDTP result is within the CI, but should be outside the CI. Again, this error is depicted in Figure 26. The β error can be calculated based on how large a discrepancy is acceptable between MDTP results and test results.

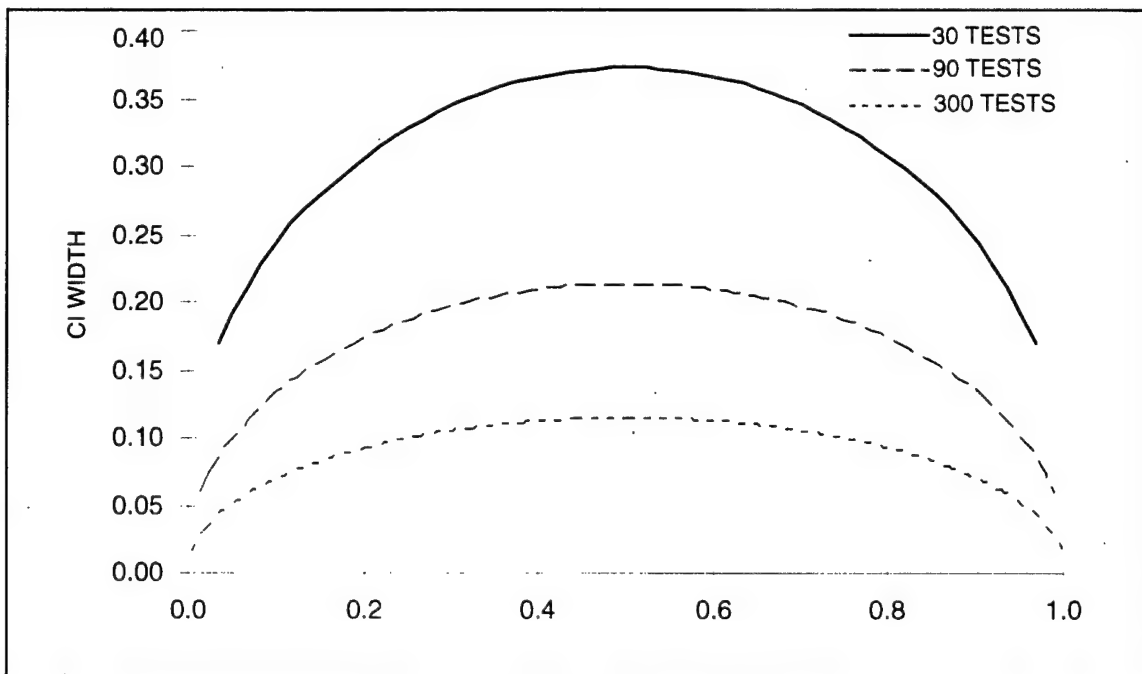


Figure 28. CI Width versus P_d

Given a true value for the P_d , it is possible to calculate the probability of accepting a false hypothesis based on the CI calculated from the test results. Given a lower and upper limit of θ_a and θ_b , the probability of accepting a false hypothesis, β , is given by:

$$\beta = P[\theta_b \geq \bar{P}d \geq \theta_a]$$

where $\bar{P}d$ is the true probability of detection. Calculation of β is then made by:

$$\beta = P[\bar{P}d \leq \theta_b] - P[\bar{P}d \leq \theta_a]$$

Assuming a normal approximation to the binomial distribution, a Z value for each of the above probabilities can be calculated by:

$$Z = \frac{\theta - \bar{P}d}{\sqrt{\frac{\bar{P}d(1 - \bar{P}d)}{n}}}$$

Using these Z values, the probabilities to use can be determined with a standard normal distribution table; or with an Excel spreadsheet function. Thus, β can be calculated.

For small sample sizes, determination of β must be based on the binomial distribution. All of the equations above are valid. Determination of the probabilities in the equation for β above (accepting a false hypothesis) is somewhat more difficult when the binomial distribution must be used. This is primarily because the binomial distribution is discrete, whereas the normal distribution is continuous. To determine β , $\bar{P}d$ is used as the mean of the binomial distribution. The number of trials, n , is the same as the number of tests used to develop the CI. The question becomes: what is the number of successes in the cumulative binomial probability equation? The number of successes is:

$$s_a = \text{int}(\theta_a n) \text{ and } s_b = \text{int}(\theta_b n)$$

The calculation of β then becomes:

$$\beta = \sum_{x=0}^{s_b} \binom{n}{x} \bar{P}_d^x (1 - \bar{P}_d)^{n-x} - \sum_{x=0}^{s_a} \binom{n}{x} \bar{P}_d^x (1 - \bar{P}_d)^{n-x}$$

This is a straightforward calculation in a spreadsheet using the previously described functions. Plotting the β error for all possible values of \bar{P}_d results in a curve known as the operating characteristic (OC) curve. Figure 29 shows the OC curve calculated for the example problem previously described. This curve shows that as the true P_d gets farther from the test P_d used to develop the CI, the probability of accepting that the true P_d is within the CI decreases. This curve yields a way of bounding the accuracy of the tested P_d .

As can be seen in Figure 29 as the number of tests increases, the range of P_d with a high β error decreases. It is possible to say that the probability of accepting the hypothesis that the true P_d is within the CI when it is not becomes high only as the true P_d is very close to the tested P_d . From this figure, it can be seen that if it is desirable to detect a shift of 0.1 in the P_d , then the probability of making a β error is very small, ~0.01.

For this validation, a minimum detectable difference between the MDTP P_d and the test P_d will be selected. From this difference, the β error will be calculated and identified in the table of results for each comparison.

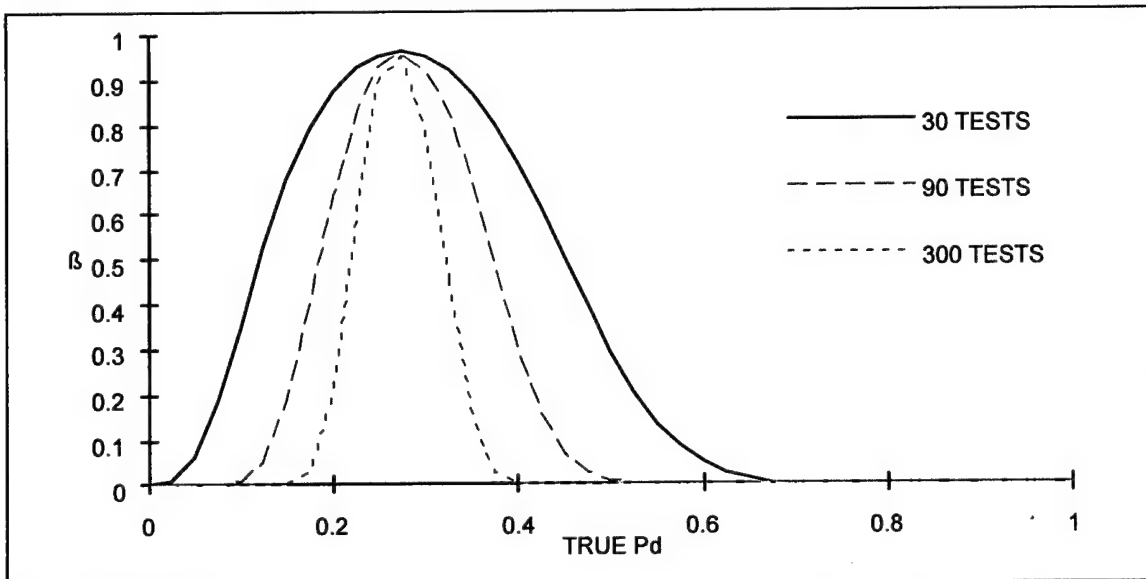


Figure 29. Effect of Number of Tests on OC Curve

3.6.6.5 DISCREPANCY ANALYSIS

It is impossible to predict all sources of error that would cause validation discrepancies. This subsection briefly introduces several potential sources of error as given in reference 4:

1. Errors in input data,
2. Errors in procedure or use of the model,
3. Errors in interpretation of results,
4. Errors in programming, and
5. Errors in design (algorithms).

The error analysis will examine, in the order listed above, the respective errors to determine if they are systemic, random, or single point. It is important to note that usage and programming errors will be examined prior to algorithm execution.

A source for error that falls under item 2 (above) is the fact that all of the measurements are taken under test conditions, and that there are multiple looks over the same vehicles and terrain. A modeling assumption is that each of the looks is uncorrelated with prior looks. This assumption will be examined during data reduction to test its validity.

As seen in Figure 24 there is a feedback loop in the validation process. This represents examination of errors and their sources and modification of MDTP inputs or algorithms to more closely represent the test results.

The support the tracker performance methodology and the validation plan, a generic tracker must be identified and used as the actual tracker. Several portions of this report allude to the use of a tracker, but are left ambiguous. The next section details the actual tracker that will be used to support the Phase II effort.

4. Tracker Algorithm

A Modular Framework for Algorithm Development and Evaluation (MFADE) and the Ground Attack Target Engagement (GATE) algorithm was recently developed the Aviation and Missile Research, Development, and Engineering Center (AMRDEC), IR Branch. This effort was performed by Dynetics and it integrated algorithms for tracking ground targets. Initially, a Hot Spot, Bayesian, and Feature-Based Correlation (FBC) algorithms were to be considered for inclusion in the GATE algorithm

MFADE can be run from its Graphic User Interface (GUI) or by using a command line version. It has hooks for acquisition, small-target, mid-course, and terminal algorithms and can support multi-channel algorithms to include hooks for data fusion. MFADE is implemented in a modular fashion to accommodate growth and expansion in the future. The modular design also can support insertion of real image data as well as integration with simulations that include seekers and/or scene generators. The GUI is focused on Microsoft OS, but all other code was developed to ANSI standards to maximize the portability to other computer platforms. MFADE is written in C++ and

calls many subroutines that are in C. Lastly, there are hooks for interfacing with 6-DOF models or external data sources (e.g. gimbal data, telemetry, range to go, etc.).

The primary algorithm within MFADE is the GATE algorithm which consists of a combination of the Anti-Median Hot Spot (AMHS) track algorithm, the Anti-Median Geometric Centroid (AMGC) track algorithm, a re-centering algorithm, and the Feature Based Correlation (FBC) track algorithm. The primary mode for the algorithm is to start in the AMHS tracker. The imagery is filtered using an Anti-Median (AM) filter of a sub-image around the target area. The AM filter tends to enhance hot and cold spots on the target while suppressing extended bodies such as roads, poles, trees, and so on. The GATE algorithm continues in the AMHS mode, each time checking to see if there is a predominate HS (in the AM filtered image) that is much higher than the surrounding background. The HS inside of the track box must be 7 background sigmas above the mean background level (measured in a background box surrounding the track box). If the HS intensity ever falls below this level, the GATE will transition to a re-centering algorithm then to a Sobel AMGC algorithm.

The re-centering algorithm is accomplished using a Sobel Geometric Centroid (GC) routine. First, the image is filtered using a Sobel routine. The Sobel filter is a gradient operator that enhances the rate of change in the original imagery, which accentuates the edges or high frequency content of the image. The idea is to highlight the target edges before performing a GC track on the image. This is repeated for 25 consecutive images in an attempt to walk the track gate onto the center of the target if it had previously been offset because of AMHS tracking on a hot spot. On each frame, the image is filtered with the Sobel filter, then the top 12% of the pixels within the track gate are used to geometrically center the new track box. Note that this re-centering algorithm is used again in the transition to FBC from either the AMHS or the AMGC.

The Sobel AMGC algorithm is a tracker that operates on an image that is first Sobel filtered, then AM filtered, as its name implies. The Sobel AMGC algorithm has demonstrated capability to track targets that do not have a prominent hot spot on them, such as the cold side (right side) of a T-72.

The final track algorithm that is invoked is the FBC algorithm. A transition to a re-centering algorithm is performed first followed by the FBC algorithm. The transition occurs when the track box has more than 750 pixels on target. For the AMS seeker in narrow field of view, this occurs at a slant range of approximately 1000 meters. The FBC algorithm uses a reference template to correlate with each succeeding image to locate the target and center the track box on the target. Additionally, the FBC uses a feature extraction and a scoremap to allow processing and correlating on a smaller portion of the image about the track box that incorporates only features that are persistent frame-to-frame. This results in fewer calculations and completing the processing more quickly. The FBC algorithm in GATE has been improved from its predecessor in ISAT for better performance in endgame. The template is updated more often, and the template is magnified, as needed, when the track box is growing at high rates, such as during endgame.

The MFADE and GATE were developed as government owned and operated source code and algorithm. All results can be openly published. And since it is a robust tracker and should represent a typical tracker used for missile seeker terminal homing, it will be used as the system tracker in the methodology implemented in the Pending Phase II effort.

5. Conclusions

In conclusion, all requirements for the completion of the Phase I SBIR have been met. A large set of infrared image sequences have been identified, ground-truthed, and processed with the metrics. Several metrics have been identified and developed that will support future analysis and the Phase II effort. A modular software metric tool has been developed that will read image sequences of any format, and process the sequences with the user selected metrics. The metric tool is designed for ease of adding additional metric algorithms as they become available. A comprehensive process for taking the metric outputs and comparing them to actual tracker performance for the training of a neural network process has been defined in some detail. And a comprehensive validation plan to prove the viability of the performance model, and then ultimately the use of the tool by

the community has been identified. The actual tracker that will be used for the validation has been identified and has been approved for use. And the proposed phase I option will allow the addition of MWIR and LWIR image sequences and ground-truthing of these sequences for use in the Phase II. All processes are defined and ready to take this effort to the next level. Clearly the feasibility of a performance prediction capability for auto-tracker and ATD systems has been demonstrated and justifies the continuation and award of the Phase II effort.

REFERENCES

- ¹ Gonzalez and Woods, *Digital Image Processing*, Prentice-Hall Inc., 2002.
- ² Margaret A. Phillips and S. Richard F. Sims, "A Signal to Clutter Measure for ATR Performance Comparison", U.S. Army Missile Command, Research Development and Engineering Center, Redstone Arsenal, AL 35898
- ³ Kimbel, Carrie, Mark Chambliss, Jay Griffin, Jay Lightfoot, Daniel Konkle, Jeff Todd, "Tracker Analysis and Groundtruth Tool Description," 2002 Ground Targets Modeling and Validation Conference, August 2002.
- ⁴ Shannon, Robert E., Systems Simulation, the Art and Science, Prentice-Hall, 1975 (UNCLASSIFIED).
- ⁵ Beyer, William H., Ed., CRC Standard Probability and Statistics, CRC Press, 1991 (UNCLASSIFIED).
- ⁶ Hicks, Charles R., Fundamental Concepts in the Design of Experiments, Saunders College Publishing, 1982 (UNCLASSIFIED)

Appendix A

Infrared Image Sequences

| Sensor | Filename | Conditions | | | | | | Resolution | | | | | | Sensor Sensitivity | | | | | |
|----------|---------------------------------|------------|-----------------|-------------|--------|--------------|--------------|-----------------|----------------|-----------------------|---------------|---------|------------------|--------------------|---------------------|---------------|---------------|--------------|-------|
| | | Location | Time | Time-of-Day | Season | Air Temp (F) | Air Temp (C) | Wind Speed (ft) | Wind Dir (deg) | Relative Humidity (%) | Dew Point (F) | Weather | FPA Size (Pixel) | Frame Rate (Hz) | Bit/Plane (Nyquist) | Spectral Band | IFOV (mrad) | NETD (mK) | Class |
| AMS | Checkout_r1_20031030091135.dat | RSA TA-3 | 9:11 Morning | Fall | 65 | 18 | 4 | 135 | 62% | 52 | Clear | 512x512 | 12 | 30 | better than 50 | MWIR | 1 to 2 | less than 50 | UN |
| AMS | Checkout_f2_20031030092023.dat | RSA TA-3 | 9:20 Morning | Fall | 66 | 19 | 4 | 133 | 61% | 52 | Clear | 512x512 | 12 | 30 | better than 50 | MWIR | 1 to 2 | less than 50 | UN |
| AMS | Checkout_f3_20031030092459.dat | RSA TA-3 | 9:24 Morning | Fall | 68 | 20 | 2 | 158 | 59% | 52 | Clear | 512x512 | 12 | 30 | better than 50 | MWIR | 1 to 2 | less than 50 | UN |
| AMS | Checkout_f4_20031030093349.dat | RSA TA-3 | 9:33 Morning | Fall | 68 | 20 | 2 | 158 | 59% | 53 | Clear | 512x512 | 12 | 30 | better than 50 | MWIR | 1 to 2 | less than 50 | UN |
| AMS | Checkout_f5_20031030093807.dat | RSA TA-3 | 9:38 Morning | Fall | 68 | 20 | 6 | 169 | 59% | 53 | Clear | 512x512 | 12 | 30 | better than 50 | MWIR | 1 to 2 | less than 50 | UN |
| AMS | Checkout_f6_20031030094315.dat | RSA TA-3 | 9:43 Morning | Fall | 70 | 21 | 6 | 169 | 57% | 54 | Clear | 512x512 | 12 | 30 | better than 50 | MWIR | 1 to 2 | less than 50 | UN |
| AMS | Checkout_f7_20031030094703.dat | RSA TA-3 | 9:47 Morning | Fall | 70 | 21 | 6 | 173 | 57% | 54 | Clear | 512x512 | 12 | 30 | better than 50 | MWIR | 1 to 2 | less than 50 | UN |
| AMS | Checkout_f8_20031030095229.dat | RSA TA-3 | 9:52 Morning | Fall | 70 | 21 | 7 | 170 | 57% | 54 | Clear | 512x512 | 12 | 30 | better than 50 | MWIR | 1 to 2 | less than 50 | UN |
| AMS | Checkout_f9_20031030100036.dat | RSA TA-3 | 10:00 Morning | Fall | 71 | 22 | 8 | 170 | 54% | 54 | Clear | 512x512 | 12 | 30 | better than 50 | MWIR | 1 to 2 | less than 50 | UN |
| AMS | Checkout_f10_20031030100252.dat | RSA TA-3 | 10:02 Morning | Fall | 71 | 22 | 7 | 168 | 54% | 54 | Clear | 512x512 | 12 | 30 | better than 50 | MWIR | 1 to 2 | less than 50 | UN |
| AMS | ChkOut2_f1_20031104131529.dat | RSA TA-3 | 13:15 Afternoon | Fall | 79 | 26 | 5 | 173 | 62% | 65 | Pt. Cloudy | 512x512 | 12 | 30 | better than 50 | MWIR | 1 to 2 | less than 50 | UN |
| AMS | ChkOut2_f2_20031104131847.dat | RSA TA-3 | 13:18 Afternoon | Fall | 79 | 26 | 4 | 172 | 62% | 65 | Pt. Cloudy | 512x512 | 12 | 30 | better than 50 | MWIR | 1 to 2 | less than 50 | UN |
| AMS | ChkOut2_f3_20031104132626.dat | RSA TA-3 | 13:26 Afternoon | Fall | 79 | 26 | 3 | 172 | 62% | 65 | Pt. Cloudy | 512x512 | 12 | 30 | better than 50 | MWIR | 1 to 2 | less than 50 | UN |
| AMS | ChkOut2_f4_20031104135707.dat | RSA TA-3 | 13:37 Afternoon | Fall | 79 | 26 | 4 | 172 | 62% | 65 | Pt. Cloudy | 512x512 | 12 | 30 | better than 50 | MWIR | 1 to 2 | less than 50 | UN |
| AMS | ChkOut2_f5_20031104134030.dat | RSA TA-3 | 13:40 Afternoon | Fall | 79 | 26 | 4 | 179 | 62% | 65 | Pt. Cloudy | 512x512 | 12 | 30 | better than 50 | MWIR | 1 to 2 | less than 50 | UN |
| AMS | ChkOut2_f6_20031104134558.dat | RSA TA-3 | 13:45 Afternoon | Fall | 79 | 26 | 3 | 179 | 61% | 65 | Pt. Cloudy | 512x512 | 12 | 30 | better than 50 | MWIR | 1 to 2 | less than 50 | UN |
| AMS | ChkOut2_f7_20031104135120.dat | RSA TA-3 | 13:51 Afternoon | Fall | 79 | 26 | 4 | 179 | 62% | 65 | Pt. Cloudy | 512x512 | 12 | 30 | better than 50 | MWIR | 1 to 2 | less than 50 | UN |
| AMS | ChkOut2_f8_20031104135540.dat | RSA TA-3 | 13:55 Afternoon | Fall | 79 | 26 | 4 | 173 | 62% | 65 | Cloudy | 512x512 | 12 | 30 | better than 50 | MWIR | 1 to 2 | less than 50 | UN |
| AMS | ChkOut2_f9_20031104135540.dat | RSA TA-3 | 14:00 Afternoon | Fall | 79 | 26 | 3 | 173 | 61% | 65 | Cloudy | 512x512 | 12 | 30 | better than 50 | MWIR | 1 to 2 | less than 50 | UN |
| AMS | ChkOut2_f10_20031104140543.dat | RSA TA-3 | 14:05 Afternoon | Fall | 79 | 26 | 3 | 172 | 62% | 65 | Cloudy | 512x512 | 12 | 30 | better than 50 | MWIR | 1 to 2 | less than 50 | UN |
| AMS | ChkOut2_f11_20031104140543.dat | RSA TA-3 | 14:09 Afternoon | Fall | 79 | 26 | 3 | 173 | 61% | 65 | Cloudy | 512x512 | 12 | 30 | better than 50 | MWIR | 1 to 2 | less than 50 | UN |
| AMS | ChkOut2_f12_20031104141854.dat | RSA TA-3 | 14:18 Afternoon | Fall | 79 | 26 | 3 | 171 | 62% | 65 | Cloudy | 512x512 | 12 | 30 | better than 50 | MWIR | 1 to 2 | less than 50 | UN |
| AMS | ChkOut2_f13_20031104142221.dat | RSA TA-3 | 14:22 Afternoon | Fall | 79 | 26 | 3 | 141 | 62% | 65 | Cloudy | 512x512 | 12 | 30 | better than 50 | MWIR | 1 to 2 | less than 50 | UN |
| AMS | Mission1_f1_20031113075241.dat | RSA TA-3 | 7:52 Morning | Fall | 44 | 7 | 8 | 357 | 45% | 24 | Clear | 512x512 | 12 | 30 | better than 50 | MWIR | 1 to 2 | less than 50 | UN |
| AMS | Mission1_f2_20031113080545.dat | RSA TA-3 | 8:04 Morning | Fall | 45 | 7 | 9 | 360 | 45% | 24 | Clear | 512x512 | 12 | 30 | better than 50 | MWIR | 1 to 2 | less than 50 | UN |
| AMS | Mission1_f3_20031113081213.dat | RSA TA-3 | 8:12 Morning | Fall | 45 | 7 | 9 | 351 | 44% | 24 | Clear | 512x512 | 12 | 30 | better than 50 | MWIR | 1 to 2 | less than 50 | UN |
| AMS | Mission1_f4_20031113081213.dat | RSA TA-3 | 8:21 Morning | Fall | 45 | 7 | 9 | 351 | 44% | 24 | Clear | 512x512 | 12 | 30 | better than 50 | MWIR | 1 to 2 | less than 50 | UN |
| AMS | Mission1_f5_20031113081208.dat | RSA TA-3 | 8:28 Morning | Fall | 45 | 7 | 8 | 351 | 44% | 25 | Clear | 512x512 | 12 | 30 | better than 50 | MWIR | 1 to 2 | less than 50 | UN |
| AMS | Mission1_f6_20031113082003.dat | RSA TA-3 | 8:30 Morning | Fall | 45 | 7 | 8 | 351 | 43% | 24 | Clear | 512x512 | 12 | 30 | better than 50 | MWIR | 1 to 2 | less than 50 | UN |
| AMS | Mission1_f7_20031113082024.dat | RSA TA-3 | 8:33 Morning | Fall | 45 | 7 | 8 | 351 | 43% | 24 | Clear | 512x512 | 12 | 30 | better than 50 | MWIR | 1 to 2 | less than 50 | UN |
| AMS | Mission1_f8_20031113083344.dat | RSA TA-3 | 14:03 Afternoon | Fall | 53 | 12 | 7 | 348 | 28% | 20 | Clear | 512x512 | 12 | 30 | better than 50 | MWIR | 1 to 2 | less than 50 | UN |
| AMS | Mission1_f9_20031113084626.dat | RSA TA-3 | 14:06 Afternoon | Fall | 53 | 12 | 7 | 357 | 28% | 20 | Clear | 512x512 | 12 | 30 | better than 50 | MWIR | 1 to 2 | less than 50 | UN |
| AMS | Mission1_f10_20031113084550.dat | RSA TA-3 | 14:09 Afternoon | Fall | 53 | 12 | 7 | 356 | 28% | 20 | Clear | 512x512 | 12 | 30 | better than 50 | MWIR | 1 to 2 | less than 50 | UN |
| AMS | Mission1_f11_20031113084556.dat | RSA TA-3 | 14:13 Afternoon | Fall | 53 | 12 | 7 | 354 | 27% | 19 | Clear | 512x512 | 12 | 30 | better than 50 | MWIR | 1 to 2 | less than 50 | UN |
| AMS | Mission2_f1_20031113135536.dat | RSA TA-3 | 13:50 Afternoon | Fall | 53 | 12 | 6 | 349 | 28% | 20 | Clear | 512x512 | 12 | 30 | better than 50 | MWIR | 1 to 2 | less than 50 | UN |
| AMS | Mission2_f2_20031113135937.dat | RSA TA-3 | 13:59 Afternoon | Fall | 53 | 12 | 6 | 348 | 28% | 20 | Clear | 512x512 | 12 | 30 | better than 50 | MWIR | 1 to 2 | less than 50 | UN |
| AMS | Mission2_f3_20031113130301.dat | RSA TA-3 | 14:03 Afternoon | Fall | 53 | 12 | 7 | 357 | 27% | 19 | Clear | 512x512 | 12 | 30 | better than 50 | MWIR | 1 to 2 | less than 50 | UN |
| AMS | Mission2_f4_20031113140626.dat | RSA TA-3 | 14:21 Afternoon | Fall | 53 | 12 | 7 | 356 | 27% | 19 | Clear | 512x512 | 12 | 30 | better than 50 | MWIR | 1 to 2 | less than 50 | UN |
| AMS | Mission2_f5_20031113140940.dat | RSA TA-3 | 14:24 Afternoon | Fall | 53 | 12 | 7 | 354 | 27% | 19 | Clear | 512x512 | 12 | 30 | better than 50 | MWIR | 1 to 2 | less than 50 | UN |
| AMS | Mission2_f6_20031113141717.dat | RSA TA-3 | 14:28 Afternoon | Fall | 53 | 12 | 8 | 354 | 26% | 19 | Clear | 512x512 | 12 | 30 | better than 50 | MWIR | 1 to 2 | less than 50 | UN |
| AMS | Mission2_f7_20031113141643.dat | RSA TA-3 | 14:32 Afternoon | Fall | 53 | 12 | 8 | 357 | 26% | 19 | Clear | 512x512 | 12 | 30 | better than 50 | MWIR | 1 to 2 | less than 50 | UN |
| AMS | Mission2_f8_20031113142027.dat | RSA TA-3 | 14:39 Afternoon | Fall | 53 | 12 | 7 | 354 | 26% | 19 | Clear | 512x512 | 12 | 30 | better than 50 | MWIR | 1 to 2 | less than 50 | UN |
| Seeker B | Flight03Run011.dat | RSA TA-3 | Afternoon | Winter | 50 | 10 | 1 | 5 | 79% | 44 | Cloudy | 384x384 | 14 | 30 | 25 to 50 | MWIR | less than 100 | UN | |
| Seeker B | Flight03Run012.dat | RSA TA-3 | Afternoon | Winter | 50 | 10 | 1 | 5 | 79% | 44 | Cloudy | 384x384 | 14 | 30 | 25 to 50 | MWIR | less than 100 | UN | |
| Seeker B | Flight03Run013.dat | RSA TA-3 | Afternoon | Winter | 50 | 10 | 1 | 5 | 79% | 44 | Cloudy | 384x384 | 14 | 30 | 25 to 50 | MWIR | less than 100 | UN | |
| Seeker B | Flight03Run017.dat | RSA TA-3 | Afternoon | Winter | 50 | 10 | 1 | 5 | 79% | 44 | Cloudy | 384x384 | 14 | 30 | 25 to 50 | MWIR | less than 100 | UN | |
| Seeker B | Flight03Run019.dat | RSA TA-3 | Afternoon | Winter | 50 | 10 | 1 | 5 | 79% | 44 | Cloudy | 384x384 | 14 | 30 | 25 to 50 | MWIR | less than 100 | UN | |

| Sensor | Filename | Conditions | | | | | | Resolution | | | | | | Sensor Sensitivity | | |
|----------|---------------------|------------|-----------------|-------------|--------|--------------|--------------|-----------------|----------------|-----------------------|---------------|-------------|-----------------|--------------------|---------------------|-----------|
| | | Location | Time | Time-of-Day | Season | Air Temp (F) | Air Temp (C) | Wind Speed (ft) | Wind Dir (deg) | Relative Humidity (%) | Dew Point (F) | Weather | Frame Rate (Hz) | Bit/Pixel | Frame Size (Pixels) | IFOV (mm) |
| Seeker B | Flight03Run022.dat | RSA TA-3 | Afternoon | Winter | 50 | 10 | 1 | 5 | 79% | 44 | Cloudy | 30.25 to 50 | MWIR | less than .1 | 50 to 100 | UN |
| Seeker B | Flight03Run023.dat | RSA TA-3 | Afternoon | Winter | 50 | 10 | 1 | 5 | 79% | 44 | Cloudy | 30.25 to 50 | MWIR | less than .1 | 50 to 100 | UN |
| Seeker B | Flight03Run034.dat | RSA TA-3 | Afternoon | Winter | 50 | 10 | 1 | 5 | 79% | 44 | Cloudy | 30.25 to 50 | MWIR | less than .1 | 50 to 100 | UN |
| Seeker B | Flight03Run040.dat | RSA TA-3 | Afternoon | Winter | 50 | 10 | 1 | 5 | 79% | 44 | Cloudy | 30.25 to 50 | MWIR | less than .1 | 50 to 100 | UN |
| Seeker B | Flight03Run043.dat0 | RSA TA-3 | Afternoon | Winter | 50 | 10 | 1 | 5 | 79% | 44 | Cloudy | 30.25 to 50 | MWIR | less than .1 | 50 to 100 | UN |
| Seeker B | Flight03Run044.dat | RSA TA-3 | Afternoon | Winter | 50 | 10 | 1 | 5 | 79% | 44 | Cloudy | 30.25 to 50 | MWIR | less than .1 | 50 to 100 | UN |
| Seeker B | Flight04Run006.dat | RSA TA-3 | Afternoon | Winter | 51 | 11 | 4 | 274 | 21% | 13 | Clear | 30.25 to 50 | MWIR | less than .1 | 50 to 100 | UN |
| Seeker B | Flight04Run007.dat | RSA TA-3 | Afternoon | Winter | 51 | 11 | 4 | 274 | 21% | 13 | Clear | 30.25 to 50 | MWIR | less than .1 | 50 to 100 | UN |
| Seeker B | Flight04Run011.dat | RSA TA-3 | Afternoon | Winter | 51 | 11 | 4 | 274 | 21% | 13 | Clear | 30.25 to 50 | MWIR | less than .1 | 50 to 100 | UN |
| Seeker B | Flight04Run017.dat | RSA TA-3 | Afternoon | Winter | 51 | 11 | 4 | 274 | 21% | 13 | Clear | 30.25 to 50 | MWIR | less than .1 | 50 to 100 | UN |
| Seeker B | Flight04Run019.dat | RSA TA-3 | Afternoon | Winter | 51 | 11 | 4 | 274 | 21% | 13 | Clear | 30.25 to 50 | MWIR | less than .1 | 50 to 100 | UN |
| Seeker B | Flight04Run021.dat | RSA TA-3 | Afternoon | Winter | 51 | 11 | 4 | 274 | 21% | 13 | Clear | 30.25 to 50 | MWIR | less than .1 | 50 to 100 | UN |
| Seeker B | Flight04Run031.dat | RSA TA-3 | Afternoon | Winter | 51 | 11 | 4 | 274 | 21% | 13 | Clear | 30.25 to 50 | MWIR | less than .1 | 50 to 100 | UN |
| Seeker B | Flight04Run037.dat | RSA TA-3 | Afternoon | Winter | 51 | 11 | 4 | 274 | 21% | 13 | Clear | 30.25 to 50 | MWIR | less than .1 | 50 to 100 | UN |
| Seeker B | Flight05Run028.dat | RSA TA-3 | Afternoon | Winter | 62 | 17 | 7 | 61 | 30% | 30 | Clear | 30.25 to 50 | MWIR | less than .1 | 50 to 100 | UN |
| Seeker B | Flight05Run032.dat | RSA TA-3 | Afternoon | Winter | 62 | 17 | 7 | 61 | 30% | 30 | Clear | 30.25 to 50 | MWIR | less than .1 | 50 to 100 | UN |
| Seeker B | Flight05Run035b.dat | RSA TA-3 | Afternoon | Winter | 62 | 17 | 7 | 61 | 30% | 30 | Clear | 30.25 to 50 | MWIR | less than .1 | 50 to 100 | UN |
| Seeker B | Flight05Run039.dat | RSA TA-3 | 9:36 Morning | Winter | 59 | 15 | 3 | 109 | 76% | 51 | Cloudy | 30.25 to 50 | MWIR | less than .1 | 50 to 100 | UN |
| Seeker B | Flight06Run012.dat | RSA TA-3 | 10:01 Morning | Winter | 59 | 15 | 3 | 108 | 76% | 51 | Cloudy | 30.25 to 50 | MWIR | less than .1 | 50 to 100 | UN |
| Seeker B | Flight06Run016.dat | RSA TA-3 | 10:12 Morning | Winter | 59 | 15 | 3 | 119 | 76% | 51 | Cloudy | 30.25 to 50 | MWIR | less than .1 | 50 to 100 | UN |
| Seeker B | Flight06Run024.dat | RSA TA-3 | 10:26 Morning | Winter | 59 | 15 | 3 | 107 | 75% | 51 | Cloudy | 30.25 to 50 | MWIR | less than .1 | 50 to 100 | UN |
| Seeker B | Flight06Run025.dat | RSA TA-3 | 10:30 Morning | Winter | 59 | 15 | 3 | 107 | 75% | 51 | Cloudy | 30.25 to 50 | MWIR | less than .1 | 50 to 100 | UN |
| Seeker B | Flight06Run026.dat | RSA TA-3 | 10:32 Morning | Winter | 59 | 15 | 3 | 107 | 75% | 51 | Cloudy | 30.25 to 50 | MWIR | less than .1 | 50 to 100 | UN |
| Seeker B | Flight06Run031.dat | RSA TA-3 | 10:43 Morning | Winter | 60 | 16 | 3 | 114 | 75% | 51 | Cloudy | 30.25 to 50 | MWIR | less than .1 | 50 to 100 | UN |
| Seeker B | Flight06Run034.dat | RSA TA-3 | 10:52 Morning | Winter | 60 | 16 | 3 | 114 | 75% | 51 | Cloudy | 30.25 to 50 | MWIR | less than .1 | 50 to 100 | UN |
| Seeker B | Flight06Run039.dat | RSA TA-3 | 11:04 Morning | Winter | 62 | 17 | 3 | 102 | 69% | 52 | Cloudy | 30.25 to 50 | MWIR | less than .1 | 50 to 100 | UN |
| Seeker B | Flight06Run046.dat | RSA TA-3 | 11:21 Morning | Winter | 60 | 16 | 3 | 94 | 81% | 54 | Cloudy | 30.25 to 50 | MWIR | less than .1 | 50 to 100 | UN |
| Seeker B | Flight06Run050.dat | RSA TA-3 | 11:28 Morning | Winter | 60 | 16 | 2 | 94 | 82% | 54 | Cloudy | 30.25 to 50 | MWIR | less than .1 | 50 to 100 | UN |
| Seeker B | Flight06Run052.dat | RSA TA-3 | 11:31 Morning | Winter | 60 | 16 | 2 | 94 | 82% | 54 | Cloudy | 30.25 to 50 | MWIR | less than .1 | 50 to 100 | UN |
| Seeker B | Flight06Run053.dat | RSA TA-3 | 11:34 Morning | Winter | 60 | 16 | 2 | 94 | 82% | 54 | Cloudy | 30.25 to 50 | MWIR | less than .1 | 50 to 100 | UN |
| Seeker B | Flight06Run055.dat | RSA TA-3 | 11:41 Morning | Winter | 60 | 16 | 2 | 94 | 82% | 54 | Cloudy | 30.25 to 50 | MWIR | less than .1 | 50 to 100 | UN |
| Seeker B | Flight06Run056.dat | RSA TA-3 | 11:43 Morning | Winter | 60 | 16 | 2 | 94 | 82% | 54 | Cloudy | 30.25 to 50 | MWIR | less than .1 | 50 to 100 | UN |
| Seeker B | Flight06Run079.dat | RSA TA-3 | 13:02 Afternoon | Winter | 60 | 16 | 3 | 54 | 83% | 54 | Cloudy | 30.25 to 50 | MWIR | less than .1 | 50 to 100 | UN |
| Seeker B | Flight10Run014.dat | RSA TA-3 | 20:23 Night | Winter | 39 | 4 | 3 | 19 | 99% | 37 | Clear | 30.25 to 50 | MWIR | less than .1 | 50 to 100 | UN |
| Seeker B | Flight10Run005.dat | RSA TA-3 | 21:05 Night | Winter | 39 | 4 | 3 | 19 | 99% | 37 | Clear | 30.25 to 50 | MWIR | less than .1 | 50 to 100 | UN |
| Seeker B | Flight10Run035.dat | RSA TA-3 | 21:08 Night | Winter | 39 | 4 | 3 | 19 | 99% | 37 | Clear | 30.25 to 50 | MWIR | less than .1 | 50 to 100 | UN |
| Seeker B | Flight10Run036.dat | RSA TA-3 | 21:11 Night | Winter | 39 | 4 | 3 | 19 | 99% | 37 | Clear | 30.25 to 50 | MWIR | less than .1 | 50 to 100 | UN |
| Seeker B | Flight10Run039.dat | RSA TA-3 | 21:18 Night | Winter | 39 | 4 | 3 | 19 | 99% | 37 | Clear | 30.25 to 50 | MWIR | less than .1 | 50 to 100 | UN |
| Seeker B | Flight10Run043.dat | RSA TA-3 | 21:23 Night | Winter | 39 | 4 | 3 | 19 | 99% | 37 | Clear | 30.25 to 50 | MWIR | less than .1 | 50 to 100 | UN |
| Seeker B | Flight10Run044.dat | RSA TA-3 | 21:29 Night | Winter | 39 | 4 | 3 | 19 | 99% | 37 | Clear | 30.25 to 50 | MWIR | less than .1 | 50 to 100 | UN |
| Seeker B | Flight10Run048.dat | RSA TA-3 | 21:33 Night | Winter | 39 | 4 | 3 | 19 | 99% | 37 | Clear | 30.25 to 50 | MWIR | less than .1 | 50 to 100 | UN |
| Seeker B | Flight10Run049.dat | RSA TA-3 | 21:41 Night | Winter | 39 | 4 | 3 | 19 | 99% | 37 | Clear | 30.25 to 50 | MWIR | less than .1 | 50 to 100 | UN |
| Seeker B | Flight10Run052.dat | RSA TA-3 | 21:40 Night | Winter | 39 | 4 | 3 | 19 | 99% | 37 | Clear | 30.25 to 50 | MWIR | less than .1 | 50 to 100 | UN |
| Seeker B | Flight10Run053.dat | RSA TA-3 | 22:12 Night | Winter | 39 | 4 | 3 | 19 | 99% | 37 | Clear | 30.25 to 50 | MWIR | less than .1 | 50 to 100 | UN |
| Seeker B | Flight10Run054.dat | RSA TA-3 | 22:16 Night | Winter | 39 | 4 | 3 | 19 | 99% | 37 | Clear | 30.25 to 50 | MWIR | less than .1 | 50 to 100 | UN |
| Seeker B | Flight10Run056.dat | RSA TA-3 | 22:22 Night | Winter | 39 | 4 | 3 | 19 | 99% | 37 | Clear | 30.25 to 50 | MWIR | less than .1 | 50 to 100 | UN |
| Seeker B | Flight10Run057.dat | RSA TA-3 | 22:30 Night | Winter | 39 | 4 | 3 | 19 | 99% | 37 | Clear | 30.25 to 50 | MWIR | less than .1 | 50 to 100 | UN |
| Seeker B | Flight10Run038.dat | RSA TA-3 | 22:45 Night | Winter | 39 | 4 | 3 | 19 | 99% | 37 | Clear | 30.25 to 50 | MWIR | less than .1 | 50 to 100 | UN |
| Seeker B | Flight10Run047.dat | RSA TA-3 | 23:15 Night | Winter | 39 | 4 | 3 | 19 | 99% | 37 | Clear | 30.25 to 50 | MWIR | less than .1 | 50 to 100 | UN |
| Seeker B | Flight10Run059.dat | RSA TA-3 | 23:15 Night | Winter | 39 | 4 | 3 | 19 | 99% | 37 | Clear | 30.25 to 50 | MWIR | less than .1 | 50 to 100 | UN |

| Sensor | Filename | Conditions | | | | | | | | | | Resolution | | | | | | Sensor Sensitivity | |
|----------|--------------------|------------|-----------------|-------------|--------------|--------------|-----------------|----------------|-----------------------|---------------|---------|------------------|-----------------|-------------------------|----------------|------------|--------------|--------------------|--|
| | | Location | Time | Time-of-Day | Air Temp (F) | Air Temp (C) | Wind Speed (ft) | Wind Dir (deg) | Relative Humidity (%) | Dew Point (F) | Weather | FPA Size (Pixel) | Frame Rate (Hz) | MTF (% at Half Nyquist) | Spectral Band | FOV (mrad) | NETT (mK) | Class | |
| Seeker B | Flight1run004.dat | RSA TA-3 | 9:25 Morning | Winter | 47 | 8 | 3 | 238 | 95% | 46 | Clear | 384 x 512 | 14 | 30 | 25 to 50 | MWIR | less than .1 | 50 to 100 | |
| Seeker B | Flight1run014.dat | RSA TA-3 | 10:05 Morning | Winter | 47 | 8 | 3 | 15 | 94% | 46 | Clear | 384 x 512 | 14 | 30 | 25 to 50 | MWIR | less than .1 | 50 to 100 | |
| Seeker B | Flight1run017.dat | RSA TA-3 | 10:16 Morning | Winter | 47 | 8 | 3 | 15 | 94% | 45 | Clear | 384 x 512 | 14 | 30 | 25 to 50 | MWIR | less than .1 | 50 to 100 | |
| Seeker B | Flight1run020.dat | RSA TA-3 | 10:20 Morning | Winter | 47 | 8 | 3 | 15 | 94% | 45 | Clear | 384 x 512 | 14 | 30 | 25 to 50 | MWIR | less than .1 | 50 to 100 | |
| Seeker B | Flight1run022.dat | RSA TA-3 | 10:40 Morning | Winter | 47 | 8 | 4 | 21 | 93% | 45 | Clear | 384 x 512 | 14 | 30 | 25 to 50 | MWIR | less than .1 | 50 to 100 | |
| Seeker B | Flight1run027.dat | RSA TA-3 | 10:45 Morning | Winter | 47 | 8 | 3 | 14 | 93% | 45 | Clear | 384 x 512 | 14 | 30 | 25 to 50 | MWIR | less than .1 | 50 to 100 | |
| Seeker B | Flight1run030.dat | RSA TA-3 | 11:23 Morning | Winter | 47 | 8 | 2 | 11 | 89% | 44 | Clear | 384 x 512 | 14 | 30 | 25 to 50 | MWIR | less than .1 | 50 to 100 | |
| Seeker B | Flight1run010.dat | RSA TA-3 | 11:40 Morning | Winter | 47 | 8 | 2 | 4 | 89% | 44 | Clear | 384 x 512 | 14 | 30 | 25 to 50 | MWIR | less than .1 | 50 to 100 | |
| Seeker B | Flight1run012.dat | RSA TA-3 | 11:50 Morning | Winter | 47 | 8 | 2 | 4 | 89% | 44 | Clear | 384 x 512 | 14 | 30 | 25 to 50 | MWIR | less than .1 | 50 to 100 | |
| Seeker B | Flight1run017.dat | RSA TA-3 | 12:00 Afternoon | Winter | 47 | 8 | 2 | 13 | 87% | 44 | Clear | 384 x 512 | 14 | 30 | 25 to 50 | MWIR | less than .1 | 50 to 100 | |
| Seeker B | Flight1run025.dat | RSA TA-3 | 12:10 Afternoon | Winter | 47 | 8 | 1 | 21 | 85% | 43 | Clear | 384 x 512 | 14 | 30 | 25 to 50 | MWIR | less than .1 | 50 to 100 | |
| Seeker B | Flight1run026.dat | RSA TA-3 | 12:25 Afternoon | Winter | 47 | 8 | 2 | 9 | 85% | 43 | Clear | 384 x 512 | 14 | 30 | 25 to 50 | MWIR | less than .1 | 50 to 100 | |
| Seeker B | Flight1run028.dat | RSA TA-3 | 12:35 Afternoon | Winter | 47 | 8 | 2 | 9 | 85% | 43 | Clear | 384 x 512 | 14 | 30 | 25 to 50 | MWIR | less than .1 | 50 to 100 | |
| Seeker B | Flight1run032.dat | RSA TA-3 | 12:50 Afternoon | Winter | 47 | 8 | 3 | 26 | 85% | 42 | Clear | 384 x 512 | 14 | 30 | 25 to 50 | MWIR | less than .1 | 50 to 100 | |
| Seeker B | Flight1run045.dat | RSA TA-3 | 13:12 Afternoon | Winter | 47 | 8 | 3 | 13 | 87% | 43 | Clear | 384 x 512 | 14 | 30 | 25 to 50 | MWIR | less than .1 | 50 to 100 | |
| AMS | BMissionCru19.dat | RSA TA-3 | Afternoon | Winter | 50 | 10 | 1 | 5 | 79% | 44 | Cloudy | 384 x 512 | 12 | 30 | better than 50 | MWIR | less than .1 | 50 to 100 | |
| AMS | BMissionCru10.dat | RSA TA-3 | Afternoon | Winter | 50 | 10 | 1 | 5 | 79% | 44 | Cloudy | 512 x 512 | 12 | 30 | better than 50 | MWIR | less than .1 | 50 to 100 | |
| AMS | BMissionCru11.dat | RSA TA-3 | Afternoon | Winter | 50 | 10 | 1 | 5 | 79% | 44 | Cloudy | 512 x 512 | 12 | 30 | better than 50 | MWIR | less than .1 | 50 to 100 | |
| AMS | BMissionCru10a.dat | RSA TA-3 | Afternoon | Winter | 50 | 10 | 1 | 5 | 79% | 44 | Cloudy | 512 x 512 | 12 | 30 | better than 50 | MWIR | less than .1 | 50 to 100 | |
| AMS | BMissionCru11a.dat | RSA TA-3 | Afternoon | Winter | 50 | 10 | 1 | 5 | 79% | 44 | Cloudy | 512 x 512 | 12 | 30 | better than 50 | MWIR | less than .1 | 50 to 100 | |
| AMS | BMissionCru13.dat | RSA TA-3 | Afternoon | Winter | 50 | 10 | 1 | 5 | 79% | 44 | Cloudy | 512 x 512 | 12 | 30 | better than 50 | MWIR | less than .1 | 50 to 100 | |
| AMS | BMissionCru14.dat | RSA TA-3 | Afternoon | Winter | 50 | 10 | 1 | 5 | 79% | 44 | Cloudy | 512 x 512 | 12 | 30 | better than 50 | MWIR | less than .1 | 50 to 100 | |
| AMS | BMissionCru15.dat | RSA TA-3 | Afternoon | Winter | 50 | 10 | 1 | 5 | 79% | 44 | Cloudy | 512 x 512 | 12 | 30 | better than 50 | MWIR | less than .1 | 50 to 100 | |
| AMS | BMissionCru27.dat | RSA TA-3 | Afternoon | Winter | 50 | 10 | 1 | 5 | 79% | 44 | Cloudy | 512 x 512 | 12 | 30 | better than 50 | MWIR | less than .1 | 50 to 100 | |
| AMS | BMissionCru28.dat | RSA TA-3 | Afternoon | Winter | 50 | 10 | 1 | 5 | 79% | 44 | Cloudy | 512 x 512 | 12 | 30 | better than 50 | MWIR | less than .1 | 50 to 100 | |
| AMS | BMissionCru29.dat | RSA TA-3 | Afternoon | Winter | 50 | 10 | 1 | 5 | 79% | 44 | Cloudy | 512 x 512 | 12 | 30 | better than 50 | MWIR | less than .1 | 50 to 100 | |
| AMS | BMissionCru30.dat | RSA TA-3 | Afternoon | Winter | 50 | 10 | 1 | 5 | 79% | 44 | Cloudy | 512 x 512 | 12 | 30 | better than 50 | MWIR | less than .1 | 50 to 100 | |
| AMS | BMissionHru03.dat | RSA TA-3 | Afternoon | Winter | 51 | 11 | 4 | 274 | 21% | 13 | Clear | 512 x 512 | 12 | 30 | better than 50 | MWIR | less than .1 | 50 to 100 | |
| AMS | BMissionHru04.dat | RSA TA-3 | Afternoon | Winter | 51 | 11 | 4 | 274 | 21% | 13 | Clear | 512 x 512 | 12 | 30 | better than 50 | MWIR | less than .1 | 50 to 100 | |
| AMS | BMissionHru05.dat | RSA TA-3 | Afternoon | Winter | 51 | 11 | 4 | 274 | 21% | 13 | Clear | 512 x 512 | 12 | 30 | better than 50 | MWIR | less than .1 | 50 to 100 | |
| AMS | BMissionHru06.dat | RSA TA-3 | Afternoon | Winter | 51 | 11 | 4 | 274 | 21% | 13 | Clear | 512 x 512 | 12 | 30 | better than 50 | MWIR | less than .1 | 50 to 100 | |
| AMS | BMissionHru09.dat | RSA TA-3 | Afternoon | Winter | 51 | 11 | 4 | 274 | 21% | 13 | Clear | 512 x 512 | 12 | 30 | better than 50 | MWIR | less than .1 | 50 to 100 | |
| AMS | BMissionHru10.dat | RSA TA-3 | Afternoon | Winter | 51 | 11 | 4 | 274 | 21% | 13 | Clear | 512 x 512 | 12 | 30 | better than 50 | MWIR | less than .1 | 50 to 100 | |
| AMS | BMissionHru11.dat | RSA TA-3 | Afternoon | Winter | 51 | 11 | 4 | 274 | 21% | 13 | Clear | 512 x 512 | 12 | 30 | better than 50 | MWIR | less than .1 | 50 to 100 | |
| AMS | BMissionHru14.dat | RSA TA-3 | 9:56 Morning | Winter | 59 | 15 | 3 | 109 | 76% | 51 | Cloudy | 512 x 512 | 12 | 30 | better than 50 | MWIR | less than .1 | 50 to 100 | |
| AMS | BMissionHru15.dat | RSA TA-3 | 10:01 Morning | Winter | 59 | 15 | 3 | 108 | 76% | 51 | Cloudy | 512 x 512 | 12 | 30 | better than 50 | MWIR | less than .1 | 50 to 100 | |
| AMS | BMissionHru18.dat | RSA TA-3 | 10:12 Morning | Winter | 59 | 15 | 3 | 119 | 76% | 51 | Cloudy | 512 x 512 | 12 | 30 | better than 50 | MWIR | less than .1 | 50 to 100 | |
| AMS | BMissionHru19.dat | RSA TA-3 | 10:26 Morning | Winter | 59 | 15 | 3 | 107 | 75% | 51 | Cloudy | 512 x 512 | 12 | 30 | better than 50 | MWIR | less than .1 | 50 to 100 | |
| AMS | BMissionHru27.dat | RSA TA-3 | 10:30 Morning | Winter | 59 | 15 | 3 | 107 | 75% | 51 | Cloudy | 512 x 512 | 12 | 30 | better than 50 | MWIR | less than .1 | 50 to 100 | |
| AMS | BMissionDrn1.dat | RSA TA-3 | 10:32 Morning | Winter | 59 | 15 | 3 | 107 | 75% | 51 | Cloudy | 512 x 512 | 12 | 30 | better than 50 | MWIR | less than .1 | 50 to 100 | |
| AMS | BMissionDrn17.dat | RSA TA-3 | 10:43 Morning | Winter | 60 | 16 | 3 | 114 | 75% | 51 | Cloudy | 512 x 512 | 12 | 30 | better than 50 | MWIR | less than .1 | 50 to 100 | |
| AMS | BMissionDrn19.dat | RSA TA-3 | 10:52 Morning | Winter | 60 | 16 | 3 | 114 | 75% | 51 | Cloudy | 512 x 512 | 12 | 30 | better than 50 | MWIR | less than .1 | 50 to 100 | |
| AMS | BMissionDrn13.dat | RSA TA-3 | 11:04 Morning | Winter | 62 | 17 | 3 | 102 | 69% | 52 | Cloudy | 512 x 512 | 12 | 30 | better than 50 | MWIR | less than .1 | 50 to 100 | |
| AMS | BMissionDrn14.dat | RSA TA-3 | 11:26 Morning | Winter | 60 | 16 | 2 | 94 | 82% | 54 | Cloudy | 512 x 512 | 12 | 30 | better than 50 | MWIR | less than .1 | 50 to 100 | |
| AMS | BMissionDrn24a.dat | RSA TA-3 | 11:31 Morning | Winter | 60 | 16 | 2 | 94 | 82% | 54 | Cloudy | 512 x 512 | 12 | 30 | better than 50 | MWIR | less than .1 | 50 to 100 | |
| AMS | BMissionDrn24a.dat | RSA TA-3 | 11:35 Morning | Winter | 60 | 16 | 2 | 94 | 82% | 54 | Cloudy | 512 x 512 | 12 | 30 | better than 50 | MWIR | less than .1 | 50 to 100 | |

| Sensor | Filename | Conditions | | | | | | | | | | Resolution | | | | | | Sensor Sensitivity | | |
|----------|------------------------------|------------|-------|-------------|--------|--------------|--------------|-----------------|----------------|-----------------------|---------------|------------|-------------------|-----------------|------------|-----------------|-------------------------|--------------------|--------------|-----------|
| | | Location | Time | Time-of-Dry | Season | Air Temp (F) | Air Temp (C) | Wind Speed (ft) | Wind Dir (deg) | Relative Humidity (%) | Dew Point (F) | Weather | IRPA Size (Pixel) | Frame Rate (Hz) | Bits/Pixel | Frame Rate (Hz) | MTF (% at Half Nyquist) | Spectral Band | IFOV (mrad) | NETT (mK) |
| AMS | BMissionDrun27.dat | RSA TA-3 | 11:41 | Morning | Winter | 60 | 16 | 2 | 94 | 82% | 54 | Cloudy | 512 x 512 | 12 | 30 | better than 50 | MWIR | 1 to .2 | less than 50 | UN |
| AMS | BMissionDrun28.dat | RSA TA-3 | 11:43 | Morning | Winter | 60 | 16 | 2 | 94 | 82% | 54 | Cloudy | 512 x 512 | 12 | 30 | better than 50 | MWIR | 1 to .2 | less than 50 | UN |
| AMS | BMissionDrun34.dat | RSA TA-3 | 13:02 | Afternoon | Winter | 60 | 16 | 3 | 54 | 83% | 54 | Cloudy | 512 x 512 | 12 | 30 | better than 50 | MWIR | 1 to .2 | less than 50 | UN |
| AMS | NightTest4.png.dat | RSA TA-3 | 21:08 | Night | Winter | 39 | 4 | 3 | 19 | 93% | 37 | Clear | 512 x 512 | 12 | 30 | better than 50 | MWIR | 1 to .2 | less than 50 | UN |
| AMS | NightTest5.dat | RSA TA-3 | 21:11 | Night | Winter | 39 | 4 | 3 | 19 | 93% | 37 | Clear | 512 x 512 | 12 | 30 | better than 50 | MWIR | 1 to .2 | less than 50 | UN |
| AMS | NightTest6.dat | RSA TA-3 | 21:18 | Night | Winter | 39 | 4 | 3 | 19 | 93% | 37 | Clear | 512 x 512 | 12 | 30 | better than 50 | MWIR | 1 to .2 | less than 50 | UN |
| AMS | NightTest8.dat | RSA TA-3 | 21:23 | Night | Winter | 39 | 4 | 3 | 19 | 93% | 37 | Clear | 512 x 512 | 12 | 30 | better than 50 | MWIR | 1 to .2 | less than 50 | UN |
| AMS | NightTest9.dat | RSA TA-3 | 21:29 | Night | Winter | 39 | 4 | 3 | 19 | 93% | 37 | Clear | 512 x 512 | 12 | 30 | better than 50 | MWIR | 1 to .2 | less than 50 | UN |
| AMS | NightTest10.dat | RSA TA-3 | 21:33 | Night | Winter | 39 | 4 | 3 | 19 | 93% | 37 | Clear | 512 x 512 | 12 | 30 | better than 50 | MWIR | 1 to .2 | less than 50 | UN |
| AMS | NightTest11.dat | RSA TA-3 | 21:34 | Night | Winter | 39 | 4 | 3 | 19 | 93% | 37 | Clear | 512 x 512 | 12 | 30 | better than 50 | MWIR | 1 to .2 | less than 50 | UN |
| AMS | NightTest12.dat | RSA TA-3 | 21:38 | Night | Winter | 39 | 4 | 3 | 19 | 93% | 37 | Clear | 512 x 512 | 12 | 30 | better than 50 | MWIR | 1 to .2 | less than 50 | UN |
| AMS | NightTest17.dat | RSA TA-3 | 22:12 | Night | Winter | 39 | 4 | 3 | 19 | 93% | 37 | Clear | 512 x 512 | 12 | 30 | better than 50 | MWIR | 1 to .2 | less than 50 | UN |
| AMS | NightTest18.dat | RSA TA-3 | 22:16 | Night | Winter | 39 | 4 | 3 | 19 | 93% | 37 | Clear | 512 x 512 | 12 | 30 | better than 50 | MWIR | 1 to .2 | less than 50 | UN |
| AMS | NightTest20.dat | RSA TA-3 | 22:22 | Night | Winter | 39 | 4 | 3 | 19 | 93% | 37 | Clear | 512 x 512 | 12 | 30 | better than 50 | MWIR | 1 to .2 | less than 50 | UN |
| AMS | NightTest21.dat | RSA TA-3 | 22:30 | Night | Winter | 39 | 4 | 3 | 19 | 93% | 37 | Clear | 512 x 512 | 12 | 30 | better than 50 | MWIR | 1 to .2 | less than 50 | UN |
| AMS | NightTest23.dat | RSA TA-3 | 22:45 | Night | Winter | 39 | 4 | 3 | 19 | 93% | 37 | Clear | 512 x 512 | 12 | 30 | better than 50 | MWIR | 1 to .2 | less than 50 | UN |
| AMS | NightTest24.dat | RSA TA-3 | 23:15 | Night | Winter | 39 | 4 | 3 | 19 | 93% | 37 | Clear | 512 x 512 | 12 | 30 | better than 50 | MWIR | 1 to .2 | less than 50 | UN |
| AMS | BMF1.dat | RSA TA-3 | 9:25 | Morning | Winter | 47 | 8 | 3 | 258 | 98% | 46 | Clear | 512 x 512 | 12 | 30 | better than 50 | MWIR | 1 to .2 | less than 50 | UN |
| AMS | BMF4.dat | RSA TA-3 | 10:05 | Morning | Winter | 47 | 8 | 3 | 15 | 94% | 46 | Clear | 512 x 512 | 12 | 30 | better than 50 | MWIR | 1 to .2 | less than 50 | UN |
| AMS | BMF5.dat | RSA TA-3 | 10:16 | Morning | Winter | 47 | 8 | 3 | 15 | 94% | 45 | Clear | 512 x 512 | 12 | 30 | better than 50 | MWIR | 1 to .2 | less than 50 | UN |
| AMS | BMF7.dat | RSA TA-3 | 10:20 | Morning | Winter | 47 | 8 | 3 | 15 | 94% | 45 | Clear | 512 x 512 | 12 | 30 | better than 50 | MWIR | 1 to .2 | less than 50 | UN |
| AMS | BMF8.dat | RSA TA-3 | 10:30 | Morning | Winter | 47 | 8 | 4 | 21 | 93% | 45 | Clear | 512 x 512 | 12 | 30 | better than 50 | MWIR | 1 to .2 | less than 50 | UN |
| AMS | BMF19.dat | RSA TA-3 | 10:45 | Morning | Winter | 47 | 8 | 3 | 14 | 93% | 45 | Clear | 512 x 512 | 12 | 30 | better than 50 | MWIR | 1 to .2 | less than 50 | UN |
| AMS | T72Run1.dat | RSA TA-3 | 11:23 | Morning | Winter | 47 | 8 | 2 | 11 | 89% | 44 | Clear | 512 x 512 | 12 | 30 | better than 50 | MWIR | 1 to .2 | less than 50 | UN |
| AMS | T72Run3.dat | RSA TA-3 | 11:40 | Morning | Winter | 47 | 8 | 2 | 4 | 89% | 44 | Clear | 512 x 512 | 12 | 30 | better than 50 | MWIR | 1 to .2 | less than 50 | UN |
| AMS | T72Run4.dat | RSA TA-3 | 11:50 | Morning | Winter | 47 | 8 | 2 | 4 | 89% | 44 | Clear | 512 x 512 | 12 | 30 | better than 50 | MWIR | 1 to .2 | less than 50 | UN |
| AMS | T72Run7.dat | RSA TA-3 | 12:00 | Afternoon | Winter | 47 | 8 | 2 | 13 | 87% | 44 | Clear | 512 x 512 | 12 | 30 | better than 50 | MWIR | 1 to .2 | less than 50 | UN |
| AMS | T72Run10.dat | RSA TA-3 | 12:10 | Afternoon | Winter | 47 | 8 | 1 | 21 | 83% | 43 | Clear | 512 x 512 | 12 | 30 | better than 50 | MWIR | 1 to .2 | less than 50 | UN |
| AMS | T72Run11.dat | RSA TA-3 | 12:25 | Afternoon | Winter | 47 | 8 | 2 | 9 | 83% | 43 | Clear | 512 x 512 | 12 | 30 | better than 50 | MWIR | 1 to .2 | less than 50 | UN |
| AMS | T72Run13.dat | RSA TA-3 | 12:34 | Afternoon | Winter | 47 | 8 | 2 | 9 | 83% | 43 | Clear | 512 x 512 | 12 | 30 | better than 50 | MWIR | 1 to .2 | less than 50 | UN |
| AMS | T72Run17.dat | RSA TA-3 | 12:50 | Afternoon | Winter | 47 | 8 | 3 | 26 | 85% | 42 | Clear | 512 x 512 | 12 | 30 | better than 50 | MWIR | 1 to .2 | less than 50 | UN |
| AMS | T72Run19.dat | RSA TA-3 | 13:12 | Afternoon | Winter | 47 | 8 | 3 | 13 | 87% | 43 | Clear | 512 x 512 | 12 | 30 | better than 50 | MWIR | 1 to .2 | less than 50 | UN |
| Seeker B | IRFrames_flight01/run002.dat | RSA TA-3 | 13:00 | Afternoon | Spring | 72.5 | 22 | 2 | 237 | 34% | 42 | Clear | 384 x 512 | 14 | 30 | 25 to 50 | MWIR | less than 1 | 50 to 100 | UN |
| Seeker B | IRFrames_flight01/run003.dat | RSA TA-3 | 13:05 | Afternoon | Spring | 72.5 | 22 | 2 | 237 | 34% | 40 | Clear | 384 x 512 | 14 | 30 | 25 to 50 | MWIR | less than 1 | 50 to 100 | UN |
| Seeker B | IRFrames_flight01/run004.dat | RSA TA-3 | 13:10 | Afternoon | Spring | 73.1 | 23 | 3 | 353 | 33% | 42 | Clear | 384 x 512 | 14 | 30 | 25 to 50 | MWIR | less than 1 | 50 to 100 | UN |
| Seeker B | IRFrames_flight01/run005.dat | RSA TA-3 | 13:15 | Afternoon | Spring | 73.1 | 23 | 3 | 353 | 32% | 42 | Clear | 384 x 512 | 14 | 30 | 25 to 50 | MWIR | less than 1 | 50 to 100 | UN |
| Seeker B | IRFrames_flight01/run008.dat | RSA TA-3 | 13:20 | Afternoon | Spring | 73.1 | 23 | 3 | 353 | 32% | 42 | Clear | 384 x 512 | 14 | 30 | 25 to 50 | MWIR | less than 1 | 50 to 100 | UN |
| Seeker B | IRFrames_flight01/run009.dat | RSA TA-3 | 13:25 | Afternoon | Spring | 73.1 | 23 | 5 | 358 | 30% | 40 | Clear | 384 x 512 | 14 | 30 | 25 to 50 | MWIR | less than 1 | 50 to 100 | UN |
| Seeker B | IRFrames_flight01/run012.dat | RSA TA-3 | 13:30 | Afternoon | Spring | 73.5 | 22 | 5 | 358 | 30% | 40 | Clear | 384 x 512 | 14 | 30 | 25 to 50 | MWIR | less than 1 | 50 to 100 | UN |
| Seeker B | IRFrames_flight01/run015.dat | RSA TA-3 | 13:35 | Afternoon | Spring | 73.1 | 23 | 3 | 329 | 29% | 40 | Clear | 384 x 512 | 14 | 30 | 25 to 50 | MWIR | less than 1 | 50 to 100 | UN |
| Seeker B | IRFrames_flight01/run016.dat | RSA TA-3 | 13:40 | Afternoon | Spring | 73.1 | 23 | 4 | 329 | 29% | 40 | Clear | 384 x 512 | 14 | 30 | 25 to 50 | MWIR | less than 1 | 50 to 100 | UN |
| Seeker B | IRFrames_flight01/run018.dat | RSA TA-3 | 14:14 | Afternoon | Spring | 73.9 | 23 | 3 | 15 | 30% | 41 | Clear | 384 x 512 | 14 | 30 | 25 to 50 | MWIR | less than 1 | 50 to 100 | UN |
| Seeker B | IRFrames_flight01/run019.dat | RSA TA-3 | 14:20 | Afternoon | Spring | 73.9 | 23 | 3 | 15 | 30% | 41 | Clear | 384 x 512 | 14 | 30 | 25 to 50 | MWIR | less than 1 | 50 to 100 | UN |
| Seeker B | IRFrames_flight02/run020.dat | RSA TA-3 | 14:00 | Afternoon | Spring | 73.6 | 23 | 4 | 4 | 29% | 40 | Clear | 384 x 512 | 14 | 30 | 25 to 50 | MWIR | less than 1 | 50 to 100 | UN |
| Seeker B | IRFrames_flight02/run021.dat | RSA TA-3 | 14:07 | Afternoon | Spring | 73.6 | 23 | 4 | 4 | 29% | 40 | Clear | 384 x 512 | 14 | 30 | 25 to 50 | MWIR | less than 1 | 50 to 100 | UN |
| Seeker B | IRFrames_flight01/run022.dat | RSA TA-3 | 14:14 | Afternoon | Spring | 73.9 | 23 | 3 | 15 | 30% | 41 | Clear | 384 x 512 | 14 | 30 | 25 to 50 | MWIR | less than 1 | 50 to 100 | UN |
| Seeker B | IRFrames_flight01/run023.dat | RSA TA-3 | 14:20 | Afternoon | Spring | 73.9 | 23 | 3 | 15 | 30% | 41 | Clear | 384 x 512 | 14 | 30 | 25 to 50 | MWIR | less than 1 | 50 to 100 | UN |
| Seeker B | IRFrames_flight01/run024.dat | RSA TA-3 | 14:20 | Afternoon | Spring | 71.8 | 22 | 5 | 155 | 41% | 47 | Clear | 384 x 512 | 14 | 30 | 25 to 50 | MWIR | less than 1 | 50 to 100 | UN |
| Seeker B | IRFrames_flight02/run003.dat | RSA TA-3 | 10:00 | Morning | Spring | 72.6 | 23 | 4 | 135 | 40% | 47 | Clear | 384 x 512 | 14 | 30 | 25 to 50 | MWIR | less than 1 | 50 to 100 | UN |
| Seeker B | IRFrames_flight02/run004.dat | RSA TA-3 | 10:10 | Morning | Spring | 72.6 | 23 | 4 | 135 | 40% | 47 | Clear | 384 x 512 | 14 | 30 | 25 to 50 | MWIR | less than 1 | 50 to 100 | UN |

| Season | File Name | Conditions | | | | | | | | | | Resolution | | | | | | Sensor Sensitivity | |
|----------|-----------------------------|------------|-----------------|-------------|--------|--------------|--------------|-----------------|----------------|-----------------------|---------------|------------|-----------------|-----------------|----------|---------------|-----------------|--------------------|-------|
| | | Location | Time | Time-of-day | Season | Air Temp (F) | Air Temp (C) | Wind Speed (mi) | Wind Dir (deg) | Relative Humidity (%) | Dew Point (F) | Weather | FPA Size (PMSH) | Frame Rate (Hz) | Bit/Fuel | Spectral Band | IFOV (infrared) | NETT (mK) | Class |
| Seeker B | IRFrames_fight02/run007.dat | RSA TA-3 | 10:20 Morning | Spring | 72.6 | 23 | 4 | 135 | 40% | 47 | Clear | 384 x 512 | 14 | 30.25 to 50 | MWIR | less than .1 | 50 to 100 | UN | |
| Seeker B | IRFrames_fight02/run010.dat | RSA TA-3 | 10:30 Morning | Spring | 74.3 | 24 | 3 | 156 | 40% | 49 | Clear | 384 x 512 | 14 | 30.25 to 50 | MWIR | less than .1 | 50 to 100 | UN | |
| Seeker B | IRFrames_fight02/run015.dat | RSA TA-3 | 10:40 Morning | Spring | 75.4 | 24 | 3 | 156 | 38% | 48 | Clear | 384 x 512 | 14 | 30.25 to 50 | MWIR | less than .1 | 50 to 100 | UN | |
| Seeker B | IRFrames_fight02/run016.dat | RSA TA-3 | 10:50 Morning | Spring | 76.4 | 25 | 3 | 174 | 38% | 49 | Clear | 384 x 512 | 14 | 30.25 to 50 | MWIR | less than .1 | 50 to 100 | UN | |
| Seeker B | IRFrames_fight02/run017.dat | RSA TA-3 | 11:00 Morning | Spring | 76.4 | 25 | 3 | 174 | 38% | 49 | Clear | 384 x 512 | 14 | 30.25 to 50 | MWIR | less than .1 | 50 to 100 | UN | |
| Seeker B | IRFrames_fight02/run018.dat | RSA TA-3 | 11:10 Morning | Spring | 77.3 | 25 | 3 | 175 | 38% | 50 | Clear | 384 x 512 | 14 | 30.25 to 50 | MWIR | less than .1 | 50 to 100 | UN | |
| Seeker B | IRFrames_fight02/run020.dat | RSA TA-3 | 11:20 Morning | Spring | 77.8 | 25 | 3 | 148 | 38% | 51 | Clear | 384 x 512 | 14 | 30.25 to 50 | MWIR | less than .1 | 50 to 100 | UN | |
| Seeker B | IRFrames_fight02/run021.dat | RSA TA-3 | 11:30 Morning | Spring | 77.8 | 25 | 3 | 148 | 38% | 51 | Clear | 384 x 512 | 14 | 30.25 to 50 | MWIR | less than .1 | 50 to 100 | UN | |
| Seeker B | IRFrames_fight02/run027.dat | RSA TA-3 | 11:45 Morning | Spring | 78.5 | 26 | 4 | 158 | 38% | 52 | Clear | 384 x 512 | 14 | 30.25 to 50 | MWIR | less than .1 | 50 to 100 | UN | |
| Seeker B | IRFrames_fight04/run002.dat | RSA TA-3 | 8:35 Morning | Spring | 67.1 | 19 | 2 | 157 | 61% | 53 | Clear | 384 x 512 | 14 | 30.25 to 50 | MWIR | less than .1 | 50 to 100 | UN | |
| Seeker B | IRFrames_fight04/run003.dat | RSA TA-3 | 8:50 Morning | Spring | 67.1 | 19 | 2 | 157 | 61% | 53 | Clear | 384 x 512 | 14 | 30.25 to 50 | MWIR | less than .1 | 50 to 100 | UN | |
| Seeker B | IRFrames_fight04/run009.dat | RSA TA-3 | 9:00 Morning | Spring | 69.0 | 21 | 2 | 152 | 58% | 54 | Clear | 384 x 512 | 14 | 30.25 to 50 | MWIR | less than .1 | 50 to 100 | UN | |
| Seeker B | IRFrames_fight04/run013.dat | RSA TA-3 | 9:10 Morning | Spring | 69.0 | 21 | 2 | 152 | 58% | 54 | Clear | 384 x 512 | 14 | 30.25 to 50 | MWIR | less than .1 | 50 to 100 | UN | |
| Seeker B | IRFrames_fight04/run016.dat | RSA TA-3 | 9:20 Morning | Spring | 71.2 | 22 | 2 | 166 | 54% | 53 | Clear | 384 x 512 | 14 | 30.25 to 50 | MWIR | less than .1 | 50 to 100 | UN | |
| Seeker B | IRFrames_fight04/run019.dat | RSA TA-3 | 9:30 Morning | Spring | 72.4 | 22 | 3 | 177 | 53% | 54 | Clear | 384 x 512 | 14 | 30.25 to 50 | MWIR | less than .1 | 50 to 100 | UN | |
| Seeker B | IRFrames_fight04/run021.dat | RSA TA-3 | 9:40 Morning | Spring | 73.4 | 23 | 3 | 180 | 48% | 53 | Clear | 384 x 512 | 14 | 30.25 to 50 | MWIR | less than .1 | 50 to 100 | UN | |
| Seeker B | IRFrames_fight04/run024.dat | RSA TA-3 | 9:50 Morning | Spring | 73.4 | 23 | 3 | 180 | 48% | 53 | Clear | 384 x 512 | 14 | 30.25 to 50 | MWIR | less than .1 | 50 to 100 | UN | |
| Seeker B | IRFrames_fight04/run027.dat | RSA TA-3 | 10:00 Morning | Spring | 75.1 | 24 | 2 | 177 | 45% | 53 | Clear | 384 x 512 | 14 | 30.25 to 50 | MWIR | less than .1 | 50 to 100 | UN | |
| Seeker B | IRFrames_fight04/run030.dat | RSA TA-3 | 10:10 Morning | Spring | 76.6 | 25 | 1 | 176 | 44% | 53 | Clear | 384 x 512 | 14 | 30.25 to 50 | MWIR | less than .1 | 50 to 100 | UN | |
| Seeker B | IRFrames_fight04/run045.dat | RSA TA-3 | 10:25 Morning | Spring | 77.3 | 25 | 1 | 149 | 42% | 53 | Clear | 384 x 512 | 14 | 30.25 to 50 | MWIR | less than .1 | 50 to 100 | UN | |
| Seeker B | IRFrames_fight05/run002.dat | RSA TA-3 | 16:00 Afternoon | Spring | 79.4 | 26 | 10 | 177 | 31% | 47 | Pt. Cloudy | 384 x 512 | 14 | 30.25 to 50 | MWIR | less than .1 | 50 to 100 | UN | |
| Seeker B | IRFrames_fight05/run002.dat | RSA TA-3 | 16:10 Afternoon | Spring | 78.4 | 26 | 13 | 180 | 32% | 47 | Pt. Cloudy | 384 x 512 | 14 | 30.25 to 50 | MWIR | less than .1 | 50 to 100 | UN | |
| Seeker B | IRFrames_fight05/run004.dat | RSA TA-3 | 16:20 Afternoon | Spring | 78.4 | 26 | 13 | 180 | 32% | 47 | Pt. Cloudy | 384 x 512 | 14 | 30.25 to 50 | MWIR | less than .1 | 50 to 100 | UN | |
| Seeker B | IRFrames_fight05/run004.dat | RSA TA-3 | 16:30 Afternoon | Spring | 77.4 | 25 | 10 | 185 | 33% | 46 | Pt. Cloudy | 384 x 512 | 14 | 30.25 to 50 | MWIR | less than .1 | 50 to 100 | UN | |
| Seeker B | IRFrames_fight05/run005.dat | RSA TA-3 | 16:40 Afternoon | Spring | 77.4 | 25 | 10 | 185 | 33% | 46 | Pt. Cloudy | 384 x 512 | 14 | 30.25 to 50 | MWIR | less than .1 | 50 to 100 | UN | |
| Seeker B | IRFrames_fight05/run005.dat | RSA TA-3 | 16:50 Afternoon | Spring | 77.8 | 25 | 11 | 175 | 35% | 48 | Pt. Cloudy | 384 x 512 | 14 | 30.25 to 50 | MWIR | less than .1 | 50 to 100 | UN | |
| Seeker B | IRFrames_fight05/run006.dat | RSA TA-3 | 17:00 Afternoon | Spring | 78.7 | 26 | 12 | 176 | 34% | 48 | Pt. Cloudy | 384 x 512 | 14 | 30.25 to 50 | MWIR | less than .1 | 50 to 100 | UN | |
| Seeker B | IRFrames_fight05/run007.dat | RSA TA-3 | 17:02 Afternoon | Spring | 78.7 | 26 | 12 | 176 | 34% | 48 | Pt. Cloudy | 384 x 512 | 14 | 30.25 to 50 | MWIR | less than .1 | 50 to 100 | UN | |
| Seeker B | IRFrames_fight05/run011.dat | RSA TA-3 | 17:08 Afternoon | Spring | 76.6 | 25 | 11 | 172 | 36% | 48 | Pt. Cloudy | 384 x 512 | 14 | 30.25 to 50 | MWIR | less than .1 | 50 to 100 | UN | |
| Seeker B | IRFrames_fight05/run011.dat | RSA TA-3 | 17:14 Afternoon | Spring | 76.6 | 25 | 11 | 172 | 36% | 48 | Pt. Cloudy | 384 x 512 | 14 | 30.25 to 50 | MWIR | less than .1 | 50 to 100 | UN | |
| Seeker B | IRFrames_fight05/run012.dat | RSA TA-3 | 17:24 Afternoon | Spring | 78.3 | 26 | 9 | 165 | 37% | 50 | Pt. Cloudy | 384 x 512 | 14 | 30.25 to 50 | MWIR | less than .1 | 50 to 100 | UN | |
| Seeker B | IRFrames_fight05/run013.dat | RSA TA-3 | 17:36 Afternoon | Spring | 78.3 | 26 | 9 | 165 | 37% | 50 | Pt. Cloudy | 384 x 512 | 14 | 30.25 to 50 | MWIR | less than .1 | 50 to 100 | UN | |
| Seeker B | IRFrames_fight05/run014.dat | RSA TA-3 | 17:45 Afternoon | Spring | 77.5 | 25 | 8 | 178 | 37% | 50 | Pt. Cloudy | 384 x 512 | 14 | 30.25 to 50 | MWIR | less than .1 | 50 to 100 | UN | |
| Seeker B | IRFrames_fight05/run019.dat | RSA TA-3 | 17:55 Afternoon | Spring | 77.5 | 25 | 8 | 178 | 37% | 50 | Pt. Cloudy | 384 x 512 | 14 | 30.25 to 50 | MWIR | less than .1 | 50 to 100 | UN | |
| Seeker B | IRFrames_fight05/run019.dat | RSA TA-3 | 18:05 Afternoon | Spring | 77.2 | 25 | 11 | 174 | 38% | 50 | Pt. Cloudy | 384 x 512 | 14 | 30.25 to 50 | MWIR | less than .1 | 50 to 100 | UN | |
| Seeker B | IRFrames_fight05/run012.dat | RSA TA-3 | 18:13 Afternoon | Spring | 75.6 | 24 | 8 | 175 | 42% | 51 | Pt. Cloudy | 384 x 512 | 14 | 30.25 to 50 | MWIR | less than .1 | 50 to 100 | UN | |
| Seeker B | IRFrames_fight05/run013.dat | RSA TA-3 | 18:20 Afternoon | Spring | 75.6 | 24 | 8 | 175 | 42% | 51 | Pt. Cloudy | 384 x 512 | 14 | 30.25 to 50 | MWIR | less than .1 | 50 to 100 | UN | |
| Seeker B | IRFrames_fight05/run014.dat | RSA TA-3 | 18:28 Afternoon | Spring | 75.1 | 24 | 6 | 187 | 42% | 51 | Pt. Cloudy | 384 x 512 | 14 | 30.25 to 50 | MWIR | less than .1 | 50 to 100 | UN | |
| Seeker B | IRFrames_fight05/run019.dat | RSA TA-3 | 18:36 Afternoon | Spring | 75.1 | 24 | 6 | 187 | 42% | 51 | Pt. Cloudy | 384 x 512 | 14 | 30.25 to 50 | MWIR | less than .1 | 50 to 100 | UN | |
| Seeker B | IRFrames_fight05/run044.dat | RSA TA-3 | 18:45 Afternoon | Spring | 75.4 | 24 | 6 | 182 | 42% | 51 | Pt. Cloudy | 384 x 512 | 14 | 30.25 to 50 | MWIR | less than .1 | 50 to 100 | UN | |
| Seeker B | IRFrames_fight05/run044.dat | RSA TA-3 | 19:00 Morning | Spring | 61.3 | 16 | 3 | 187 | 93% | 59 | Pt. Cloudy | 384 x 512 | 14 | 30.25 to 50 | MWIR | less than .1 | 50 to 100 | UN | |
| Seeker B | IRFrames_fight05/run024.dat | RSA TA-3 | 10:08 Morning | Spring | 61.3 | 16 | 3 | 187 | 93% | 59 | Pt. Cloudy | 384 x 512 | 14 | 30.25 to 50 | MWIR | less than .1 | 50 to 100 | UN | |
| Seeker B | IRFrames_fight05/run038.dat | RSA TA-3 | 10:17 Morning | Spring | 61.6 | 16 | 3 | 188 | 94% | 60 | Pt. Cloudy | 384 x 512 | 14 | 30.25 to 50 | MWIR | less than .1 | 50 to 100 | UN | |
| Seeker B | IRFrames_fight05/run012.dat | RSA TA-3 | 10:25 Morning | Spring | 61.9 | 17 | 4 | 185 | 92% | 60 | Pt. Cloudy | 384 x 512 | 14 | 30.25 to 50 | MWIR | less than .1 | 50 to 100 | UN | |
| Seeker B | IRFrames_fight05/run014.dat | RSA TA-3 | 10:46 Morning | Spring | 61.9 | 17 | 3 | 185 | 90% | 60 | Pt. Cloudy | 384 x 512 | 14 | 30.25 to 50 | MWIR | less than .1 | 50 to 100 | UN | |
| Seeker B | IRFrames_fight05/run017.dat | RSA TA-3 | 10:53 Morning | Spring | 62.7 | 17 | 3 | 195 | 90% | 60 | Pt. Cloudy | 384 x 512 | 14 | 30.25 to 50 | MWIR | less than .1 | 50 to 100 | UN | |
| Seeker B | IRFrames_fight05/run018.dat | RSA TA-3 | 11:02 Morning | Spring | 63.5 | 18 | 4 | 192 | 88% | 60 | Pt. Cloudy | 384 x 512 | 14 | 30.25 to 50 | MWIR | less than .1 | 50 to 100 | UN | |
| Seeker B | IRFrames_fight05/run020.dat | RSA TA-3 | 11:09 Morning | Spring | 63.5 | 18 | 4 | 192 | 86% | 60 | Pt. Cloudy | 384 x 512 | 14 | 30.25 to 50 | MWIR | less than .1 | 50 to 100 | UN | |
| Seeker B | IRFrames_fight05/run021.dat | RSA TA-3 | 11:16 Morning | Spring | 64.1 | 18 | 4 | 186 | 85% | 60 | Pt. Cloudy | 384 x 512 | 14 | 30.25 to 50 | MWIR | less than .1 | 50 to 100 | UN | |

| Sensor | Filename | Conditions | | | | | | | | | | Resolution | | | | | | Sensor Sensitivity | | |
|----------|-----------------------------|------------|-------|-------------|--------|--------------|--------------|-------------------|----------------|-----------------------|---------------|------------|-----------|------------|-----------------|-------------------------|---------------|--------------------|--------------|-------|
| | | Location | Time | Time-of-Day | Season | Air Temp (F) | Air Temp (C) | Wind Speed (ft/s) | Wind Dir (deg) | Relative Humidity (%) | Dew Point (F) | Weather | FPA Size | Bits/Pixel | Frame Rate (Hz) | MTF (% at Half Nyquist) | Spectral Band | IPOV (mrad) | NIR&T (mK) | Class |
| Seeker B | IRFrames_flight06run022.dat | RSA TA-3 | 11:21 | Morning | Spring | 64.1 | 18 | 4 | 186 | 85% | 60 | Pr. Cloudy | 384 x 512 | 14 | 30 | 25 to 50 | MWIR | less than 1 | 50 to 100 | UN |
| Seeker B | IRFrames_flight06run023.dat | RSA TA-3 | 11:26 | Morning | Spring | 66.6 | 19 | 4 | 188 | 80% | 60 | Pr. Cloudy | 384 x 512 | 14 | 30 | 25 to 50 | MWIR | less than 1 | 50 to 100 | UN |
| Seeker B | IRFrames_flight06run024.dat | RSA TA-3 | 11:34 | Morning | Spring | 66.6 | 19 | 4 | 188 | 80% | 60 | Pr. Cloudy | 384 x 512 | 14 | 30 | 25 to 50 | MWIR | less than 1 | 50 to 100 | UN |
| Seeker B | IRFrames_flight06run025.dat | RSA TA-3 | 11:42 | Morning | Spring | 67.1 | 20 | 2 | 223 | 76% | 59 | Pr. Cloudy | 384 x 512 | 14 | 30 | 25 to 50 | MWIR | less than 1 | 50 to 100 | UN |
| Seeker B | IRFrames_flight06run027.dat | RSA TA-3 | 11:50 | Morning | Spring | 67.1 | 20 | 2 | 223 | 76% | 59 | Pr. Cloudy | 384 x 512 | 14 | 30 | 25 to 50 | MWIR | less than 1 | 50 to 100 | UN |
| Seeker B | IRFrames_flight06run029.dat | RSA TA-3 | 11:55 | Morning | Spring | 68.3 | 20 | 2 | 204 | 76% | 61 | Pr. Cloudy | 384 x 512 | 14 | 30 | 25 to 50 | MWIR | less than 1 | 50 to 100 | UN |
| Seeker B | IRFrames_flight06run031.dat | RSA TA-3 | 12:00 | Afternoon | Spring | 68.3 | 20 | 2 | 204 | 76% | 61 | Pr. Cloudy | 384 x 512 | 14 | 30 | 25 to 50 | MWIR | less than 1 | 50 to 100 | UN |
| Seeker A | M05_P04_T01_File002_irRaw | RSA TA-3 | 10:10 | Morning | Spring | 50.5 | 10 | 3 | 338 | 37% | 26 | Clear | 256 x 256 | 14 | 30 | 25 to 50 | MWIR | .1 to .2 | less than 50 | S |
| Seeker A | M05_P05_T01_File003_irRaw | RSA TA-3 | 10:30 | Morning | Spring | 51.3 | 11 | 3 | 309 | 32% | 23 | Clear | 256 x 256 | 14 | 30 | 25 to 50 | MWIR | .1 to .2 | less than 50 | S |
| Seeker A | M05_P06_T01_File004_irRaw | RSA TA-3 | 10:50 | Morning | Spring | 51.3 | 11 | 3 | 312 | 31% | 22 | Clear | 256 x 256 | 14 | 30 | 25 to 50 | MWIR | .1 to .2 | less than 50 | S |
| Seeker A | M05_P07_T01_File005_irRaw | RSA TA-3 | 11:10 | Morning | Spring | 52.9 | 12 | 2 | 345 | 30% | 23 | Clear | 256 x 256 | 14 | 30 | 25 to 50 | MWIR | .1 to .2 | less than 50 | S |
| Seeker A | M05_P08_T01_File006_irRaw | RSA TA-3 | 11:30 | Morning | Spring | 53.1 | 12 | 3 | 323 | 30% | 23 | Clear | 256 x 256 | 14 | 30 | 25 to 50 | MWIR | .1 to .2 | less than 50 | S |
| Seeker A | M05_P12_T01_File010_irRaw | RSA TA-3 | 11:50 | Morning | Spring | 54.0 | 12 | 3 | 290 | 30% | 24 | Clear | 256 x 256 | 14 | 30 | 25 to 50 | MWIR | .1 to .2 | less than 50 | S |
| Seeker A | M05_P13_T01_File011_irRaw | RSA TA-3 | 12:10 | Afternoon | Spring | 54.3 | 12 | 3 | 310 | 30% | 24 | Clear | 256 x 256 | 14 | 30 | 25 to 50 | MWIR | .1 to .2 | less than 50 | S |
| Seeker A | M06_P10_T01_File001_irRaw | RSA TA-3 | 16:20 | Afternoon | Spring | 74.3 | 23 | 197 | 28% | 40 | Clear | 256 x 256 | 14 | 30 | 25 to 50 | MWIR | .1 to .2 | less than 50 | S | |
| Seeker A | M06_P11_T01_File002_irRaw | RSA TA-3 | 16:40 | Afternoon | Spring | 73.8 | 23 | 5 | 197 | 28% | 40 | Clear | 256 x 256 | 14 | 30 | 25 to 50 | MWIR | .1 to .2 | less than 50 | S |
| Seeker A | M06_P12_T01_File003_irRaw | RSA TA-3 | 17:00 | Afternoon | Spring | 72.6 | 23 | 5 | 197 | 28% | 40 | Clear | 256 x 256 | 14 | 30 | 25 to 50 | MWIR | .1 to .2 | less than 50 | S |
| Seeker A | M07_P06_T01_File004_irRaw | RSA TA-3 | 17:30 | Afternoon | Spring | 71.8 | 22 | 6 | 190 | 38% | 45 | Clear | 256 x 256 | 14 | 30 | 25 to 50 | MWIR | .1 to .2 | less than 50 | S |
| Seeker A | M08_P03_T01_File001_irRaw | RSA TA-3 | 8:40 | Morning | Spring | 67.4 | 12 | 8 | 182 | 73% | 59 | Cloudy | 256 x 256 | 14 | 30 | 25 to 50 | MWIR | .1 to .2 | less than 50 | S |
| Seeker A | M08_P10_T01_File002_irRaw | RSA TA-3 | 8:56 | Morning | Spring | 68.3 | 20 | 8 | 184 | 70% | 58 | Cloudy | 256 x 256 | 14 | 30 | 25 to 50 | MWIR | .1 to .2 | less than 50 | S |
| Seeker A | M08_P11_T01_File003_irRaw | RSA TA-3 | 9:12 | Morning | Spring | 69.4 | 21 | 5 | 201 | 67% | 58 | Cloudy | 256 x 256 | 14 | 30 | 25 to 50 | MWIR | .1 to .2 | less than 50 | S |
| Seeker A | M08_P12_T01_File004_irRaw | RSA TA-3 | 9:35 | Morning | Spring | 69.0 | 21 | 7 | 180 | 68% | 58 | Cloudy | 256 x 256 | 14 | 30 | 25 to 50 | MWIR | .1 to .2 | less than 50 | S |
| Seeker A | M08_P07_T01_File005_irRaw | RSA TA-3 | 9:50 | Morning | Spring | 69.8 | 21 | 8 | 177 | 66% | 58 | Cloudy | 256 x 256 | 14 | 30 | 25 to 50 | MWIR | .1 to .2 | less than 50 | S |
| Seeker A | M09_P01_T01_File001_irRaw | RSA TA-3 | 10:16 | Afternoon | Spring | 72.3 | 22 | 8 | 189 | 66% | 61 | Cloudy | 256 x 256 | 14 | 30 | 25 to 50 | MWIR | .1 to .2 | less than 50 | S |
| Seeker A | M09_P02_T01_File002_irRaw | RSA TA-3 | 10:30 | Afternoon | Spring | 71.7 | 22 | 9 | 183 | 68% | 61 | Cloudy | 256 x 256 | 14 | 30 | 25 to 50 | MWIR | .1 to .2 | less than 50 | S |
| Seeker A | M09_P03_T01_File003_irRaw | RSA TA-3 | 10:46 | Afternoon | Spring | 71.3 | 22 | 7 | 185 | 70% | 61 | Cloudy | 256 x 256 | 14 | 30 | 25 to 50 | MWIR | .1 to .2 | less than 50 | S |
| Seeker A | M09_P04_T01_File004_irRaw | RSA TA-3 | 11:02 | Afternoon | Spring | 70.8 | 22 | 7 | 183 | 72% | 62 | Cloudy | 256 x 256 | 14 | 30 | 25 to 50 | MWIR | .1 to .2 | less than 50 | S |
| Seeker A | M09_P05_T01_File005_irRaw | RSA TA-3 | 11:22 | Afternoon | Spring | 70.8 | 22 | 8 | 188 | 72% | 62 | Cloudy | 256 x 256 | 14 | 30 | 25 to 50 | MWIR | .1 to .2 | less than 50 | S |
| Seeker A | M09_P06_T01_File006_irRaw | RSA TA-3 | 11:45 | Afternoon | Spring | 69.5 | 21 | 5 | 191 | 76% | 62 | Cloudy | 256 x 256 | 14 | 30 | 25 to 50 | MWIR | .1 to .2 | less than 50 | S |
| Seeker A | M09_P07_T01_File007_irRaw | RSA TA-3 | 12:00 | Afternoon | Spring | 69.0 | 21 | 6 | 177 | 74% | 62 | Cloudy | 256 x 256 | 14 | 30 | 25 to 50 | MWIR | .1 to .2 | less than 50 | S |
| Seeker A | M09_P08_T01_File008_irRaw | RSA TA-3 | 12:15 | Afternoon | Spring | 68.7 | 20 | 6 | 17 | 74% | 39 | Cloudy | 256 x 256 | 14 | 30 | 25 to 50 | MWIR | .1 to .2 | less than 50 | S |
| Seeker A | M09_P09_T01_File009_irRaw | RSA TA-3 | 12:30 | Afternoon | Spring | 67.1 | 20 | 5 | 14 | 38% | 40 | Pr. Cloudy | 256 x 256 | 14 | 30 | 25 to 50 | MWIR | .1 to .2 | less than 50 | S |
| Seeker A | M09_P10_T01_File010_irRaw | RSA TA-3 | 12:45 | Afternoon | Spring | 68.7 | 20 | 6 | 186 | 79% | 62 | Cloudy | 256 x 256 | 14 | 30 | 25 to 50 | MWIR | .1 to .2 | less than 50 | S |
| Seeker A | M09_P11_T01_File011_irRaw | RSA TA-3 | 13:00 | Afternoon | Spring | 70.4 | 21 | 6 | 20 | 37% | 43 | Pr. Cloudy | 256 x 256 | 14 | 30 | 25 to 50 | MWIR | .1 to .2 | less than 50 | S |
| Seeker A | M09_P12_T01_File012_irRaw | RSA TA-3 | 13:15 | Afternoon | Spring | 69.9 | 21 | 6 | 188 | 72% | 41 | Pr. Cloudy | 256 x 256 | 14 | 30 | 25 to 50 | MWIR | .1 to .2 | less than 50 | S |
| Seeker A | M09_P13_T01_File013_irRaw | RSA TA-3 | 13:30 | Afternoon | Spring | 68.7 | 20 | 5 | 360 | 42% | 41 | Pr. Cloudy | 256 x 256 | 14 | 30 | 25 to 50 | MWIR | .1 to .2 | less than 50 | S |
| Seeker A | M10_P06_T01_File001_irRaw | RSA TA-3 | 13:45 | Afternoon | Spring | 63.6 | 18 | 5 | 2 | 47% | 43 | Pr. Cloudy | 256 x 256 | 14 | 30 | 25 to 50 | MWIR | .1 to .2 | less than 50 | S |
| Seeker A | M10_P07_T01_File002_irRaw | RSA TA-3 | 14:00 | Afternoon | Spring | 63.6 | 18 | 5 | 2 | 47% | 43 | Pr. Cloudy | 256 x 256 | 14 | 30 | 25 to 50 | MWIR | .1 to .2 | less than 50 | S |
| Seeker A | M10_P08_T01_File003_irRaw | RSA TA-3 | 14:15 | Afternoon | Spring | 73.7 | 23 | 4 | 152 | 61% | 46 | Pr. Cloudy | 256 x 256 | 14 | 30 | 25 to 50 | MWIR | .1 to .2 | less than 50 | S |
| Seeker A | M10_P09_T01_File004_irRaw | RSA TA-3 | 14:30 | Afternoon | Spring | 62.3 | 17 | 5 | 1 | 55% | 61 | Cloudy | 256 x 256 | 14 | 30 | 25 to 50 | MWIR | .1 to .2 | less than 50 | S |
| Seeker A | M10_P10_T01_File005_irRaw | RSA TA-3 | 14:45 | Afternoon | Spring | 73.0 | 23 | 6 | 167 | 61% | 59 | Cloudy | 256 x 256 | 14 | 30 | 25 to 50 | MWIR | .1 to .2 | less than 50 | S |
| Seeker A | M10_P11_T01_File006_irRaw | RSA TA-3 | 15:00 | Afternoon | Spring | 64.5 | 18 | 5 | 360 | 42% | 59 | Cloudy | 256 x 256 | 14 | 30 | 25 to 50 | MWIR | .1 to .2 | less than 50 | S |
| Seeker A | M10_P12_T01_File007_irRaw | RSA TA-3 | 15:15 | Afternoon | Spring | 63.6 | 18 | 5 | 147 | 61% | 59 | Cloudy | 256 x 256 | 14 | 30 | 25 to 50 | MWIR | .1 to .2 | less than 50 | S |
| Seeker A | M10_P13_T01_File008_irRaw | RSA TA-3 | 15:30 | Afternoon | Spring | 63.6 | 18 | 5 | 152 | 61% | 60 | Cloudy | 256 x 256 | 14 | 30 | 25 to 50 | MWIR | .1 to .2 | less than 50 | S |
| Seeker A | M10_P14_T01_File009_irRaw | RSA TA-3 | 15:45 | Afternoon | Spring | 63.6 | 18 | 5 | 152 | 61% | 60 | Cloudy | 256 x 256 | 14 | 30 | 25 to 50 | MWIR | .1 to .2 | less than 50 | S |
| Seeker A | M10_P15_T01_File010_irRaw | RSA TA-3 | 16:00 | Afternoon | Spring | 63.6 | 18 | 5 | 152 | 61% | 60 | Cloudy | 256 x 256 | 14 | 30 | 25 to 50 | MWIR | .1 to .2 | less than 50 | S |
| Seeker A | M11_P01_T01_File001_irRaw | RSA TA-3 | 14:01 | Afternoon | Spring | 73.2 | 23 | 5 | 147 | 61% | 59 | Cloudy | 256 x 256 | 14 | 30 | 25 to 50 | MWIR | .1 to .2 | less than 50 | S |
| Seeker A | M11_P02_T01_File002_irRaw | RSA TA-3 | 14:16 | Afternoon | Spring | 73.7 | 23 | 4 | 152 | 61% | 60 | Cloudy | 256 x 256 | 14 | 30 | 25 to 50 | MWIR | .1 to .2 | less than 50 | S |
| Seeker A | M11_P03_T01_File003_irRaw | RSA TA-3 | 14:31 | Afternoon | Spring | 73.7 | 23 | 4 | 152 | 61% | 60 | Cloudy | 256 x 256 | 14 | 30 | 25 to 50 | MWIR | .1 to .2 | less than 50 | S |
| Seeker A | M11_P04_T01_File004_irRaw | RSA TA-3 | 14:46 | Afternoon | Spring | 73.7 | 23 | 6 | 145 | 62% | 60 | Cloudy | 256 x 256 | 14 | 30 | 25 to 50 | MWIR | .1 to .2 | less than 50 | S |
| Seeker A | M11_P05_T01_File005_irRaw | RSA TA-3 | 15:01 | Afternoon | Spring | 73.8 | 23 | 5 | 141 | 63% | 61 | Cloudy | 256 x 256 | 14 | 30 | 25 to 50 | MWIR | .1 to .2 | less than 50 | S |
| Seeker A | M11_P06_T01_File006_irRaw | RSA TA-3 | 15:16 | Afternoon | Spring | 73.7 | 23 | 7 | 138 | 62% | 60 | Cloudy | 256 x 256 | 14 | 30 | 25 to 50 | MWIR | .1 to .2 | less than 50 | S |
| Seeker A | M11_P07_T01_File007_irRaw | RSA TA-3 | 15:31 | Afternoon | Spring | 73.3 | 23 | 6 | 139 | 63% | 60 | Cloudy | 256 x 256 | 14 | 30 | 25 to 50 | MWIR | .1 to .2 | less than 50 | S |
| Seeker A | M11_P08_T01_File008_irRaw | RSA TA-3 | 15:46 | Afternoon | Spring | 72.9 | 23 | 5 | 136 | 63% | 60 | Cloudy | 256 x 256 | 14 | 30 | 25 to 50 | MWIR | .1 to .2 | less than 50 | S |

| Sensor | File Name | Conditions | | | | | | | | | | Resolution | | | | | | Sensor Sensitivity | | | |
|----------|---------------------------|------------|-------|-----------|--------------|--------|--------------|--------------|-----------------|----------------|-----------------------|---------------|-----------|-------------------|------------|-----------------|-------------------------|--------------------|--------------|-----------|-------|
| | | Location | | Time | Time-off Day | Season | Air Temp (F) | Air Temp (C) | Wind Speed (ft) | Wind Dir (deg) | Relative Humidity (%) | Dew Point (F) | Weather | FPA Size (Pixels) | Bits/Pixel | Frame Rate (Hz) | MTF (% at Half Nyquist) | Spectral Band | IFOV (mrad) | NEAT (mK) | Class |
| | | Time | Day | | | | | | | | | | | | | | | | | | |
| Secker A | M12_P04_TO1_File004_irRaw | RSA TA-3 | 16:40 | Afternoon | Spring | 76.3 | 25 | 1 | 222 | 63% | 63 | Cloudy | 256 x 256 | 14 | 30 | 25 to 50 | MWIR | .1 to .2 | less than 50 | \$ | |
| Secker A | M12_P05_TO1_File005_irRaw | RSA TA-3 | 16:52 | Afternoon | Spring | 76.0 | 24 | 1 | 211 | 62% | 62 | Cloudy | 256 x 256 | 14 | 30 | 25 to 50 | MWIR | .1 to .2 | less than 50 | \$ | |
| Secker A | M12_P06_TO1_File006_irRaw | RSA TA-3 | 17:00 | Afternoon | Spring | 76.0 | 24 | 1 | 211 | 62% | 62 | Cloudy | 256 x 256 | 14 | 30 | 25 to 50 | MWIR | .1 to .2 | less than 50 | \$ | |
| Secker A | M12_P07_TO1_File007_irRaw | RSA TA-3 | 17:11 | Afternoon | Spring | 75.5 | 24 | 0 | 278 | 64% | 63 | Cloudy | 256 x 256 | 14 | 30 | 25 to 50 | MWIR | .1 to .2 | less than 50 | \$ | |
| Secker A | M12_P08_TO1_File008_irRaw | RSA TA-3 | 17:20 | Afternoon | Spring | 74.8 | 24 | 1 | 163 | 68% | 64 | Cloudy | 256 x 256 | 14 | 30 | 25 to 50 | MWIR | .1 to .2 | less than 50 | \$ | |
| Secker A | M12_P09_TO1_File009_irRaw | RSA TA-3 | 17:30 | Afternoon | Spring | 74.8 | 24 | 1 | 165 | 68% | 64 | Cloudy | 256 x 256 | 14 | 30 | 25 to 50 | MWIR | .1 to .2 | less than 50 | \$ | |
| Secker A | M12_P10_TO1_File010_irRaw | RSA TA-3 | 17:45 | Afternoon | Spring | 74.1 | 23 | 2 | 177 | 73% | 65 | Cloudy | 256 x 256 | 14 | 30 | 25 to 50 | MWIR | .1 to .2 | less than 50 | \$ | |
| Secker A | M12_P11_TO1_File011_irRaw | RSA TA-3 | 17:55 | Afternoon | Spring | 73.8 | 23 | 0 | 180 | 74% | 65 | Cloudy | 256 x 256 | 14 | 30 | 25 to 50 | MWIR | .1 to .2 | less than 50 | \$ | |
| Secker A | M12_P12_TO1_File012_irRaw | RSA TA-3 | 18:05 | Afternoon | Spring | 73.8 | 23 | 0 | 180 | 74% | 65 | Cloudy | 256 x 256 | 14 | 30 | 25 to 50 | MWIR | .1 to .2 | less than 50 | \$ | |
| Secker A | M12_P14_TO1_File014_irRaw | RSA TA-3 | 18:20 | Afternoon | Spring | 72.8 | 23 | 1 | 180 | 79% | 66 | Cloudy | 256 x 256 | 14 | 30 | 25 to 50 | MWIR | .1 to .2 | less than 50 | \$ | |
| Secker A | M12_P15_TO1_File015_irRaw | RSA TA-3 | 18:30 | Afternoon | Spring | 71.6 | 22 | 1 | 180 | 83% | 66 | Cloudy | 256 x 256 | 14 | 30 | 25 to 50 | MWIR | .1 to .2 | less than 50 | \$ | |
| Secker A | M14_P04_TO1_File004_irRaw | RSA TA-3 | 8:40 | Morning | Spring | 51.3 | 11 | 4 | 339 | 65% | 40 | Clear | 256 x 256 | 14 | 30 | 25 to 50 | MWIR | .1 to .2 | less than 50 | \$ | |
| Secker A | M14_P05_TO1_File005_irRaw | RSA TA-3 | 8:52 | Morning | Spring | 51.3 | 11 | 4 | 339 | 65% | 40 | Clear | 256 x 256 | 14 | 30 | 25 to 50 | MWIR | .1 to .2 | less than 50 | \$ | |
| Secker A | M14_P06_TO1_File006_irRaw | RSA TA-3 | 9:02 | Morning | Spring | 51.9 | 11 | 7 | 5 | 66% | 41 | Clear | 256 x 256 | 14 | 30 | 25 to 50 | MWIR | .1 to .2 | less than 50 | \$ | |
| Secker A | M14_P07_TO1_File007_irRaw | RSA TA-3 | 9:14 | Morning | Spring | 52.7 | 12 | 6 | 4 | 65% | 41 | Clear | 256 x 256 | 14 | 30 | 25 to 50 | MWIR | .1 to .2 | less than 50 | \$ | |
| Secker A | M14_P15_TO1_File015_irRaw | RSA TA-3 | 9:24 | Morning | Spring | 53.7 | 12 | 4 | 345 | 62% | 41 | Clear | 256 x 256 | 14 | 30 | 25 to 50 | MWIR | .1 to .2 | less than 50 | \$ | |
| Secker A | M14_P16_TO1_File009_irRaw | RSA TA-3 | 9:36 | Morning | Spring | 54.7 | 13 | 4 | 345 | 62% | 42 | Clear | 256 x 256 | 14 | 30 | 25 to 50 | MWIR | .1 to .2 | less than 50 | \$ | |
| Secker A | M14_P17_TO1_File016_irRaw | RSA TA-3 | 10:40 | Morning | Spring | 54.7 | 13 | 4 | 345 | 62% | 42 | Clear | 256 x 256 | 14 | 30 | 25 to 50 | MWIR | .1 to .2 | less than 50 | \$ | |
| Secker A | M14_P18_TO1_File018_irRaw | RSA TA-3 | 9:55 | Morning | Spring | 55.7 | 13 | 3 | 322 | 60% | 42 | Clear | 256 x 256 | 14 | 30 | 25 to 50 | MWIR | .1 to .2 | less than 50 | \$ | |
| Secker A | M14_P09_TO1_File009_irRaw | RSA TA-3 | 10:05 | Morning | Spring | 55.7 | 13 | 3 | 322 | 60% | 42 | Clear | 256 x 256 | 14 | 30 | 25 to 50 | MWIR | .1 to .2 | less than 50 | \$ | |
| Secker A | M14_P10_TO1_File010_irRaw | RSA TA-3 | 10:20 | Morning | Spring | 56.8 | 14 | 3 | 330 | 59% | 43 | Clear | 256 x 256 | 14 | 30 | 25 to 50 | MWIR | .1 to .2 | less than 50 | \$ | |
| Secker A | M14_P11_TO1_File009_irRaw | RSA TA-3 | 10:30 | Morning | Spring | 57.5 | 14 | 4 | 332 | 58% | 43 | Clear | 256 x 256 | 14 | 30 | 25 to 50 | MWIR | .1 to .2 | less than 50 | \$ | |
| Secker A | M14_P12_TO1_File012_irRaw | RSA TA-3 | 10:50 | Morning | Spring | 58.1 | 15 | 6 | 357 | 57% | 43 | Clear | 256 x 256 | 14 | 30 | 25 to 50 | MWIR | .1 to .2 | less than 50 | \$ | |
| Secker A | M14_P13_TO1_File011_irRaw | RSA TA-3 | 21:08 | Night | Winter | 39 | 4 | 3 | 19 | 93% | 37 | Clear | 512 x 512 | 12 | 30 | better than 30 | MWIR | .1 to .2 | less than 50 | UN | |
| Secker A | M14_P14_TO1_File012_irRaw | RSA TA-3 | 21:08 | Night | Winter | 39 | 4 | 3 | 19 | 93% | 37 | Clear | 512 x 512 | 12 | 30 | better than 30 | MWIR | .1 to .2 | less than 50 | UN | |
| Secker A | M14_P15_TO1_File013_irRaw | RSA TA-3 | 21:08 | Night | Winter | 39 | 4 | 3 | 19 | 93% | 37 | Clear | 512 x 512 | 12 | 30 | better than 30 | MWIR | .1 to .2 | less than 50 | UN | |
| Secker A | M14_P16_TO1_File014_irRaw | RSA TA-3 | 21:11 | Night | Winter | 39 | 4 | 3 | 19 | 93% | 37 | Clear | 512 x 512 | 12 | 30 | better than 30 | MWIR | .1 to .2 | less than 50 | UN | |
| Secker A | M14_P17_TO1_File016_irRaw | RSA TA-3 | 21:11 | Night | Winter | 39 | 4 | 3 | 19 | 93% | 37 | Clear | 512 x 512 | 12 | 30 | better than 30 | MWIR | .1 to .2 | less than 50 | UN | |
| AMS | NightTest4a.ams | RSA TA-3 | 21:18 | Night | Winter | 39 | 4 | 3 | 19 | 93% | 37 | Clear | 512 x 512 | 12 | 30 | better than 30 | MWIR | .1 to .2 | less than 50 | UN | |
| AMS | NightTest4b.ams | RSA TA-3 | 21:18 | Night | Winter | 39 | 4 | 3 | 19 | 93% | 37 | Clear | 512 x 512 | 12 | 30 | better than 30 | MWIR | .1 to .2 | less than 50 | UN | |
| AMS | NightTest4c.ams | RSA TA-3 | 21:18 | Night | Winter | 39 | 4 | 3 | 19 | 93% | 37 | Clear | 512 x 512 | 12 | 30 | better than 30 | MWIR | .1 to .2 | less than 50 | UN | |
| AMS | NightTest4d.ams | RSA TA-3 | 21:18 | Night | Winter | 39 | 4 | 3 | 19 | 93% | 37 | Clear | 512 x 512 | 12 | 30 | better than 30 | MWIR | .1 to .2 | less than 50 | UN | |
| AMS | NightTest5a.ams | RSA TA-3 | 21:23 | Night | Winter | 39 | 4 | 3 | 19 | 93% | 37 | Clear | 512 x 512 | 12 | 30 | better than 30 | MWIR | .1 to .2 | less than 50 | UN | |
| AMS | NightTest5b.ams | RSA TA-3 | 21:29 | Night | Winter | 39 | 4 | 3 | 19 | 93% | 37 | Clear | 512 x 512 | 12 | 30 | better than 30 | MWIR | .1 to .2 | less than 50 | UN | |
| AMS | NightTest5c.ams | RSA TA-3 | 21:33 | Night | Winter | 39 | 4 | 3 | 19 | 93% | 37 | Clear | 512 x 512 | 12 | 30 | better than 30 | MWIR | .1 to .2 | less than 50 | UN | |
| AMS | NightTest5d.ams | RSA TA-3 | 21:33 | Night | Winter | 39 | 4 | 3 | 19 | 93% | 37 | Clear | 512 x 512 | 12 | 30 | better than 30 | MWIR | .1 to .2 | less than 50 | UN | |
| AMS | NightTest6a.ams | RSA TA-3 | 21:35 | Night | Winter | 39 | 4 | 3 | 19 | 93% | 37 | Clear | 512 x 512 | 12 | 30 | better than 30 | MWIR | .1 to .2 | less than 50 | UN | |
| AMS | NightTest6b.ams | RSA TA-3 | 21:39 | Night | Winter | 39 | 4 | 3 | 19 | 93% | 37 | Clear | 512 x 512 | 12 | 30 | better than 30 | MWIR | .1 to .2 | less than 50 | UN | |
| AMS | NightTest6c.ams | RSA TA-3 | 21:38 | Night | Winter | 39 | 4 | 3 | 19 | 93% | 37 | Clear | 512 x 512 | 12 | 30 | better than 30 | MWIR | .1 to .2 | less than 50 | UN | |
| AMS | NightTest6d.ams | RSA TA-3 | 21:38 | Night | Winter | 39 | 4 | 3 | 19 | 93% | 37 | Clear | 512 x 512 | 12 | 30 | better than 30 | MWIR | .1 to .2 | less than 50 | UN | |
| AMS | NightTest7a.ams | RSA TA-3 | 21:38 | Night | Winter | 39 | 4 | 3 | 19 | 93% | 37 | Clear | 512 x 512 | 12 | 30 | better than 30 | MWIR | .1 to .2 | less than 50 | UN | |
| AMS | NightTest7b.ams | RSA TA-3 | 21:38 | Night | Winter | 39 | 4 | 3 | 19 | 93% | 37 | Clear | 512 x 512 | 12 | 30 | better than 30 | MWIR | .1 to .2 | less than 50 | UN | |
| AMS | NightTest7c.ams | RSA TA-3 | 21:38 | Night | Winter | 39 | 4 | 3 | 19 | 93% | 37 | Clear | 512 x 512 | 12 | 30 | better than 30 | MWIR | .1 to .2 | less than 50 | UN | |
| AMS | NightTest7d.ams | RSA TA-3 | 21:38 | Night | Winter | 39 | 4 | 3 | 19 | 93% | 37 | Clear | 512 x 512 | 12 | 30 | better than 30 | MWIR | .1 to .2 | less than 50 | UN | |
| AMS | NightTest8a.ams | RSA TA-3 | 21:38 | Night | Winter | 39 | 4 | 3 | 19 | 93% | 37 | Clear | 512 x 512 | 12 | 30 | better than 30 | MWIR | .1 to .2 | less than 50 | UN | |
| AMS | NightTest8b.ams | RSA TA-3 | 22:12 | Night | Winter | 39 | 4 | 3 | 19 | 93% | 37 | Clear | 512 x 512 | 12 | 30 | better than 30 | MWIR | .1 to .2 | less than 50 | UN | |
| AMS | NightTest8c.ams | RSA TA-3 | 22:12 | Night | Winter | 39 | 4 | 3 | 19 | 93% | 37 | Clear | 512 x 512 | 12 | 30 | better than 30 | MWIR | .1 to .2 | less than 50 | UN | |
| AMS | NightTest8d.ams | RSA TA-3 | 22:12 | Night | Winter | 39 | 4 | 3 | 19 | 93% | 37 | Clear | 512 x 512 | 12 | 30 | better than 30 | MWIR | .1 to .2 | less than 50 | UN | |
| AMS | NightTest9a.ams | RSA TA-3 | 21:38 | Night | Winter | 39 | 4 | 3 | 19 | 93% | 37 | Clear | 512 x 512 | 12 | 30 | better than 30 | MWIR | .1 to .2 | less than 50 | UN | |
| AMS | NightTest9b.ams | RSA TA-3 | 21:38 | Night | Winter | 39 | 4 | 3 | 19 | 93% | 37 | Clear | 512 x 512 | 12 | 30 | better than 30 | MWIR | .1 to .2 | less than 50 | UN | |
| AMS | NightTest9c.ams | RSA TA-3 | 21:38 | Night | Winter | 39 | 4 | 3 | 19 | 93% | 37 | Clear | 512 x 512 | 12 | 30 | better than 30 | MWIR | .1 to .2 | less than 50 | UN | |
| AMS | NightTest9d.ams | RSA TA-3 | 21:38 | Night | Winter | 39 | 4 | 3 | 19 | 93% | 37 | Clear | 512 x 512 | 12 | 30 | better than 30 | MWIR | .1 to .2 | less than 50 | UN | |
| AMS | NightTest10a.ams | RSA TA-3 | 22:12 | Night | Winter | 39 | 4 | 3 | 19 | 93% | 37 | Clear | 512 x 512 | 12 | 30 | better than 30 | MWIR | .1 to .2 | less than 50 | UN | |
| AMS | NightTest10b.ams | RSA TA-3 | 22:12 | Night | Winter | 39 | 4 | 3 | 19 | 93% | 37 | Clear | 512 x 512 | 12 | 30 | better than 30 | MWIR | .1 to .2 | less than 50 | UN | |
| AMS | NightTest10c.ams | RSA TA-3 | 22:12 | Night | Winter | 39 | 4 | 3 | 19 | 93% | 37 | Clear | 512 x 512 | 12 | 30 | better than 30 | MWIR | .1 to .2 | less than 50 | UN | |
| AMS | NightTest10d.ams | RSA TA-3 | 22:12 | Night | Winter | 39 | 4 | 3 | 19 | 93% | 37 | Clear | 512 x 512 | 12 | 30 | better than 30 | MWIR | .1 to .2 | less than 50 | UN | |
| AMS | NightTest11a.ams | RSA TA-3 | 22:12 | Night | Winter | 39 | 4 | 3 | 19 | 93% | 37 | Clear | 512 x 512 | 12 | 30 | better than 30 | MWIR | .1 to .2 | less than 50 | UN | |
| AMS | NightTest11b.ams | RSA TA-3 | 22:12 | Night | Winter | 39 | 4 | 3 | 19 | 93% | 37 | Clear | 512 x 512 | 12 | 30 | better than 30 | MWIR | .1 to .2 | less than 50 | UN | |
| AMS | NightTest11c.ams | RSA TA-3 | 22:12 | Night | Winter | 39 | 4 | 3 | | | | | | | | | | | | | |

| Sensor | Filename | Conditions | | | | | | | | | | Resolution | | | | | | Senior Sensitivity | | |
|--------|--------------------|------------|-------|-------------|--------|--------------|--------------|-----------------|----------------|-----------------------|---------------|------------|------------------|------------|-----------------|-------------------------|---------------|--------------------|--------------|-------|
| | | Location | Time | Time-of-Day | Season | Air Temp (F) | Air Temp (C) | Wind Speed (ft) | Wind Dir (deg) | Relative Humidity (%) | Dew Point (F) | Weather | FPA Size (Pixel) | Bits/Frame | Frame Rate (Hz) | MTF (% at Half Nyquist) | Spectral Band | IFOV (mrad) | NETT (mK) | Class |
| AMS | NightTest20b.ams | RSA TA-3 | 22:12 | Night | Winter | 39 | 4 | 3 | 19 | 93% | 37 | Clear | 512 x 512 | 12 | 30 | better than 50 | MWIR | .1 to .2 | less than 50 | UN |
| AMS | NightTest21a.ams | RSA TA-3 | 22:12 | Night | Winter | 39 | 4 | 3 | 19 | 93% | 37 | Clear | 512 x 512 | 12 | 30 | better than 50 | MWIR | .1 to .2 | less than 50 | UN |
| AMS | NightTest21b.ams | RSA TA-3 | 22:12 | Night | Winter | 39 | 4 | 3 | 19 | 93% | 37 | Clear | 512 x 512 | 12 | 30 | better than 50 | MWIR | .1 to .2 | less than 50 | UN |
| AMS | NightTest23a.ams | RSA TA-3 | 22:12 | Night | Winter | 39 | 4 | 3 | 19 | 93% | 37 | Clear | 512 x 512 | 12 | 30 | better than 50 | MWIR | .1 to .2 | less than 50 | UN |
| AMS | NightTest23b.ams | RSA TA-3 | 22:12 | Night | Winter | 39 | 4 | 3 | 19 | 93% | 37 | Clear | 512 x 512 | 12 | 30 | better than 50 | MWIR | .1 to .2 | less than 50 | UN |
| AMS | NightTest27a_a.ams | RSA TA-3 | 22:12 | Night | Winter | 39 | 4 | 3 | 19 | 93% | 37 | Clear | 512 x 512 | 12 | 30 | better than 50 | MWIR | .1 to .2 | less than 50 | UN |
| AMS | NightTest27a_b.ams | RSA TA-3 | 22:12 | Night | Winter | 39 | 4 | 3 | 19 | 93% | 37 | Clear | 512 x 512 | 12 | 30 | better than 50 | MWIR | .1 to .2 | less than 50 | UN |
| AMS | NightTest27a_c.ams | RSA TA-3 | 22:12 | Night | Winter | 39 | 4 | 3 | 19 | 93% | 37 | Clear | 512 x 512 | 12 | 30 | better than 50 | MWIR | .1 to .2 | less than 50 | UN |
| AMS | BMP1a.ams | RSA TA-3 | 9:25 | Morning | Winter | 47 | 8 | 3 | 258 | 95% | 46 | Clear | 512 x 512 | 12 | 30 | better than 50 | MWIR | .1 to .2 | less than 50 | UN |
| AMS | BMP1b.ams | RSA TA-3 | 9:25 | Morning | Winter | 47 | 8 | 3 | 258 | 95% | 46 | Clear | 512 x 512 | 12 | 30 | better than 50 | MWIR | .1 to .2 | less than 50 | UN |
| AMS | BMP1d.ams | RSA TA-3 | 9:25 | Morning | Winter | 47 | 8 | 3 | 258 | 95% | 46 | Clear | 512 x 512 | 12 | 30 | better than 50 | MWIR | .1 to .2 | less than 50 | UN |
| AMS | BMP24a.ams | RSA TA-3 | 10:05 | Morning | Winter | 47 | 8 | 3 | 15 | 94% | 46 | Clear | 512 x 512 | 12 | 30 | better than 50 | MWIR | .1 to .2 | less than 50 | UN |
| AMS | BMP24b.ams | RSA TA-3 | 10:05 | Morning | Winter | 47 | 8 | 3 | 15 | 94% | 46 | Clear | 512 x 512 | 12 | 30 | better than 50 | MWIR | .1 to .2 | less than 50 | UN |
| AMS | BMP24c.ams | RSA TA-3 | 10:05 | Morning | Winter | 47 | 8 | 3 | 15 | 94% | 46 | Clear | 512 x 512 | 12 | 30 | better than 50 | MWIR | .1 to .2 | less than 50 | UN |
| AMS | BMP5a.ams | RSA TA-3 | 10:16 | Morning | Winter | 47 | 8 | 3 | 15 | 94% | 45 | Clear | 512 x 512 | 12 | 30 | better than 50 | MWIR | .1 to .2 | less than 50 | UN |
| AMS | BMP5b.ams | RSA TA-3 | 10:16 | Morning | Winter | 47 | 8 | 3 | 15 | 94% | 45 | Clear | 512 x 512 | 12 | 30 | better than 50 | MWIR | .1 to .2 | less than 50 | UN |
| AMS | BMP5c.ams | RSA TA-3 | 10:16 | Morning | Winter | 47 | 8 | 3 | 15 | 94% | 45 | Clear | 512 x 512 | 12 | 30 | better than 50 | MWIR | .1 to .2 | less than 50 | UN |
| AMS | BMP77.ams | RSA TA-3 | 10:20 | Morning | Winter | 47 | 8 | 3 | 15 | 94% | 45 | Clear | 512 x 512 | 12 | 30 | better than 50 | MWIR | .1 to .2 | less than 50 | UN |
| AMS | BMP8.ams | RSA TA-3 | 10:30 | Morning | Winter | 47 | 8 | 4 | 21 | 93% | 45 | Clear | 512 x 512 | 12 | 30 | better than 50 | MWIR | .1 to .2 | less than 50 | UN |
| AMS | BMP19a.ams | RSA TA-3 | 10:45 | Morning | Winter | 47 | 8 | 3 | 14 | 93% | 45 | Clear | 512 x 512 | 12 | 30 | better than 50 | MWIR | .1 to .2 | less than 50 | UN |
| AMS | BMP19b.ams | RSA TA-3 | 10:45 | Morning | Winter | 47 | 8 | 3 | 14 | 93% | 45 | Clear | 512 x 512 | 12 | 30 | better than 50 | MWIR | .1 to .2 | less than 50 | UN |
| AMS | BMP19c.ams | RSA TA-3 | 10:45 | Morning | Winter | 47 | 8 | 3 | 14 | 93% | 45 | Clear | 512 x 512 | 12 | 30 | better than 50 | MWIR | .1 to .2 | less than 50 | UN |
| AMS | T72Run1a.ams | RSA TA-3 | 11:23 | Morning | Winter | 47 | 8 | 2 | 11 | 89% | 44 | Clear | 512 x 512 | 12 | 30 | better than 50 | MWIR | .1 to .2 | less than 50 | UN |
| AMS | T72Run1b.ams | RSA TA-3 | 11:23 | Morning | Winter | 47 | 8 | 2 | 11 | 89% | 44 | Clear | 512 x 512 | 12 | 30 | better than 50 | MWIR | .1 to .2 | less than 50 | UN |
| AMS | T72Run1c.ams | RSA TA-3 | 11:23 | Morning | Winter | 47 | 8 | 2 | 11 | 89% | 44 | Clear | 512 x 512 | 12 | 30 | better than 50 | MWIR | .1 to .2 | less than 50 | UN |
| AMS | T72Run1d.ams | RSA TA-3 | 11:23 | Morning | Winter | 47 | 8 | 2 | 11 | 89% | 44 | Clear | 512 x 512 | 12 | 30 | better than 50 | MWIR | .1 to .2 | less than 50 | UN |
| AMS | T72Run1e.ams | RSA TA-3 | 11:40 | Morning | Winter | 47 | 8 | 2 | 4 | 89% | 44 | Clear | 512 x 512 | 12 | 30 | better than 50 | MWIR | .1 to .2 | less than 50 | UN |
| AMS | T72Run1f.ams | RSA TA-3 | 11:40 | Morning | Winter | 47 | 8 | 2 | 4 | 89% | 44 | Clear | 512 x 512 | 12 | 30 | better than 50 | MWIR | .1 to .2 | less than 50 | UN |
| AMS | T72Run1g.ams | RSA TA-3 | 11:50 | Morning | Winter | 47 | 8 | 2 | 4 | 89% | 44 | Clear | 512 x 512 | 12 | 30 | better than 50 | MWIR | .1 to .2 | less than 50 | UN |
| AMS | T72Run1h.ams | RSA TA-3 | 11:50 | Morning | Winter | 47 | 8 | 2 | 4 | 89% | 44 | Clear | 512 x 512 | 12 | 30 | better than 50 | MWIR | .1 to .2 | less than 50 | UN |
| AMS | T72Run1i.ams | RSA TA-3 | 12:00 | Morning | Winter | 47 | 8 | 2 | 4 | 89% | 44 | Clear | 512 x 512 | 12 | 30 | better than 50 | MWIR | .1 to .2 | less than 50 | UN |
| AMS | T72Run1j.ams | RSA TA-3 | 12:00 | Morning | Winter | 47 | 8 | 2 | 4 | 89% | 44 | Clear | 512 x 512 | 12 | 30 | better than 50 | MWIR | .1 to .2 | less than 50 | UN |
| AMS | T72Run1k.ams | RSA TA-3 | 12:00 | Morning | Winter | 47 | 8 | 1 | 21 | 85% | 43 | Clear | 512 x 512 | 12 | 30 | better than 50 | MWIR | .1 to .2 | less than 50 | UN |
| AMS | T72Run1l.ams | RSA TA-3 | 12:25 | Afternoon | Winter | 47 | 8 | 2 | 9 | 85% | 43 | Clear | 512 x 512 | 12 | 30 | better than 50 | MWIR | .1 to .2 | less than 50 | UN |
| AMS | T72Run1m.ams | RSA TA-3 | 12:25 | Afternoon | Winter | 47 | 8 | 2 | 9 | 85% | 43 | Clear | 512 x 512 | 12 | 30 | better than 50 | MWIR | .1 to .2 | less than 50 | UN |
| AMS | T72Run1n.ams | RSA TA-3 | 12:35 | Afternoon | Winter | 47 | 8 | 2 | 9 | 85% | 43 | Clear | 512 x 512 | 12 | 30 | better than 50 | MWIR | .1 to .2 | less than 50 | UN |
| AMS | T72Run1o.ams | RSA TA-3 | 12:50 | Afternoon | Winter | 47 | 8 | 2 | 9 | 85% | 42 | Clear | 512 x 512 | 12 | 30 | better than 50 | MWIR | .1 to .2 | less than 50 | UN |
| AMS | T72Run1p.ams | RSA TA-3 | 13:12 | Afternoon | Winter | 47 | 8 | 3 | 13 | 87% | 43 | Clear | 512 x 512 | 12 | 30 | better than 50 | MWIR | .1 to .2 | less than 50 | UN |
| AMS | T72Run1q.ams | RSA TA-3 | 13:12 | Afternoon | Winter | 47 | 8 | 3 | 13 | 87% | 43 | Clear | 512 x 512 | 12 | 30 | better than 50 | MWIR | .1 to .2 | less than 50 | UN |
| AMS | T72Run1r.ams | RSA TA-3 | 13:12 | Afternoon | Winter | 47 | 8 | 3 | 13 | 87% | 43 | Clear | 512 x 512 | 12 | 30 | better than 50 | MWIR | .1 to .2 | less than 50 | UN |

| Sensor Sequence | Location | Season | Time-of-Day | AIR TEMP | | | Wind Speed | | | Bar Pressure | | | Global Radiation | | | FPA Size (Pixels) | | | Frame Rate (Hz) | | | MTF (% at Half Nyquist) | | | IFOV (mrad) | | | Class |
|-----------------|-------------------|------------|-------------|-----------|----------|------|------------|-------|-------------|-------------------|--------------|--------------|-------------------|---------|----------------------------|--------------------|---------|--------------------|-----------------|--------------------|--------------|-------------------------|---------|--------------------|-------------|-------------|-----------|-------|
| | | | | Time | °F | Dir | Wind m/s | Dir | Air Temp °C | Relative Humidity | Dew Point °C | Soil Temp °C | Bar Pressure (mb) | Rain mm | Global Radiation watts/m^2 | Frame Rate at Half | MTF (%) | Frame Rate at Half | MTF (%) | Frame Rate at Half | MTF (%) | Frame Rate at Half | MTF (%) | Frame Rate at Half | MTF (%) | IFOV (mrad) | NEDT (mK) | |
| Skyball | TS2 1000 16 000 M | Eglin B-70 | Spring | Afternoon | 14:03:44 | 81.7 | 3.2 | 159.5 | 27.6 | 67% | 20.7 | 23.4 | 1013.0 | 0.0 | 913.0 | 512x512 | 12.0 | 30.0 | 77 | MWIR | less than .1 | 77 | S | | | | | |
| Skyball | TS2 1000 16 090 M | Eglin B-70 | Spring | Afternoon | 14:07:33 | 82.1 | 3.7 | 175.2 | 27.9 | 64% | 20.6 | 29.5 | 1013.0 | 0.0 | 843.0 | 512x512 | 12.0 | 30.0 | 77 | MWIR | less than .1 | 77 | S | | | | | |
| Skyball | TS2 1000 16 135 M | Eglin B-70 | Spring | Afternoon | 14:06:01 | 82.0 | 3.9 | 174.5 | 27.8 | 66% | 20.9 | 29.5 | 1013.0 | 0.0 | 867.0 | 512x512 | 12.0 | 30.0 | 77 | MWIR | less than .1 | 77 | S | | | | | |
| Skyball | TS2 1000 16 180 M | Eglin B-70 | Spring | Afternoon | 14:06:52 | 82.0 | 3.9 | 174.5 | 27.8 | 66% | 20.9 | 29.5 | 1013.0 | 0.0 | 867.0 | 512x512 | 12.0 | 30.0 | 77 | MWIR | less than .1 | 77 | S | | | | | |
| Skyball | TS2 1000 16 225 M | Eglin B-70 | Spring | Afternoon | 14:04:25 | 82.0 | 4.3 | 149.0 | 27.8 | 66% | 20.7 | 29.5 | 1013.0 | 0.0 | 952.0 | 512x512 | 12.0 | 30.0 | 77 | MWIR | less than .1 | 77 | S | | | | | |
| Skyball | TS2 1000 16 270 M | Eglin B-70 | Spring | Afternoon | 14:02:55 | 81.3 | 4.4 | 179.3 | 27.4 | 67% | 20.4 | 29.4 | 1013.0 | 0.0 | 947.0 | 512x512 | 12.0 | 30.0 | 77 | MWIR | less than .1 | 77 | S | | | | | |
| Skyball | TS2 1000 17 000 M | Eglin B-70 | Spring | Afternoon | 14:10:14 | 82.0 | 5.4 | 148.3 | 27.8 | 65% | 20.6 | 29.6 | 1013.0 | 0.0 | 844.0 | 512x512 | 12.0 | 30.0 | 77 | MWIR | less than .1 | 77 | S | | | | | |
| Skyball | TS2 1000 17 090 M | Eglin B-70 | Spring | Afternoon | 14:12:21 | 81.8 | 4.0 | 160.9 | 27.7 | 65% | 20.5 | 29.6 | 1013.0 | 0.0 | 844.0 | 512x512 | 12.0 | 30.0 | 77 | MWIR | less than .1 | 77 | S | | | | | |
| Skyball | TS2 1000 17 135 M | Eglin B-70 | Spring | Afternoon | 14:12:53 | 81.8 | 4.0 | 160.9 | 27.7 | 65% | 20.5 | 29.6 | 1013.0 | 0.0 | 734.0 | 512x512 | 12.0 | 30.0 | 77 | MWIR | less than .1 | 77 | S | | | | | |
| Skyball | TS2 1000 17 180 M | Eglin B-70 | Spring | Afternoon | 14:10:50 | 82.0 | 5.4 | 148.3 | 27.8 | 65% | 20.6 | 29.6 | 1013.0 | 0.0 | 844.0 | 512x512 | 12.0 | 30.0 | 77 | MWIR | less than .1 | 77 | S | | | | | |
| Skyball | TS2 1000 17 225 M | Eglin B-70 | Spring | Afternoon | 14:09:24 | 82.0 | 4.1 | 149.8 | 27.8 | 65% | 20.6 | 29.6 | 1013.0 | 0.0 | 828.0 | 512x512 | 12.0 | 30.0 | 77 | MWIR | less than .1 | 77 | S | | | | | |
| Skyball | TS2 1000 17 270 M | Eglin B-70 | Spring | Afternoon | 14:07:54 | 81.8 | 3.8 | 192.7 | 27.7 | 66% | 20.7 | 29.4 | 1013.0 | 0.0 | 933.0 | 512x512 | 12.0 | 30.0 | 77 | MWIR | less than .1 | 77 | S | | | | | |
| Skyball | TS2 1000 17 300 M | Eglin B-70 | Spring | Afternoon | 14:09:13 | 81.5 | 4.8 | 185.6 | 27.5 | 65% | 20.5 | 29.4 | 1013.0 | 0.0 | 944.0 | 512x512 | 12.0 | 30.0 | 77 | MWIR | less than .1 | 77 | S | | | | | |
| Skyball | TS2 1000 17 350 M | Eglin B-70 | Spring | Afternoon | 14:09:51 | 81.8 | 4.3 | 176.2 | 27.7 | 66% | 20.6 | 29.4 | 1013.0 | 0.0 | 916.0 | 512x512 | 12.0 | 30.0 | 77 | MWIR | less than .1 | 77 | S | | | | | |
| Skyball | TS2 1000 17 380 M | Eglin B-70 | Spring | Afternoon | 14:00:33 | 81.7 | 5.3 | 174.8 | 27.6 | 66% | 20.7 | 29.4 | 1013.0 | 0.0 | 937.0 | 512x512 | 12.0 | 30.0 | 77 | MWIR | less than .1 | 77 | S | | | | | |
| Skyball | TS2 1000 17 382 M | Eglin B-70 | Spring | Afternoon | 13:58:38 | 82.0 | 4.3 | 185.6 | 27.8 | 64% | 20.6 | 29.4 | 1013.0 | 0.0 | 948.0 | 512x512 | 12.0 | 30.0 | 77 | MWIR | less than .1 | 77 | S | | | | | |
| Skyball | TS2 1000 17 390 M | Eglin B-70 | Spring | Afternoon | 13:57:03 | 81.8 | 3.8 | 192.7 | 27.7 | 66% | 20.7 | 29.4 | 1013.0 | 0.0 | 933.0 | 512x512 | 12.0 | 30.0 | 77 | MWIR | less than .1 | 77 | S | | | | | |
| Skyball | TS2 2000 16 000 M | Eglin B-70 | Spring | Afternoon | 9:57:42 | 69.5 | 0.8 | 177.5 | 20.9 | 64% | 13.5 | 21.5 | 1015.0 | 0.0 | 726.0 | 512x512 | 12.0 | 30.0 | 77 | MWIR | less than .1 | 77 | S | | | | | |
| Skyball | TS2 2000 16 045 M | Eglin B-70 | Spring | Afternoon | 9:55:04 | 69.7 | 1.8 | 298.3 | 21.0 | 61% | 13.4 | 21.4 | 1015.0 | 0.0 | 741.0 | 512x512 | 12.0 | 30.0 | 77 | MWIR | less than .1 | 77 | S | | | | | |
| Skyball | TS2 2000 16 090 M | Eglin B-70 | Spring | Afternoon | 9:52:06 | 69.5 | 0.8 | 177.5 | 20.9 | 64% | 13.5 | 21.3 | 1015.0 | 0.0 | 740.0 | 512x512 | 12.0 | 30.0 | 77 | MWIR | less than .1 | 77 | S | | | | | |
| Skyball | TS2 2000 16 130 M | Eglin B-70 | Spring | Afternoon | 9:50:06 | 69.8 | 1.5 | 318.2 | 21.0 | 63% | 13.5 | 21.4 | 1015.0 | 0.0 | 744.0 | 512x512 | 12.0 | 30.0 | 77 | MWIR | less than .1 | 77 | S | | | | | |
| Skyball | TS2 2000 16 180 M | Eglin B-70 | Spring | Afternoon | 9:56:01 | 69.8 | 1.8 | 331.5 | 21.0 | 62% | 13.7 | 21.3 | 1015.0 | 0.0 | 727.0 | 512x512 | 12.0 | 30.0 | 77 | MWIR | less than .1 | 77 | S | | | | | |
| Skyball | TS2 2000 16 225 M | Eglin B-70 | Spring | Afternoon | 9:53:32 | 69.8 | 1.5 | 318.2 | 21.0 | 63% | 13.5 | 21.4 | 1015.0 | 0.0 | 747.0 | 512x512 | 12.0 | 30.0 | 77 | MWIR | less than .1 | 77 | S | | | | | |
| Skyball | TS2 2000 16 270 M | Eglin B-70 | Spring | Afternoon | 9:52:00 | 69.8 | 1.5 | 318.2 | 21.0 | 63% | 13.5 | 21.4 | 1015.0 | 0.0 | 734.0 | 512x512 | 12.0 | 30.0 | 77 | MWIR | less than .1 | 77 | S | | | | | |
| Skyball | TS2 2000 17 000 M | Eglin B-70 | Spring | Afternoon | 9:59:06 | 70.1 | 2.3 | 21.2 | 21.2 | 60% | 13.2 | 21.5 | 1015.0 | 0.0 | 747.0 | 512x512 | 12.0 | 30.0 | 77 | MWIR | less than .1 | 77 | S | | | | | |
| Skyball | TS2 2000 17 045 M | Eglin B-70 | Spring | Afternoon | 10:01:11 | 70.1 | 1.5 | 55.6 | 21.2 | 60% | 12.9 | 21.5 | 1014.0 | 0.0 | 754.0 | 512x512 | 12.0 | 30.0 | 77 | MWIR | less than .1 | 77 | S | | | | | |
| Skyball | TS2 2000 16 090 M | Eglin B-70 | Spring | Afternoon | 9:58:22 | 70.0 | 2.3 | 51.2 | 21.1 | 59% | 13.1 | 21.4 | 1015.0 | 0.0 | 744.0 | 512x512 | 12.0 | 30.0 | 77 | MWIR | less than .1 | 77 | S | | | | | |
| Skyball | TS2 2000 16 130 M | Eglin B-70 | Spring | Afternoon | 10:02:03 | 70.2 | 1.1 | 66.7 | 21.2 | 58% | 12.9 | 21.5 | 1014.0 | 0.0 | 757.0 | 512x512 | 12.0 | 30.0 | 77 | MWIR | less than .1 | 77 | S | | | | | |
| Skyball | TS2 2000 16 180 M | Eglin B-70 | Spring | Afternoon | 9:59:50 | 70.1 | 2.3 | 55.2 | 21.2 | 60% | 13.2 | 21.5 | 1015.0 | 0.0 | 747.0 | 512x512 | 12.0 | 30.0 | 77 | MWIR | less than .1 | 77 | S | | | | | |
| Skyball | TS2 2000 16 225 M | Eglin B-70 | Spring | Afternoon | 10:02:50 | 70.2 | 1.1 | 66.7 | 21.2 | 58% | 12.9 | 21.5 | 1014.0 | 0.0 | 757.0 | 512x512 | 12.0 | 30.0 | 77 | MWIR | less than .1 | 77 | S | | | | | |
| Skyball | TS2 2000 16 270 M | Eglin B-70 | Spring | Afternoon | 9:59:06 | 70.1 | 1.6 | 146.7 | 21.2 | 63% | 13.4 | 21.2 | 1015.0 | 0.0 | 767.0 | 512x512 | 12.0 | 30.0 | 77 | MWIR | less than .1 | 77 | S | | | | | |
| Skyball | TS2 2000 16 300 M | Eglin B-70 | Spring | Afternoon | 9:49:07 | 69.3 | 2.0 | 131.5 | 20.7 | 63% | 13.7 | 21.2 | 1015.0 | 0.0 | 716.0 | 512x512 | 12.0 | 30.0 | 77 | MWIR | less than .1 | 77 | S | | | | | |
| Skyball | TS2 2000 16 345 M | Eglin B-70 | Spring | Afternoon | 9:46:04 | 69.2 | 1.6 | 146.7 | 20.7 | 63% | 13.4 | 21.2 | 1015.0 | 0.0 | 707.0 | 512x512 | 12.0 | 30.0 | 77 | MWIR | less than .1 | 77 | S | | | | | |
| Skyball | TS2 2000 16 380 M | Eglin B-70 | Spring | Afternoon | 9:49:53 | 69.3 | 2.0 | 131.5 | 20.7 | 63% | 13.7 | 21.2 | 1015.0 | 0.0 | 716.0 | 512x512 | 12.0 | 30.0 | 77 | MWIR | less than .1 | 77 | S | | | | | |
| Skyball | TS2 2000 16 225 M | Eglin B-70 | Spring | Afternoon | 9:47:38 | 69.1 | 2.3 | 152.5 | 20.6 | 63% | 13.2 | 21.2 | 1015.0 | 0.0 | 757.0 | 512x512 | 12.0 | 30.0 | 77 | MWIR | less than .1 | 77 | S | | | | | |
| Skyball | TS2 2000 16 270 M | Eglin B-70 | Spring | Afternoon | 9:50:39 | 69.4 | 1.9 | 145.6 | 20.8 | 63% | 13.6 | 21.3 | 1015.0 | 0.0 | 720.0 | 512x512 | 12.0 | 30.0 | 77 | MWIR | less than .1 | 77 | S | | | | | |
| Skyball | TS2 2000 16 300 M | Eglin B-70 | Spring | Afternoon | 12:53:58 | 72.2 | 2.1 | 309.2 | 25.1 | 43% | 12.3 | 26.6 | 1014.0 | 0.0 | 990.0 | 512x512 | 12.0 | 30.0 | 77 | MWIR | less than .1 | 77 | S | | | | | |
| Skyball | TS2 2500 16 000 M | Eglin B-70 | Spring | Afternoon | 12:54:06 | 76.8 | 0.9 | 284.1 | 24.9 | 45% | 12.3 | 26.7 | 1014.0 | 0.0 | 985.0 | 512x512 | 12.0 | 30.0 | 77 | MWIR | less than .1 | 77 | S | | | | | |
| Skyball | TS2 2500 16 045 M | Eglin B-70 | Spring | Afternoon | 12:51:18 | 76.6 | 2.0 | 308.2 | 25.1 | 43% | 12.3 | 26.6 | 1014.0 | 0.0 | 990.0 | 512x512 | 12.0 | 30.0 | 77 | MWIR | less than .1 | 77 | S | | | | | |
| Skyball | TS2 2500 16 090 M | Eglin B-70 | Spring | Afternoon | 12:49:01 | 77.2 | 1.5 | 27.5 | 21.1 | 47% | 12.7 | 26.4 | 1014.0 | 0.0 | 980.0 | 512x512 | 12.0 | 30.0 | 77 | MWIR | less than .1 | 77 | S | | | | | |
| Skyball | TS2 2500 16 135 M | Eglin B-70 | Spring | Afternoon | 12:49:01 | 77.7 | 1.4 | 303.1 | 25.3 | 45% | 12.1 | 26.5 | 1014.0 | 0.0 | 969.0 | 512x512 | 12.0 | 30.0 | 77 | MWIR | less than .1 | 77 | S | | | | | |
| Skyball | TS2 2500 16 180 M | Eglin B-70 | Spring | Afternoon | 12:48:50 | 76.9 | 2.5 | 310.0 | 25.4 | 46% | 12.2 | 26.8 | 1014.0 | 0.0 | 971.0 | 512x512 | 12.0 | 30.0 | 77 | MWIR | less than .1 | 77 | S | | | | | |
| Skyball | TS2 2500 16 225 M | Eglin B-70 | Spring | Afternoon | 12:48:50 | 76.8 | 2.0 | 309.9 | 24.9 | 46% | 12.3 | 26.7 | 1014.0 | 0.0 | 969.0 | 512x512 | 12.0 | 30.0 | 77 | MWIR | less than .1 | 77 | S | | | | | |
| Skyball | TS2 2500 16 270 M | Eglin B-70 | Spring | Afternoon | 12:49:01 | 77.6 | 1.2 | 303.1 | 25.3 | 48% | 12.9 | 26.9 | 1014.0 | 0.0 | 981.0 | 512x512 | 12.0 | 30.0 | 77 | MWIR | less than .1 | 77 | S | | | | | |
| Skyball | TS2 2500 16 300 M | Eglin B-70 | Spring | Afternoon | 12:49:15 | 77.4 | 2.2 | 351.4 | 25.2 | 46% | 12.1 | 26.8 | 1014.0 | 0.0 | 983.0 | 512x512 | 12.0 | 30.0 | 77 | MWIR | less than .1 | 77 | S | | | | | |
| Skyball | TS2 2500 16 045 M | Eglin B-70 | Spring | Afternoon | 13:00:16 | 77.8 | 2.1 | 304.9 | 25.1 | 43% | 13.0 | 26.8 | 1014.0 | 0.0 | 987.0 | 512x512 | 12.0 | 30.0 | 77 | | | | | | | | | |

| Sensor | SEQUENCE | Location | Season | Time-of-Day | TIME | AIR TEMP °F | Wind Speed | Wind Dir | AIR TEMP °C | Relative Humidity | Dew Point °C | Soil Temp °C | Bar Pressure (mb) | Rain mm | Global Radiation watt/m^2 | FPA Size (Pixel) | Frame Rate (Hz) | MTF (%) at Half Nyquist | Spectral Band | IFOV (mrad) | NET (mK) | Class |
|---------|-------------------|------------|--------|-------------|----------|-------------|------------|----------|-------------|-------------------|--------------|--------------|-------------------|---------|---------------------------|------------------|-----------------|-------------------------|---------------|-------------|--------------|-------|
| Skyball | TS2_4000_16_270_M | Eglin B-70 | Spring | Morning | 10:52:48 | 80.3 | 2.6 | 159.5 | 26.9 | 69% | 20.6 | 25.2 | 1015.0 | 0.0 | 755.0 | 512 x 512 | 12.0 | 30.0 | ?? | MWIR | less than .1 | ?? |
| Skyball | TS2_4000_3_060_M | Eglin B-70 | Spring | Morning | 10:47:48 | 79.6 | 3.9 | 166.0 | 26.5 | 70% | 20.4 | 25.1 | 1015.0 | 0.0 | 869.0 | 512 x 512 | 12.0 | 30.0 | ?? | MWIR | less than .1 | ?? |
| Skyball | TS2_4000_3_090_M | Eglin B-70 | Spring | Morning | 10:51:19 | 80.4 | 3.5 | 157.6 | 26.9 | 68% | 20.5 | 25.2 | 1015.0 | 0.0 | 862.0 | 512 x 512 | 12.0 | 30.0 | ?? | MWIR | less than .1 | ?? |
| Skyball | TS2_4000_3_135_M | Eglin B-70 | Spring | Morning | 10:50:10 | 80.4 | 3.6 | 189.5 | 26.9 | 67% | 20.4 | 25.2 | 1015.0 | 0.0 | 862.0 | 512 x 512 | 12.0 | 30.0 | ?? | MWIR | less than .1 | ?? |
| Skyball | TS2_4000_3_180_M | Eglin B-70 | Spring | Morning | 10:50:50 | 80.4 | 3.6 | 189.5 | 26.9 | 67% | 20.4 | 25.2 | 1015.0 | 0.0 | 862.0 | 512 x 512 | 12.0 | 30.0 | ?? | MWIR | less than .1 | ?? |
| Skyball | TS2_4000_3_225_M | Eglin B-70 | Spring | Morning | 10:48:56 | 79.7 | 3.2 | 179.3 | 26.5 | 70% | 20.6 | 25.1 | 1015.0 | 0.0 | 808.0 | 512 x 512 | 12.0 | 30.0 | ?? | MWIR | less than .1 | ?? |
| Skyball | TS2_4000_3_270_M | Eglin B-70 | Spring | Morning | 10:46:13 | 79.6 | 3.5 | 173.6 | 26.5 | 70% | 20.4 | 25.1 | 1015.0 | 0.0 | 751.0 | 512 x 512 | 12.0 | 30.0 | ?? | MWIR | less than .1 | ?? |
| Skyball | TS2_5000_16_090_M | Eglin B-70 | Spring | Afternoon | 12:09:00 | 75.2 | 0.9 | 330.0 | 24.0 | 52% | 13.2 | 25.2 | 1008.0 | 0.0 | 975.0 | 512 x 512 | 12.0 | 30.0 | ?? | MWIR | less than .1 | ?? |
| Skyball | TS2_5000_16_090_M | Eglin B-70 | Spring | Afternoon | 12:06:01 | 75.0 | 0.8 | 352.1 | 23.9 | 53% | 13.2 | 25.1 | 1008.0 | 0.0 | 974.0 | 512 x 512 | 12.0 | 30.0 | ?? | MWIR | less than .1 | ?? |
| Skyball | TS2_5000_16_135_M | Eglin B-70 | Spring | Afternoon | 12:07:59 | 75.0 | 2.5 | 349.8 | 23.9 | 51% | 13.0 | 25.1 | 1008.0 | 0.0 | 976.0 | 512 x 512 | 12.0 | 30.0 | ?? | MWIR | less than .1 | ?? |
| Skyball | TS2_5000_16_180_M | Eglin B-70 | Spring | Afternoon | 12:10:27 | 75.3 | 1.1 | 296.6 | 24.1 | 49% | 13.2 | 25.2 | 1008.0 | 0.0 | 976.0 | 512 x 512 | 12.0 | 30.0 | ?? | MWIR | less than .1 | ?? |
| Skyball | TS2_5000_16_225_M | Eglin B-70 | Spring | Afternoon | 12:07:09 | 75.0 | 2.5 | 349.8 | 23.9 | 51% | 13.0 | 25.1 | 1008.0 | 0.0 | 976.0 | 512 x 512 | 12.0 | 30.0 | ?? | MWIR | less than .1 | ?? |
| Skyball | TS2_5000_16_270_M | Eglin B-70 | Spring | Afternoon | 12:14:30 | 75.8 | 2.8 | 345.3 | 24.4 | 54% | 14.0 | 25.3 | 1008.0 | 0.0 | 975.0 | 512 x 512 | 12.0 | 30.0 | ?? | MWIR | less than .1 | ?? |
| Skyball | TS2_5000_17_090_M | Eglin B-70 | Spring | Afternoon | 12:14:55 | 75.8 | 2.8 | 345.3 | 24.4 | 54% | 14.0 | 25.3 | 1008.0 | 0.0 | 975.0 | 512 x 512 | 12.0 | 30.0 | ?? | MWIR | less than .1 | ?? |
| Skyball | TS2_5000_17_135_M | Eglin B-70 | Spring | Afternoon | 12:12:08 | 75.5 | 3.5 | 315.5 | 24.2 | 50% | 13.4 | 25.2 | 1008.0 | 0.0 | 975.0 | 512 x 512 | 12.0 | 30.0 | ?? | MWIR | less than .1 | ?? |
| Skyball | TS2_5000_17_180_M | Eglin B-70 | Spring | Afternoon | 12:13:32 | 75.6 | 2.3 | 334.6 | 24.2 | 53% | 13.3 | 25.3 | 1008.0 | 0.0 | 974.0 | 512 x 512 | 12.0 | 30.0 | ?? | MWIR | less than .1 | ?? |
| Skyball | TS2_5000_17_225_M | Eglin B-70 | Spring | Afternoon | 12:15:35 | 76.0 | 3.1 | 354.6 | 24.4 | 51% | 13.5 | 25.3 | 1008.0 | 0.0 | 975.0 | 512 x 512 | 12.0 | 30.0 | ?? | MWIR | less than .1 | ?? |
| Skyball | TS2_5000_17_270_M | Eglin B-70 | Spring | Afternoon | 12:12:49 | 75.5 | 3.5 | 315.5 | 24.2 | 50% | 13.4 | 25.3 | 1008.0 | 0.0 | 975.0 | 512 x 512 | 12.0 | 30.0 | ?? | MWIR | less than .1 | ?? |
| Skyball | TS2_5000_17_300_M | Eglin B-70 | Spring | Afternoon | 12:03:22 | 74.8 | 1.5 | 337.5 | 23.8 | 52% | 12.5 | 25.0 | 1008.0 | 0.0 | 965.0 | 512 x 512 | 12.0 | 30.0 | ?? | MWIR | less than .1 | ?? |
| Skyball | TS2_5000_17_335_M | Eglin B-70 | Spring | Afternoon | 12:03:48 | 74.8 | 1.5 | 337.5 | 23.8 | 52% | 12.5 | 25.0 | 1008.0 | 0.0 | 974.0 | 512 x 512 | 12.0 | 30.0 | ?? | MWIR | less than .1 | ?? |
| Skyball | TS2_5000_17_370_M | Eglin B-70 | Spring | Afternoon | 12:04:04 | 74.7 | 3.1 | 313.0 | 23.7 | 51% | 13.0 | 24.9 | 1008.0 | 0.0 | 968.0 | 512 x 512 | 12.0 | 30.0 | ?? | MWIR | less than .1 | ?? |
| Skyball | TS2_5000_17_405_M | Eglin B-70 | Spring | Afternoon | 12:01:44 | 74.8 | 1.8 | 287.2 | 23.8 | 48% | 12.4 | 25.0 | 1008.0 | 0.0 | 969.0 | 512 x 512 | 12.0 | 30.0 | ?? | MWIR | less than .1 | ?? |
| Skyball | TS2_5000_17_440_M | Eglin B-70 | Spring | Afternoon | 12:05:00 | 70.2 | 1.2 | 99.4 | 21.2 | 59% | 13.1 | 21.6 | 1014.0 | 0.0 | 762.0 | 512 x 512 | 12.0 | 30.0 | ?? | MWIR | less than .1 | ?? |
| Skyball | TS2_1000_6_030_M | Eglin B-70 | Spring | Morning | 10:08:08 | 70.4 | 0.9 | 313.7 | 21.3 | 60% | 13.2 | 21.7 | 1014.0 | 0.0 | 967.0 | 512 x 512 | 12.0 | 30.0 | ?? | MWIR | less than .1 | ?? |
| Skyball | TS2_1000_6_065_M | Eglin B-70 | Spring | Morning | 10:05:02 | 70.1 | 1.2 | 127.3 | 21.1 | 60% | 13.1 | 21.6 | 1014.0 | 0.0 | 758.0 | 512 x 512 | 12.0 | 30.0 | ?? | MWIR | less than .1 | ?? |
| Skyball | TS2_1000_6_100_M | Eglin B-70 | Spring | Morning | 10:09:12 | 70.5 | 1.3 | 331.5 | 21.4 | 59% | 13.1 | 21.7 | 1014.0 | 0.0 | 774.0 | 512 x 512 | 12.0 | 30.0 | ?? | MWIR | less than .1 | ?? |
| Skyball | TS2_1000_6_135_M | Eglin B-70 | Spring | Morning | 10:06:40 | 70.2 | 1.2 | 99.4 | 21.2 | 59% | 13.1 | 21.6 | 1014.0 | 0.0 | 762.0 | 512 x 512 | 12.0 | 30.0 | ?? | MWIR | less than .1 | ?? |
| Skyball | TS2_1000_6_170_M | Eglin B-70 | Spring | Morning | 10:10:04 | 70.5 | 1.5 | 311.2 | 21.4 | 59% | 13.1 | 21.7 | 1014.0 | 0.0 | 774.0 | 512 x 512 | 12.0 | 30.0 | ?? | MWIR | less than .1 | ?? |
| Skyball | TS2_1000_6_205_M | Eglin B-70 | Spring | Morning | 10:04:32 | 77.3 | 2.1 | 349.1 | 25.2 | 46% | 12.5 | 26.9 | 1014.0 | 0.0 | 967.0 | 512 x 512 | 12.0 | 30.0 | ?? | MWIR | less than .1 | ?? |
| Skyball | TS2_1000_6_240_M | Eglin B-70 | Spring | Morning | 10:06:49 | 77.5 | 2.2 | 44.2 | 25.3 | 44% | 12.7 | 27.0 | 1014.0 | 0.0 | 964.0 | 512 x 512 | 12.0 | 30.0 | ?? | MWIR | less than .1 | ?? |
| Skyball | TS2_1000_6_275_M | Eglin B-70 | Spring | Morning | 10:07:35 | 77.4 | 2.2 | 50.1 | 25.2 | 46% | 12.5 | 27.0 | 1014.0 | 0.0 | 977.0 | 512 x 512 | 12.0 | 30.0 | ?? | MWIR | less than .1 | ?? |
| Skyball | TS2_1000_6_310_M | Eglin B-70 | Spring | Morning | 10:05:10 | 77.4 | 2.6 | 45.2 | 25.2 | 45% | 12.7 | 27.0 | 1014.0 | 0.0 | 965.0 | 512 x 512 | 12.0 | 30.0 | ?? | MWIR | less than .1 | ?? |
| Skyball | TS2_1000_6_345_M | Eglin B-70 | Spring | Morning | 10:08:20 | 77.3 | 2.1 | 113.2 | 25.4 | 45% | 12.4 | 27.0 | 1014.0 | 0.0 | 980.0 | 512 x 512 | 12.0 | 30.0 | ?? | MWIR | less than .1 | ?? |
| Skyball | TS2_1000_6_380_M | Eglin B-70 | Spring | Morning | 10:13:19 | 77.3 | 1.9 | 124.0 | 25.5 | 44% | 12.5 | 27.2 | 1014.0 | 0.0 | 940.0 | 512 x 512 | 12.0 | 30.0 | ?? | MWIR | less than .1 | ?? |
| Skyball | TS2_1000_6_415_M | Eglin B-70 | Spring | Morning | 10:13:20 | 77.9 | 2.8 | 345.5 | 25.5 | 43% | 12.2 | 27.4 | 1014.0 | 0.0 | 980.0 | 512 x 512 | 12.0 | 30.0 | ?? | MWIR | less than .1 | ?? |
| Skyball | TS2_1500_6_030_M | Eglin B-70 | Spring | Afternoon | 13:09:49 | 77.3 | 1.5 | 127.0 | 25.2 | 45% | 12.3 | 27.3 | 1014.0 | 0.0 | 977.0 | 512 x 512 | 12.0 | 30.0 | ?? | MWIR | less than .1 | ?? |
| Skyball | TS2_1500_6_065_M | Eglin B-70 | Spring | Afternoon | 13:14:33 | 78.0 | 1.8 | 45.3 | 25.5 | 44% | 12.5 | 27.2 | 1014.0 | 0.0 | 969.0 | 512 x 512 | 12.0 | 30.0 | ?? | MWIR | less than .1 | ?? |
| Skyball | TS2_1500_6_100_M | Eglin B-70 | Spring | Afternoon | 13:18:17 | 77.3 | 1.3 | 112.6 | 26.0 | 45% | 12.1 | 27.3 | 1014.0 | 0.0 | 977.0 | 512 x 512 | 12.0 | 30.0 | ?? | MWIR | less than .1 | ?? |
| Skyball | TS2_1500_6_135_M | Eglin B-70 | Spring | Afternoon | 13:22:25 | 78.0 | 1.0 | 359.2 | 25.6 | 46% | 12.5 | 27.4 | 1014.0 | 0.0 | 977.0 | 512 x 512 | 12.0 | 30.0 | ?? | MWIR | less than .1 | ?? |
| Skyball | TS2_1500_6_170_M | Eglin B-70 | Spring | Afternoon | 13:18:11 | 78.1 | 8.6 | 319.3 | 27.6 | 65% | 20.6 | 29.1 | 1013.0 | 0.0 | 874.0 | 512 x 512 | 12.0 | 30.0 | ?? | MWIR | less than .1 | ?? |
| Skyball | TS2_1500_6_205_M | Eglin B-70 | Spring | Afternoon | 13:40:30 | 81.4 | 5.0 | 205.0 | 27.4 | 65% | 12.1 | 27.3 | 1014.0 | 0.0 | 975.0 | 512 x 512 | 12.0 | 30.0 | ?? | MWIR | less than .1 | ?? |
| Skyball | TS2_1500_6_240_M | Eglin B-70 | Spring | Afternoon | 13:41:15 | 81.3 | 3.0 | 196.8 | 27.4 | 67% | 20.6 | 29.0 | 1013.0 | 0.0 | 909.0 | 512 x 512 | 12.0 | 30.0 | ?? | MWIR | less than .1 | ?? |
| Skyball | TS2_1500_6_275_M | Eglin B-70 | Spring | Afternoon | 13:17:22 | 77.4 | 1.9 | 110.4 | 27.6 | 65% | 20.5 | 29.0 | 1013.0 | 0.0 | 942.0 | 512 x 512 | 12.0 | 30.0 | ?? | MWIR | less than .1 | ?? |
| Skyball | TS2_1500_6_310_M | Eglin B-70 | Spring | Afternoon | 13:18:13 | 81.7 | 4.2 | 193.1 | 27.6 | 65% | 20.5 | 29.0 | 1013.0 | 0.0 | 942.0 | 512 x 512 | 12.0 | 30.0 | ?? | MWIR | less than .1 | ?? |
| Skyball | TS2_1500_6_345_M | Eglin B-70 | Spring | Afternoon | 13:47:12 | 81.8 | 3.1 | 189.9 | 27.7 | 67% | 21.0 | 29.1 | 1013.0 | 0.0 | 858.0 | 512 x 512 | 12.0 | 30.0 | ?? | MWIR | less than .1 | ?? |
| Skyball | TS2_1500_6_380_M | Eglin B-70 | Spring | Afternoon | 13:46:02 | 82.3 | 4.1 | 188.8 | 27.9 | 66% | 21.0 | 29.1 | 1013.0 | 0.0 | 856.0 | 512 x 512 | 12.0 | 30.0 | ?? | MWIR | less than .1 | ?? |
| Skyball | TS2_1500_6_415_M | Eglin B-70 | Spring | Afternoon | 13:44:48 | 82.2 | 4.0 | 169.8 | 27.9 | 65% | 20.8 | 29.0 | 1013.0 | 0.0 | 980.0 | 512 x 512 | 12.0 | 30.0 | ?? | MWIR | less than .1 | ?? |
| Skyball | TS2_1500_6_450_M | Eglin B-70 | Spring | Afternoon | 13:38:40 | 82.0 | 4.7 | 189.3 | 27.8 | 66% | 20.6 | 29.1 | 1013.0 | 0.0 | 855.0 | 512 x 512 | 12.0 | 30.0 | ?? | MWIR | less than .1 | ?? |
| Skyball | TS2_1500_6_485_M | Eglin B-70 | Spring | Afternoon | 13:34:54 | 81.8 | 5.0 | 199.3 | 27.7 | 66% | 20.8 | 29.3 | 1013.0 | 0.0 | 920.0 | 512 x 512 | 12.0 | 30.0 | ?? | MWIR | less than .1 | ?? |
| Skyball | TS2_1500_6_520_M | Eglin B-70 | Spring | Afternoon | 13:35:45 | 81.5 | 4.6 | 204.3 | 27.5 | 67% | 20.7 | 29.3 | 1013.0 | 0.0 | 921.0 | 512 x 512 | 12.0 | 30.0 | ?? | MWIR | less than .1 | |

| Sensor | SEQUENCE | Location | Season | Time-of-Day | AIR TEMP °F | | Wind Speed m/s | | Wind Dir | | Air Temp °C | | Relative Humidity | | Soil Temp °C | | Bar Pressure (mb) | | Global Radiation watt/m²•s² | | FPA Size (Pixels) | | Frame Rate (Hz) | | MTF % at Half Nyquist | | FOV (mrad) | | NET (mK) | | Class |
|---------|--------------------|------------|--------|-------------|-------------|------|----------------|-------|----------|-----|-------------|------|-------------------|-----|--------------|---------|-------------------|------|-----------------------------|------|-------------------|-----|-----------------|-----|-----------------------|-----|------------|-----|----------|-----|-------|
| | | | | | TIME | TEMP | DIR | SPD | DIR | SPD | TEMP | DIR | TEMP | DIR | TEMP | DIR | TEMP | DIR | TEMP | DIR | TEMP | DIR | TEMP | DIR | TEMP | DIR | TEMP | DIR | TEMP | DIR | |
| Skyball | T58_2500_19_225_M | Eglin B-70 | Spring | Morning | 11:18:52 | 80.9 | 1.1 | 82.5 | 27.2 | 80% | 23.4 | 25.9 | 1015.0 | 0.0 | 836.0 | 512x512 | 12.0 | 30.0 | ??? | MWIR | less than .1 | ??? | S | | | | | | | | |
| Skyball | T58_2500_19_270_M | Eglin B-70 | Spring | Morning | 11:25:00 | 81.0 | 1.2 | 29.6 | 27.2 | 81% | 23.7 | 25.9 | 1015.0 | 0.0 | 854.0 | 512x512 | 12.0 | 30.0 | ??? | MWIR | less than .1 | ??? | S | | | | | | | | |
| Skyball | T58_2500_20_000_M | Eglin B-70 | Spring | Morning | 11:28:53 | 81.0 | 1.0 | 22.2 | 27.2 | 81% | 23.6 | 26.1 | 1015.0 | 0.0 | 801.0 | 512x512 | 12.0 | 30.0 | ??? | MWIR | less than .1 | ??? | S | | | | | | | | |
| Skyball | T58_2500_20_090_M | Eglin B-70 | Spring | Morning | 11:27:28 | 81.0 | 1.0 | 31.8 | 27.2 | 80% | 23.5 | 26.1 | 1015.0 | 0.0 | 830.0 | 512x512 | 12.0 | 30.0 | ??? | MWIR | less than .1 | ??? | S | | | | | | | | |
| Skyball | T58_2500_20_135_M | Eglin B-70 | Spring | Morning | 11:26:14 | 81.1 | 1.0 | 30.4 | 27.3 | 80% | 23.4 | 26.1 | 1015.0 | 0.0 | 815.0 | 512x512 | 12.0 | 30.0 | ??? | MWIR | less than .1 | ??? | S | | | | | | | | |
| Skyball | T58_2500_20_270_M | Eglin B-70 | Spring | Morning | 11:24:57 | 81.1 | 2.1 | 317.9 | 27.3 | 78% | 23.3 | 26.0 | 1015.0 | 0.0 | 814.0 | 512x512 | 12.0 | 30.0 | ??? | MWIR | less than .1 | ??? | S | | | | | | | | |
| Skyball | T58_3000_19_000_M | Eglin B-70 | Spring | Afternoon | 12:33:55 | 84.6 | 1.6 | 219.2 | 29.2 | 65% | 22.0 | 27.7 | 1014.0 | 0.0 | 834.0 | 512x512 | 12.0 | 30.0 | ??? | MWIR | less than .1 | ??? | S | | | | | | | | |
| Skyball | T58_3000_19_090_M | Eglin B-70 | Spring | Afternoon | 12:37:00 | 85.0 | 1.8 | 213.7 | 29.5 | 64% | 22.0 | 27.8 | 1014.0 | 0.0 | 567.9 | 512x512 | 12.0 | 30.0 | ??? | MWIR | less than .1 | ??? | S | | | | | | | | |
| Skyball | T58_3000_19_135_M | Eglin B-70 | Spring | Afternoon | 12:36:06 | 84.7 | 1.9 | 207.9 | 29.3 | 64% | 22.0 | 27.8 | 1014.0 | 0.0 | 764.0 | 512x512 | 12.0 | 30.0 | ??? | MWIR | less than .1 | ??? | S | | | | | | | | |
| Skyball | T58_3000_19_180_M | Eglin B-70 | Spring | Afternoon | 12:36:44 | 84.7 | 1.9 | 207.9 | 29.3 | 64% | 22.0 | 27.8 | 1014.0 | 0.0 | 838.0 | 512x512 | 12.0 | 30.0 | ??? | MWIR | less than .1 | ??? | S | | | | | | | | |
| Skyball | T58_3000_19_225_M | Eglin B-70 | Spring | Afternoon | 12:34:24 | 84.6 | 1.6 | 182.9 | 29.2 | 64% | 21.9 | 27.8 | 1014.0 | 0.0 | 834.0 | 512x512 | 12.0 | 30.0 | ??? | MWIR | less than .1 | ??? | S | | | | | | | | |
| Skyball | T58_3000_19_270_M | Eglin B-70 | Spring | Afternoon | 12:33:17 | 84.6 | 1.6 | 219.2 | 29.2 | 65% | 22.0 | 27.7 | 1014.0 | 0.0 | 834.0 | 512x512 | 12.0 | 30.0 | ??? | MWIR | less than .1 | ??? | S | | | | | | | | |
| Skyball | T58_3000_20_000_M | Eglin B-70 | Spring | Afternoon | 12:39:46 | 84.8 | 1.6 | 212.8 | 29.4 | 64% | 22.0 | 27.9 | 1014.0 | 0.0 | 394.4 | 512x512 | 12.0 | 30.0 | ??? | MWIR | less than .1 | ??? | S | | | | | | | | |
| Skyball | T58_3000_20_090_M | Eglin B-70 | Spring | Afternoon | 12:33:24 | 85.4 | 1.5 | 217.0 | 29.7 | 63% | 22.1 | 28.0 | 1014.0 | 0.0 | 729.0 | 512x512 | 12.0 | 30.0 | ??? | MWIR | less than .1 | ??? | S | | | | | | | | |
| Skyball | T58_3000_20_135_M | Eglin B-70 | Spring | Afternoon | 12:41:45 | 84.9 | 1.4 | 228.3 | 29.4 | 64% | 22.0 | 27.9 | 1014.0 | 0.0 | 668.7 | 512x512 | 12.0 | 30.0 | ??? | MWIR | less than .1 | ??? | S | | | | | | | | |
| Skyball | T58_3000_20_225_M | Eglin B-70 | Spring | Afternoon | 12:40:17 | 84.8 | 1.0 | 217.8 | 29.4 | 65% | 22.1 | 27.9 | 1014.0 | 0.0 | 564.7 | 512x512 | 12.0 | 30.0 | ??? | MWIR | less than .1 | ??? | S | | | | | | | | |
| Skyball | T58_3000_20_270_M | Eglin B-70 | Spring | Afternoon | 12:39:01 | 84.8 | 1.6 | 212.8 | 29.4 | 64% | 22.0 | 27.9 | 1014.0 | 0.0 | 394.4 | 512x512 | 12.0 | 30.0 | ??? | MWIR | less than .1 | ??? | S | | | | | | | | |
| Skyball | T58_4000_19_000_M | Eglin B-70 | Spring | Afternoon | 12:48:09 | 74.2 | 4.2 | 171.4 | 23.5 | 69% | 17.3 | 24.7 | 1011.0 | 0.0 | 977.0 | 512x512 | 12.0 | 30.0 | ??? | MWIR | less than .1 | ??? | S | | | | | | | | |
| Skyball | T58_4000_19_045_M | Eglin B-70 | Spring | Afternoon | 12:30:53 | 74.4 | 6.2 | 187.0 | 23.6 | 66% | 16.8 | 24.7 | 1011.0 | 0.0 | 924.0 | 512x512 | 12.0 | 30.0 | ??? | MWIR | less than .1 | ??? | S | | | | | | | | |
| Skyball | T58_4000_19_090_M | Eglin B-70 | Spring | Afternoon | 12:46:50 | 74.2 | 4.3 | 156.4 | 23.4 | 68% | 17.0 | 24.7 | 1011.0 | 0.0 | 1016.0 | 512x512 | 12.0 | 30.0 | ??? | MWIR | less than .1 | ??? | S | | | | | | | | |
| Skyball | T58_4000_19_180_M | Eglin B-70 | Spring | Afternoon | 12:52:13 | 74.1 | 5.0 | 168.1 | 23.4 | 69% | 17.2 | 24.8 | 1011.0 | 0.0 | 959.0 | 512x512 | 12.0 | 30.0 | ??? | MWIR | less than .1 | ??? | S | | | | | | | | |
| Skyball | T58_4000_19_225_M | Eglin B-70 | Spring | Afternoon | 12:48:50 | 74.2 | 4.2 | 171.4 | 23.5 | 69% | 17.3 | 24.8 | 1011.0 | 0.0 | 977.0 | 512x512 | 12.0 | 30.0 | ??? | MWIR | less than .1 | ??? | S | | | | | | | | |
| Skyball | T58_4000_19_270_M | Eglin B-70 | Spring | Afternoon | 12:52:46 | 74.1 | 5.0 | 168.1 | 23.4 | 69% | 17.2 | 24.8 | 1011.0 | 0.0 | 959.0 | 512x512 | 12.0 | 30.0 | ??? | MWIR | less than .1 | ??? | S | | | | | | | | |
| Skyball | T58_4000_20_000_M | Eglin B-70 | Spring | Afternoon | 12:57:05 | 74.4 | 4.7 | 162.5 | 23.6 | 69% | 17.0 | 24.8 | 1011.0 | 0.0 | 757.0 | 512x512 | 12.0 | 30.0 | ??? | MWIR | less than .1 | ??? | S | | | | | | | | |
| Skyball | T58_4000_20_045_M | Eglin B-70 | Spring | Afternoon | 12:59:16 | 74.2 | 5.8 | 155.1 | 23.5 | 67% | 17.1 | 24.8 | 1011.0 | 0.0 | 741.0 | 512x512 | 12.0 | 30.0 | ??? | MWIR | less than .1 | ??? | S | | | | | | | | |
| Skyball | T58_4000_20_090_M | Eglin B-70 | Spring | Afternoon | 12:55:30 | 74.0 | 3.8 | 162.2 | 23.3 | 69% | 17.3 | 24.8 | 1011.0 | 0.0 | 819.0 | 512x512 | 12.0 | 30.0 | ??? | MWIR | less than .1 | ??? | S | | | | | | | | |
| Skyball | T58_4000_20_180_M | Eglin B-70 | Spring | Afternoon | 13:00:30 | 74.0 | 4.4 | 160.1 | 23.4 | 69% | 17.0 | 24.9 | 1011.0 | 0.0 | 687.3 | 512x512 | 12.0 | 30.0 | ??? | MWIR | less than .1 | ??? | S | | | | | | | | |
| Skyball | T58_4000_20_225_M | Eglin B-70 | Spring | Afternoon | 12:57:45 | 74.4 | 4.7 | 162.5 | 23.6 | 69% | 17.0 | 24.8 | 1011.0 | 0.0 | 757.0 | 512x512 | 12.0 | 30.0 | ??? | MWIR | less than .1 | ??? | S | | | | | | | | |
| Skyball | T58_4000_20_270_M | Eglin B-70 | Spring | Afternoon | 13:00:52 | 74.0 | 4.4 | 160.1 | 23.4 | 69% | 17.0 | 24.9 | 1011.0 | 0.0 | 687.3 | 512x512 | 12.0 | 30.0 | ??? | MWIR | less than .1 | ??? | S | | | | | | | | |
| Skyball | T58_5000_19_000_M | Eglin B-70 | Spring | Morning | 11:47:10 | 72.9 | 5.1 | 165.0 | 22.7 | 67% | 16.5 | 23.9 | 1011.0 | 0.0 | 562.5 | 512x512 | 12.0 | 30.0 | ??? | MWIR | less than .1 | ??? | S | | | | | | | | |
| Skyball | T58_5000_19_045_M | Eglin B-70 | Spring | Morning | 11:49:00 | 72.5 | 4.3 | 164.4 | 22.5 | 69% | 16.6 | 23.9 | 1011.0 | 0.0 | 741.0 | 512x512 | 12.0 | 30.0 | ??? | MWIR | less than .1 | ??? | S | | | | | | | | |
| Skyball | T58_5000_19_045b_M | Eglin B-70 | Spring | Morning | 11:53:03 | 72.5 | 4.0 | 178.8 | 22.5 | 70% | 16.7 | 23.9 | 1011.0 | 0.0 | 468.4 | 512x512 | 12.0 | 30.0 | ??? | MWIR | less than .1 | ??? | S | | | | | | | | |
| Skyball | T58_5000_19_090_M | Eglin B-70 | Spring | Morning | 11:46:19 | 73.0 | 4.4 | 168.8 | 22.8 | 68% | 16.4 | 23.8 | 1011.0 | 0.0 | 547.8 | 512x512 | 12.0 | 30.0 | ??? | MWIR | less than .1 | ??? | S | | | | | | | | |
| Skyball | T58_5000_19_180_M | Eglin B-70 | Spring | Morning | 11:54:37 | 72.6 | 2.7 | 174.1 | 22.6 | 65% | 16.8 | 24.0 | 1011.0 | 0.0 | 504.2 | 512x512 | 12.0 | 30.0 | ??? | MWIR | less than .1 | ??? | S | | | | | | | | |
| Skyball | T58_5000_19_225_M | Eglin B-70 | Spring | Morning | 11:47:40 | 72.9 | 5.1 | 165.0 | 22.7 | 67% | 16.5 | 23.9 | 1011.0 | 0.0 | 562.5 | 512x512 | 12.0 | 30.0 | ??? | MWIR | less than .1 | ??? | S | | | | | | | | |
| Skyball | T58_5000_19_270_M | Eglin B-70 | Spring | Morning | 11:55:20 | 72.9 | 3.4 | 179.6 | 22.7 | 69% | 16.9 | 24.0 | 1011.0 | 0.0 | 593.2 | 512x512 | 12.0 | 30.0 | ??? | MWIR | less than .1 | ??? | S | | | | | | | | |
| Skyball | T58_5000_20_000_M | Eglin B-70 | Spring | Morning | 11:58:00 | 73.2 | 6.0 | 159.5 | 22.9 | 65% | 15.9 | 24.1 | 1011.0 | 0.0 | 789.0 | 512x512 | 12.0 | 30.0 | ??? | MWIR | less than .1 | ??? | S | | | | | | | | |
| Skyball | T58_5000_20_045_M | Eglin B-70 | Spring | Morning | 11:59:54 | 73.3 | 6.5 | 175.6 | 22.9 | 65% | 16.2 | 24.0 | 1011.0 | 0.0 | 803.0 | 512x512 | 12.0 | 30.0 | ??? | MWIR | less than .1 | ??? | S | | | | | | | | |
| Skyball | T58_5000_20_090_M | Eglin B-70 | Spring | Morning | 11:57:01 | 73.2 | 5.3 | 174.6 | 22.9 | 65% | 16.2 | 24.0 | 1011.0 | 0.0 | 787.0 | 512x512 | 12.0 | 30.0 | ??? | MWIR | less than .1 | ??? | S | | | | | | | | |
| Skyball | T58_5000_20_180_M | Eglin B-70 | Spring | Morning | 12:00:30 | 73.5 | 4.8 | 164.3 | 23.1 | 67% | 16.3 | 24.0 | 1011.0 | 0.0 | 840.0 | 512x512 | 12.0 | 30.0 | ??? | MWIR | less than .1 | ??? | S | | | | | | | | |
| Skyball | T58_5000_20_225_M | Eglin B-70 | Spring | Morning | 11:58:43 | 73.2 | 6.0 | 159.5 | 23.1 | 65% | 15.9 | 24.1 | 1011.0 | 0.0 | 789.0 | 512x512 | 12.0 | 30.0 | ??? | MWIR | less than .1 | ??? | S | | | | | | | | |
| Skyball | T58_5000_20_270_M | Eglin B-70 | Spring | Morning | 12:01:26 | 73.9 | 4.3 | 180.5 | 23.3 | 65% | 16.5 | 24.1 | 1011.0 | 0.0 | 847.0 | 512x512 | 12.0 | 30.0 | ??? | MWIR | less than .1 | ??? | S | | | | | | | | |

| Sensor Sequence | Location | Season | Time-of-Day | AIR TEMP °F | AIR TEMP °C | Wind Speed m/s | Wind Dir | Air Temp | Relative Humidity | Dew Point | Temp °C | Soil Temp °C | Bar Pressure (mb) | Rain mm | Global Radiation | FPA Size (Pixels) | Bits/watt/s/m ⁻² | Frame Rate (Hz) | MTF (%) at Half Nyquist | Spectral Band | IFOV (mrad) | NETT (mK) | Class |
|----------------------------|------------|--------|-------------|-------------|-------------|----------------|----------|----------|-------------------|-----------|---------|--------------|-------------------|---------|------------------|-------------------|-----------------------------|-----------------|-------------------------|---------------|-------------|-----------|-------|
| mission_run1_151941 | Eglin B-70 | Spring | Morning | 10:19:41 | 80.2 | 4.5 | 187.5 | 26.8 | 88% | 24.7 | 27.4 | 1017.0 | 0.0 | 365.5 | 512x512 | 12 | better than 50 | MWIR | 1 to 2 | less than 50 | S | | |
| AMS mission_run2_152455 | Eglin B-70 | Spring | Morning | 10:24:55 | 80.3 | 3.7 | 185.2 | 26.8 | 89% | 24.8 | 27.4 | 1017.0 | 0.0 | 409.5 | 512x512 | 12 | better than 50 | MWIR | 1 to 2 | less than 50 | S | | |
| AMS mission_run3_153036 | Eglin B-70 | Spring | Morning | 10:30:36 | 80.3 | 3.8 | 200.1 | 26.8 | 89% | 24.8 | 27.2 | 1018.0 | 0.0 | 240.5 | 512x512 | 12 | better than 50 | MWIR | 1 to 2 | less than 50 | S | | |
| AMS mission_run4_153605 | Eglin B-70 | Spring | Morning | 10:36:05 | 80.1 | 2.6 | 203.9 | 26.7 | 90% | 24.8 | 27.4 | 1018.0 | 0.0 | 360.5 | 512x512 | 12 | better than 50 | MWIR | 1 to 2 | less than 50 | S | | |
| AMS mission_run5_154653 | Eglin B-70 | Spring | Morning | 10:46:53 | 80.6 | 4.9 | 217.6 | 27.0 | 88% | 24.9 | 27.5 | 1018.0 | 0.0 | 261.0 | 512x512 | 12 | better than 50 | MWIR | 1 to 2 | less than 50 | S | | |
| AMS mission_run6_155058 | Eglin B-70 | Spring | Morning | 10:50:58 | 80.8 | 4.3 | 215.0 | 27.1 | 87% | 24.9 | 27.5 | 1018.0 | 0.0 | 336.4 | 512x512 | 12 | better than 50 | MWIR | 1 to 2 | less than 50 | S | | |
| AMS mission_run7_155411 | Eglin B-70 | Spring | Morning | 10:57:44 | 80.7 | 3.1 | 192.5 | 27.1 | 88% | 25.0 | 27.5 | 1018.0 | 0.0 | 364.5 | 512x512 | 12 | better than 50 | MWIR | 1 to 2 | less than 50 | S | | |
| AMS mission_run8_155742 | Eglin B-70 | Spring | Morning | 10:57:42 | 80.9 | 4.2 | 197.4 | 27.2 | 87% | 24.9 | 27.6 | 1018.0 | 0.0 | 383.0 | 512x512 | 12 | better than 50 | MWIR | 1 to 2 | less than 50 | S | | |
| AMS mission_run9_160708 | Eglin B-70 | Spring | Morning | 11:07:08 | 81.2 | 3.9 | 199.9 | 27.3 | 87% | 25.0 | 27.6 | 1018.0 | 0.0 | 409.5 | 512x512 | 12 | better than 50 | MWIR | 1 to 2 | less than 50 | S | | |
| AMS mission_run10_161203 | Eglin B-70 | Spring | Morning | 11:12:03 | 82.2 | 4.2 | 214.6 | 27.9 | 84% | 25.1 | 27.7 | 1018.0 | 0.0 | 412.0 | 512x512 | 12 | better than 50 | MWIR | 1 to 2 | less than 50 | S | | |
| AMS mission_run11_161651 | Eglin B-70 | Spring | Morning | 11:16:51 | 81.8 | 4.1 | 214.6 | 27.7 | 86% | 25.1 | 27.7 | 1018.0 | 0.0 | 360.5 | 512x512 | 12 | better than 50 | MWIR | 1 to 2 | less than 50 | S | | |
| AMS mission_run12_162109 | Eglin B-70 | Spring | Morning | 11:21:09 | 82.0 | 3.5 | 197.1 | 27.8 | 85% | 24.9 | 27.8 | 1018.0 | 0.0 | 461.5 | 512x512 | 12 | better than 50 | MWIR | 1 to 2 | less than 50 | S | | |
| AMS mission2_run1_174123 | Eglin B-70 | Spring | Afternoon | 12:41:23 | 83.2 | 4.0 | 193.9 | 28.5 | 89% | 25.0 | 28.7 | 1017.0 | 0.0 | 760.0 | 512x512 | 12 | better than 50 | MWIR | 1 to 2 | less than 50 | S | | |
| AMS mission2_run2_174447 | Eglin B-70 | Spring | Afternoon | 12:44:47 | 83.5 | 4.1 | 206.5 | 28.6 | 81% | 25.1 | 28.7 | 1017.0 | 0.0 | 836.0 | 512x512 | 12 | better than 50 | MWIR | 1 to 2 | less than 50 | S | | |
| AMS mission2_run3_175007 | Eglin B-70 | Spring | Afternoon | 12:50:07 | 82.8 | 4.8 | 206.9 | 28.2 | 83% | 25.1 | 28.8 | 1017.0 | 0.0 | 442.5 | 512x512 | 12 | better than 50 | MWIR | 1 to 2 | less than 50 | S | | |
| AMS mission2_run4_175526 | Eglin B-70 | Spring | Afternoon | 12:55:26 | 82.7 | 4.2 | 186.6 | 28.1 | 84% | 25.1 | 28.9 | 1017.0 | 0.0 | 347.5 | 512x512 | 12 | better than 50 | MWIR | 1 to 2 | less than 50 | S | | |
| AMS mission2_run5_180738 | Eglin B-70 | Spring | Afternoon | 13:07:38 | 84.0 | 3.9 | 202.4 | 28.9 | 80% | 25.2 | 29.0 | 1017.0 | 0.0 | 503.1 | 512x512 | 12 | better than 50 | MWIR | 1 to 2 | less than 50 | S | | |
| AMS mission2_run6_181106 | Eglin B-70 | Spring | Afternoon | 13:11:06 | 84.2 | 5.2 | 193.5 | 29.0 | 80% | 25.2 | 29.1 | 1016.0 | 0.0 | 768.0 | 512x512 | 12 | better than 50 | MWIR | 1 to 2 | less than 50 | S | | |
| AMS mission2_run7_181535 | Eglin B-70 | Spring | Afternoon | 13:15:35 | 84.1 | 3.6 | 200.8 | 28.9 | 80% | 25.2 | 29.1 | 1016.0 | 0.0 | 760.0 | 512x512 | 12 | better than 50 | MWIR | 1 to 2 | less than 50 | S | | |
| AMS mission2_run8_181858 | Eglin B-70 | Spring | Afternoon | 13:18:58 | 83.7 | 3.9 | 187.7 | 28.7 | 81% | 25.0 | 29.2 | 1016.0 | 0.0 | 364.2 | 512x512 | 12 | better than 50 | MWIR | 1 to 2 | less than 50 | S | | |
| AMS mission2_run9_182319 | Eglin B-70 | Spring | Afternoon | 13:23:19 | 83.8 | 5.4 | 209.6 | 28.8 | 79% | 25.0 | 29.3 | 1016.0 | 0.0 | 526.8 | 512x512 | 12 | better than 50 | MWIR | 1 to 2 | less than 50 | S | | |
| AMS mission2_run10_182759 | Eglin B-70 | Spring | Afternoon | 13:27:59 | 84.2 | 5.4 | 218.3 | 29.0 | 78% | 24.8 | 29.8 | 1016.0 | 0.0 | 980.0 | 512x512 | 12 | better than 50 | MWIR | 1 to 2 | less than 50 | S | | |
| AMS mission2_run11_183937 | Eglin B-70 | Spring | Afternoon | 13:59:37 | 84.3 | 4.7 | 191.5 | 29.1 | 79% | 25.0 | 29.3 | 1016.0 | 0.0 | 464.1 | 512x512 | 12 | better than 50 | MWIR | 1 to 2 | less than 50 | S | | |
| AMS mission2_run12_184448 | Eglin B-70 | Spring | Afternoon | 13:44:48 | 83.8 | 5.2 | 183.4 | 28.8 | 79% | 24.8 | 29.6 | 1016.0 | 0.0 | 492.0 | 512x512 | 12 | better than 50 | MWIR | 1 to 2 | less than 50 | S | | |
| AMS mission2_run13_184935 | Eglin B-70 | Spring | Afternoon | 13:54:35 | 83.2 | 4.7 | 193.7 | 28.4 | 79% | 24.5 | 29.7 | 1016.0 | 0.0 | 359.2 | 512x512 | 12 | better than 50 | MWIR | 1 to 2 | less than 50 | S | | |
| AMS mission2_run14_185240 | Eglin B-70 | Spring | Afternoon | 13:52:40 | 83.5 | 5.4 | 192.8 | 28.6 | 79% | 24.5 | 29.7 | 1016.0 | 0.0 | 937.0 | 512x512 | 12 | better than 50 | MWIR | 1 to 2 | less than 50 | S | | |
| AMS mission2_run15_185555 | Eglin B-70 | Spring | Afternoon | 13:55:55 | 84.2 | 5.8 | 207.7 | 29.0 | 79% | 25.0 | 29.5 | 1016.0 | 0.0 | 526.8 | 512x512 | 12 | better than 50 | MWIR | 1 to 2 | less than 50 | S | | |
| AMS mission2_run16_190011 | Eglin B-70 | Spring | Afternoon | 14:00:11 | 84.0 | 4.2 | 211.8 | 28.9 | 78% | 24.8 | 29.8 | 1016.0 | 0.0 | 845.0 | 512x512 | 12 | better than 50 | MWIR | 1 to 2 | less than 50 | S | | |
| AMS mission2_run17_190211 | Eglin B-70 | Spring | Afternoon | 14:02:11 | 84.0 | 4.0 | 211.8 | 28.9 | 78% | 24.9 | 29.8 | 1016.0 | 0.0 | 840.0 | 512x512 | 12 | better than 50 | MWIR | 1 to 2 | less than 50 | S | | |
| AMS mission6_run1_155218 | Eglin B-70 | Spring | Morning | 10:52:18 | 85.1 | 1.2 | 155.9 | 29.5 | 76% | 23.4 | 29.5 | 1019.0 | 0.0 | 840.0 | 512x512 | 12 | better than 50 | MWIR | 1 to 2 | less than 50 | S | | |
| AMS mission6_run2_155330 | Eglin B-70 | Spring | Morning | 10:53:30 | 84.7 | 2.7 | 207.2 | 29.3 | 72% | 23.4 | 29.7 | 1019.0 | 0.0 | 492.0 | 512x512 | 12 | better than 50 | MWIR | 1 to 2 | less than 50 | S | | |
| AMS mission6_run3_160046 | Eglin B-70 | Spring | Morning | 11:00:46 | 83.6 | 3.3 | 253.9 | 28.6 | 73% | 23.6 | 29.0 | 1019.0 | 0.0 | 660.0 | 512x512 | 12 | better than 50 | MWIR | 1 to 2 | less than 50 | S | | |
| AMS mission6_run4_160458 | Eglin B-70 | Spring | Morning | 11:04:58 | 84.9 | 4.0 | 299.2 | 29.4 | 69% | 22.9 | 29.2 | 1019.0 | 0.0 | 1004.0 | 512x512 | 12 | better than 50 | MWIR | 1 to 2 | less than 50 | S | | |
| AMS mission6_run5_161009 | Eglin B-70 | Spring | Morning | 11:10:09 | 83.9 | 3.7 | 194.9 | 28.9 | 79% | 23.3 | 29.4 | 1019.0 | 0.0 | 1038.0 | 512x512 | 12 | better than 50 | MWIR | 1 to 2 | less than 50 | S | | |
| AMS mission6_run6_161328 | Eglin B-70 | Spring | Morning | 11:13:28 | 83.8 | 2.3 | 223.3 | 28.8 | 71% | 23.0 | 29.4 | 1019.0 | 0.0 | 288.0 | 512x512 | 12 | better than 50 | MWIR | 1 to 2 | less than 50 | S | | |
| AMS mission6_run7_161926 | Eglin B-70 | Spring | Morning | 11:19:26 | 83.6 | 3.7 | 186.5 | 28.7 | 73% | 23.4 | 29.6 | 1019.0 | 0.0 | 889.0 | 512x512 | 12 | better than 50 | MWIR | 1 to 2 | less than 50 | S | | |
| AMS mission6_run8_162341 | Eglin B-70 | Spring | Morning | 11:24:41 | 84.1 | 2.3 | 178.8 | 29.0 | 75% | 23.9 | 29.7 | 1018.0 | 0.0 | 363.5 | 512x512 | 12 | better than 50 | MWIR | 1 to 2 | less than 50 | S | | |
| AMS mission6_run9_162938 | Eglin B-70 | Spring | Morning | 11:29:38 | 83.7 | 2.8 | 194.3 | 28.7 | 76% | 24.0 | 29.8 | 1018.0 | 0.0 | 1108.0 | 512x512 | 12 | better than 50 | MWIR | 1 to 2 | less than 50 | S | | |
| AMS mission6_run10_163249 | Eglin B-70 | Spring | Morning | 11:32:49 | 84.5 | 4.5 | 158.6 | 29.2 | 76% | 24.2 | 29.8 | 1018.0 | 0.0 | 352.0 | 512x512 | 12 | better than 50 | MWIR | 1 to 2 | less than 50 | S | | |
| AMS mission6_run11_163655 | Eglin B-70 | Spring | Morning | 11:36:55 | 83.7 | 3.0 | 168.4 | 28.7 | 78% | 24.0 | 29.9 | 1018.0 | 0.0 | 343.5 | 512x512 | 12 | better than 50 | MWIR | 1 to 2 | less than 50 | S | | |
| AMS mission6_run12_164019 | Eglin B-70 | Spring | Morning | 11:40:19 | 83.0 | 4.0 | 174.4 | 28.3 | 77% | 23.0 | 29.4 | 1018.0 | 0.0 | 444.5 | 512x512 | 12 | better than 50 | MWIR | 1 to 2 | less than 50 | S | | |
| AMS mission6_run13_164409 | Eglin B-70 | Spring | Morning | 11:44:09 | 84.8 | 3.8 | 203.1 | 28.1 | 79% | 24.1 | 30.0 | 1018.0 | 0.0 | 118.0 | 512x512 | 12 | better than 50 | MWIR | 1 to 2 | less than 50 | S | | |
| AMS mission6_run14_164728 | Eglin B-70 | Spring | Morning | 11:47:28 | 83.4 | 2.2 | 152.6 | 28.6 | 77% | 23.9 | 29.7 | 1018.0 | 0.0 | 442.0 | 512x512 | 12 | better than 50 | MWIR | 1 to 2 | less than 50 | S | | |
| AMS mission6_run15_165042 | Eglin B-70 | Spring | Morning | 11:50:42 | 83.8 | 3.1 | 181.7 | 28.8 | 72% | 23.3 | 30.1 | 1018.0 | 0.0 | 327.1 | 512x512 | 12 | better than 50 | MWIR | 1 to 2 | less than 50 | S | | |
| AMS mission6_run16_165354 | Eglin B-70 | Spring | Morning | 11:53:54 | 83.5 | 2.0 | 144.2 | 28.6 | 73% | 23.4 | 30.2 | 1018.0 | 0.0 | 595.7 | 512x512 | 12 | better than 50 | MWIR | 1 to 2 | less than 50 | S | | |
| AMS mission6_run17_165747 | Eglin B-70 | Spring | Morning | 11:57:47 | 83.4 | 1.9 | 167.1 | 28.5 | 75% | 23.5 | 30.3 | 1018.0 | 0.0 | 343.5 | 512x512 | 12 | better than 50 | MWIR | 1 to 2 | less than 50 | S | | |
| AMS mission6_run18_170323 | Eglin B-70 | Spring | Morning | 12:03:23 | 84.0 | 3.5 | 203.0 | 28.9 | 70% | 23.0 | 30.4 | 1018.0 | 0.0 | 463.5 | 512x512 | 12 | better than 50 | MWIR | 1 to 2 | less than 50 | S | | |
| AMS mission6_run19_170759 | Eglin B-70 | Spring | Morning | 12:07:59 | 84.8 | 3.8 | 203.0 | 29.3 | 69% | 23.2 | 30.4 | 1018.0 | 0.0 | 1126.0 | 512x512 | 12 | better than 50 | MWIR | 1 to 2 | less than 50 | S | | |
| AMS mission6_run20_171220 | Eglin B-70 | Spring | Morning | 12:12:20 | 85.1 | 3.7 | 186.8 | 29.5 | 70% | 23.5 | 30.1 | 1017.0 | 0.0 | 446.0 | 512x512 | 12 | better than 50 | MWIR | 1 to 2 | less than 50 | S | | |
| AMS mission6_run21_175444 | Eglin B-70 | Spring | Morning | 10:44:44 | 84.0 | 2.8 | 179.7 | 28.9 | 75% | 23.6 | 29.6 | 1017.0 | 0.0 | 1064.0 | 512x512 | 12 | better than 50 | MWIR | 1 to 2 | less than 50 | S | | |
| AMS mission6_run22_180121a | Eglin B-70 | Spring | Morning | 11:01:21 | 84.8 | 3.8 | 207.2 | 29.3 | 72% | 23.7 | 29.8 | 1017.0 | 0.0 | 686.0 | 512x512 | 12 | better than 50 | MWIR | 1 to 2 | less than 50 | S | | |
| AMS mission6_run23_180445 | Eglin B-70 | Spring | Morning | 11:04:45 | 84.8 | 4.4 | 190.7 | 29.4 | 71% | 23.7 | 29.8 | 1017.0 | 0.0 | 1096.0 | 512x512</td | | | | | | | | |

| Sensor | SEQUENCE | Location | Session | Time-of-Day | AIR TEMP °F | Wind Speed m/s | Wind Dir | Air Temp °C | Relative Humidity | Dew Point Temp °C | Soil Temp °C | Bar Pressure (mb) | Rain mm | Global Radiation | FPA Size (Pixels) | Bias/errs/m^2 | Frame Rate (Hz) | MTF (%) at Half Nyquist | Spectral Band | IFOV (mrad) | NET (mK) | Class | |
|--------|------------------------|-----------|---------|-------------|-------------|----------------|----------|-------------|-------------------|-------------------|--------------|-------------------|---------|------------------|-------------------|---------------|-----------------|-------------------------|----------------|-------------|----------|--------------|---|
| AMS | mission8 run5a 161428 | Edin B-70 | Spring | Morning | 11:14:28 | 85.1 | 4.9 | 214.2 | 29.5 | 71% | 23.8 | 30.0 | 1017.0 | 0.0 | 1094.0 | 512x512 | 12 | 30 | better than 50 | NAIR | 1 to 2 | less than 50 | S |
| AMS | mission9 run1b 162045 | Edin B-70 | Spring | Morning | 11:20:45 | 86.0 | 3.9 | 208.0 | 30.0 | 71% | 24.0 | 30.1 | 1017.0 | 0.0 | 1096.0 | 512x512 | 12 | 30 | better than 50 | NAIR | 1 to 2 | less than 50 | S |
| AMS | mission10 run1 180450 | Edin B-70 | Spring | Afternoon | 13:04:50 | 88.8 | 7.5 | 261.4 | 31.5 | 65% | 24.1 | 32.0 | 1016.0 | 0.0 | 1087.0 | 512x512 | 12 | 30 | better than 50 | NAIR | 1 to 2 | less than 50 | S |
| AMS | mission10 run2 181027 | Edin B-70 | Spring | Afternoon | 13:10:27 | 87.9 | 6.5 | 236.5 | 31.0 | 68% | 24.3 | 32.2 | 1016.0 | 0.0 | 988.0 | 512x512 | 12 | 30 | better than 50 | NAIR | 1 to 2 | less than 50 | S |
| AMS | mission10 run3 181722 | Edin B-70 | Spring | Afternoon | 13:17:22 | 89.0 | 6.0 | 243.4 | 31.7 | 64% | 24.0 | 32.2 | 1016.0 | 0.0 | 877.0 | 512x512 | 12 | 30 | better than 50 | NAIR | 1 to 2 | less than 50 | S |
| AMS | mission10 run4 182321 | Edin B-70 | Spring | Afternoon | 13:23:21 | 89.3 | 5.3 | 270.5 | 31.9 | 63% | 23.9 | 32.3 | 1016.0 | 0.0 | 342.2 | 512x512 | 12 | 30 | better than 50 | NAIR | 1 to 2 | less than 50 | S |
| AMS | mission10 run5 183207 | Edin B-70 | Spring | Afternoon | 13:32:07 | 89.5 | 6.2 | 250.5 | 32.0 | 63% | 24.2 | 32.4 | 1015.0 | 0.0 | 530.0 | 512x512 | 12 | 30 | better than 50 | NAIR | 1 to 2 | less than 50 | S |
| AMS | mission10 run6 183333 | Edin B-70 | Spring | Afternoon | 13:33:33 | 89.7 | 6.3 | 241.4 | 32.1 | 64% | 24.2 | 32.5 | 1015.0 | 0.0 | 772.0 | 512x512 | 12 | 30 | better than 50 | NAIR | 1 to 2 | less than 50 | S |
| AMS | mission10 run7 183905 | Edin B-70 | Spring | Afternoon | 13:39:05 | 88.6 | 5.4 | 244.6 | 31.4 | 66% | 24.4 | 32.5 | 1015.0 | 0.0 | 1096.0 | 512x512 | 12 | 30 | better than 50 | NAIR | 1 to 2 | less than 50 | S |
| AMS | mission10 run8 184456 | Edin B-70 | Spring | Afternoon | 13:44:56 | 89.3 | 6.7 | 245.9 | 31.9 | 65% | 24.4 | 32.6 | 1015.0 | 0.0 | 1091.0 | 512x512 | 12 | 30 | better than 50 | NAIR | 1 to 2 | less than 50 | S |
| AMS | mission10 run9 184656 | Edin B-70 | Spring | Afternoon | 13:46:56 | 89.1 | 7.6 | 252.0 | 31.7 | 63% | 23.9 | 32.6 | 1015.0 | 0.0 | 147.8 | 512x512 | 12 | 30 | better than 50 | NAIR | 1 to 2 | less than 50 | S |
| AMS | mission10 run10 190043 | Edin B-70 | Spring | Afternoon | 14:00:43 | 89.3 | 6.4 | 244.1 | 31.8 | 65% | 24.5 | 32.8 | 1015.0 | 0.0 | 989.0 | 512x512 | 12 | 30 | better than 50 | NAIR | 1 to 2 | less than 50 | S |
| AMS | mission10 run11 190328 | Edin B-70 | Spring | Afternoon | 14:03:28 | 88.6 | 6.7 | 249.9 | 31.5 | 67% | 24.4 | 32.8 | 1015.0 | 0.0 | 241.7 | 512x512 | 12 | 30 | better than 50 | NAIR | 1 to 2 | less than 50 | S |
| AMS | mission10 run12 190718 | Edin B-70 | Spring | Afternoon | 14:07:18 | 87.5 | 7.0 | 256.4 | 30.8 | 67% | 24.1 | 32.9 | 1015.0 | 0.0 | 903.0 | 512x512 | 12 | 30 | better than 50 | NAIR | 1 to 2 | less than 50 | S |
| AMS | mission10 run13 19143 | Edin B-70 | Spring | Afternoon | 14:11:43 | 88.6 | 6.4 | 238.4 | 31.5 | 65% | 24.3 | 32.9 | 1015.0 | 0.0 | 773.0 | 512x512 | 12 | 30 | better than 50 | NAIR | 1 to 2 | less than 50 | S |
| AMS | mission10 run14 191522 | Edin B-70 | Spring | Afternoon | 14:15:22 | 88.5 | 6.8 | 247.5 | 31.4 | 68% | 24.1 | 33.0 | 1015.0 | 0.0 | 991.0 | 512x512 | 12 | 30 | better than 50 | NAIR | 1 to 2 | less than 50 | S |
| AMS | mission10 run15 191810 | Edin B-70 | Spring | Afternoon | 14:18:10 | 89.2 | 5.4 | 262.7 | 31.8 | 63% | 23.9 | 33.0 | 1015.0 | 0.0 | 945.0 | 512x512 | 12 | 30 | better than 50 | NAIR | 1 to 2 | less than 50 | S |
| AMS | mission10 run16 192112 | Edin B-70 | Spring | Afternoon | 14:21:12 | 89.2 | 6.9 | 246.9 | 31.8 | 61% | 24.0 | 33.1 | 1015.0 | 0.0 | 322.5 | 512x512 | 12 | 30 | better than 50 | NAIR | 1 to 2 | less than 50 | S |
| AMS | mission10 run17 192407 | Edin B-70 | Spring | Afternoon | 14:24:07 | 88.9 | 7.1 | 262.0 | 31.6 | 66% | 24.3 | 33.1 | 1015.0 | 0.0 | 1075.0 | 512x512 | 12 | 30 | better than 50 | NAIR | 1 to 2 | less than 50 | S |
| AMS | mission10 run18 193132 | Edin B-70 | Spring | Afternoon | 14:13:32 | 89.5 | 6.2 | 252.5 | 31.9 | 66% | 24.6 | 32.1 | 1016.0 | 0.0 | 1029.0 | 512x512 | 12 | 30 | better than 50 | NAIR | 1 to 2 | less than 50 | S |
| AMS | mission10 run19 193717 | Edin B-70 | Spring | Afternoon | 14:27:17 | 88.1 | 7.3 | 256.2 | 31.2 | 67% | 24.1 | 32.3 | 1016.0 | 0.0 | 1129.0 | 512x512 | 12 | 30 | better than 50 | NAIR | 1 to 2 | less than 50 | S |
| AMS | mission10 run20 194247 | Edin B-70 | Spring | Afternoon | 15:42:47 | 87.4 | 2.2 | 338.5 | 30.8 | 30% | 11.3 | 33.9 | 1017.0 | 0.0 | 665.0 | 512x512 | 12 | 30 | better than 50 | NAIR | 1 to 2 | less than 50 | S |
| AMS | mission11 run1 205049 | Edin B-70 | Spring | Afternoon | 15:50:49 | 87.2 | 4.1 | 309.4 | 30.7 | 25% | 9.1 | 33.9 | 1017.0 | 0.0 | 673.1 | 512x512 | 12 | 30 | better than 50 | NAIR | 1 to 2 | less than 50 | S |
| AMS | mission11 run2 205727 | Edin B-70 | Spring | Afternoon | 15:57:27 | 87.1 | 1.4 | 360.0 | 30.6 | 28% | 9.7 | 33.9 | 1017.0 | 0.0 | 573.2 | 512x512 | 12 | 30 | better than 50 | NAIR | 1 to 2 | less than 50 | S |
| AMS | mission11 run3 210058 | Edin B-70 | Spring | Afternoon | 16:00:58 | 87.4 | 3.7 | 354.3 | 30.8 | 29% | 10.2 | 34.0 | 1017.0 | 0.0 | 660.2 | 512x512 | 12 | 30 | better than 50 | NAIR | 1 to 2 | less than 50 | S |
| AMS | mission11 run4 210611 | Edin B-70 | Spring | Afternoon | 16:05:11 | 87.3 | 2.4 | 323.1 | 30.7 | 29% | 10.2 | 34.1 | 1017.0 | 0.0 | 608.5 | 512x512 | 12 | 30 | better than 50 | NAIR | 1 to 2 | less than 50 | S |
| AMS | mission11 run5 210811 | Edin B-70 | Spring | Afternoon | 16:10:08 | 88.0 | 3.0 | 355.6 | 31.1 | 26% | 10.0 | 34.1 | 1017.0 | 0.0 | 598.0 | 512x512 | 12 | 30 | better than 50 | NAIR | 1 to 2 | less than 50 | S |
| AMS | mission11 run6 211008 | Edin B-70 | Spring | Afternoon | 16:14:12 | 87.4 | 3.5 | 321.2 | 30.8 | 25% | 8.7 | 34.1 | 1017.0 | 0.0 | 522.0 | 512x512 | 12 | 30 | better than 50 | NAIR | 1 to 2 | less than 50 | S |
| AMS | mission11 run7 211412 | Edin B-70 | Spring | Afternoon | 16:18:11 | 87.5 | 3.5 | 321.4 | 30.9 | 25% | 9.0 | 34.1 | 1017.0 | 0.0 | 598.0 | 512x512 | 12 | 30 | better than 50 | NAIR | 1 to 2 | less than 50 | S |
| AMS | mission11 run8 211811 | Edin B-70 | Spring | Afternoon | 16:23:24 | 87.4 | 3.1 | 332.3 | 30.8 | 26% | 9.7 | 34.2 | 1017.0 | 0.0 | 593.1 | 512x512 | 12 | 30 | better than 50 | NAIR | 1 to 2 | less than 50 | S |
| AMS | mission11 run9 212324 | Edin B-70 | Spring | Afternoon | 16:28:42 | 87.2 | 2.8 | 314.5 | 30.7 | 27% | 9.4 | 34.2 | 1017.0 | 0.0 | 579.7 | 512x512 | 12 | 30 | better than 50 | NAIR | 1 to 2 | less than 50 | S |
| AMS | mission11 run10 212842 | Edin B-70 | Spring | Afternoon | 16:31:53 | 87.5 | 3.0 | 342.6 | 30.8 | 28% | 10.3 | 34.2 | 1017.0 | 0.0 | 545.7 | 512x512 | 12 | 30 | better than 50 | NAIR | 1 to 2 | less than 50 | S |
| AMS | mission11 run11 213333 | Edin B-70 | Spring | Afternoon | 16:38:48 | 87.7 | 3.1 | 8.6 | 31.0 | 28% | 10.4 | 34.2 | 1017.0 | 0.0 | 517.0 | 512x512 | 12 | 30 | better than 50 | NAIR | 1 to 2 | less than 50 | S |
| AMS | mission11 run12 213948 | Edin B-70 | Spring | Afternoon | 16:45:32 | 87.9 | 2.6 | 327.0 | 31.1 | 27% | 10.2 | 34.2 | 1017.0 | 0.0 | 507.1 | 512x512 | 12 | 30 | better than 50 | NAIR | 1 to 2 | less than 50 | S |

Appendix B

Invariant Corporation

ImgMetrics Analysis Tool

User's Manual

Table of Contents

| | |
|---|-----------|
| 1. Introduction..... | 3 |
| 2. Installation | 3 |
| 2.1 Prerequisites..... | 4 |
| 2.2 Source and Configuration Files | 4 |
| 2.3 GUI Version..... | 6 |
| 2.4 Console Version..... | 6 |
| 3. Configuration | 6 |
| 4. Operation | 6 |
| 4.1 Console Application..... | 7 |
| 4.2 GUI Application..... | 7 |
| 4.2.1 Analysis File Creation/Editing..... | 7 |
| 4.2.2 Executing the Analysis | 11 |
| 4.2.3 Inspecting the Execution Results | 12 |
| 4.2.4 Other Operations..... | 13 |
| 5. New Metric Creation | 13 |
| 5.1 MetricTemplate.pro | 13 |
| 5.2 MetricTemplate.h..... | 14 |
| 5.3 MetricTemplate.cpp | 14 |
| 5.4 Finishing Up..... | 14 |
| 6. Metric Template Source..... | 15 |
| 6.1 MetricTemplate.h..... | 15 |
| 6.2 MetricTemplate.cpp | 16 |
| 6.3 Sample XML File | 17 |

1. Introduction

The Invariant Corporation ImgMetrics program enables the user to perform various metric calculations on an image sequence. The metrics are calculated on a “per frame” basis, resulting in a set of metric values for each image contained in the given sequence.

The tool is extendable by allowing for end user’s to create their own metric calculations. The tool is also versatile in that the set of metrics calculated for each analysis can be easily changed between runs. The list of sequences on which to perform these calculations may also be added to and deleted from easily.

The tool may be used to configure the analysis, run the configuration to calculate the metrics, and finally, to inspect the results of these calculations. The tool provides three views for the inspection of the analysis runs. These are a VCR type viewer for the image sequence, a window showing the exact values calculated on a frame by frame basis, and a graphical representation of the values calculated presented over the range of the sequence. The graph allows for the selection of up to five different metrics to be graphed. The graphs for each metric are distinguished by using different colors for the plot lines.

There is also a version of the tool which provides only the ability to run the metric calculations. This tool runs in a command line mode and produces a text output file. This file is saved in CSV format and may be viewed using a text editor or spreadsheet program, such as Excel. The command line version takes either all of the parameters listed individually on the command line at program invocation, or alternatively, will read these values from an XML file. This file can be generated by the GUI version of the tool, or by hand using any text editor or and XML editor. The format of the XML file is provided in the appendix.

2. Installation

A self extracting executable install file named ImgMetric_Setup.exe is provided to install the ImgMetrics tool. This install file has been created using Inno Setup. For more information on Inno Setup please see <http://www.jrsoftware.org/isinfo.php>.

The install file contains three install options. These options are “Source and Configuration files”, “GUI Version”, and “Console Application”.

2.1 Prerequisites

There are a few pre-requisites to the build process. One of these is the QT development environment. QT is a multi platform graphical user interface programming environment and was used to build the GUI version of the tool. QT is a product of Trolltech Corporation and more information, as well as directions on obtaining QT can be found by going to Trolltech's web site at <http://www.trolltech.com>.

The GUI version also uses the QWT library. The QWT library is used to generate the graphical representation of the metric values. This API can be found by going to this website, <http://qwt.sourceforge.net/index.html>. The website will provide further information on the use of the QWT library, and also instructions for downloading and installing the QWT API.

The console and GUI version of the tool also use the Xerces XML API. More information about Xerces and instructions on how to obtain the API can be found by going to this website, <http://xml.apache.org/>.

Each section contains a list of environment variables which must be added to the target system and then to that system's path environment variable. There are exceptions to these lists if the target system is already using Invariant's codec and ITools libraries. If this is the case, these variables will already exist on the system and should also be in the path. If it is known that this is the case ignore the directions for setting the codecs and ITools environment variables.

Another thing to be careful of, if the libraries already exist on the target machine, is version incompatibility. It may be necessary to update the existing versions of the libraries with the new ones from this installation. Simply copy the dlls from their installed locations to the existing location on the target machine. This may cause unexpected results in the previously existing applications dependant upon these libraries.

2.2 Source and Configuration Files

This option installs all of the files necessary to build the tool on the target machine.

The configuration files depend on the existence of several environment variables. These variables are used by the configuration scripts to generate the makefile and also by the software as it runs.

The environment variables that must be set are as follows:

| Environment Variable | Description |
|----------------------|---|
| Metricsdir | The location of the metric dlls. |
| Itools | The location of the ITools header files. |
| Codecs | The location of the codecs header files. |
| QTDIR | The location of the QT and QWT libraries, as well as the qmake utility. |
| ImgMetricsLibs | The location of the AnalysisCodec and Metric Base libraries. |
| QMAKESPEC | List of possible values can be found by looking in the QT/mkspecs directory. For example the value for Microsoft Visual C++.Net would be win32-msvc.net |
| XERCES | The location of the Xerces install. |

These variables must also be added to the path environment variable.

When these pre-requisites have been met, the system specific makefiles can be generated using the Trolltech utility qmake.

There are several items that must be built before the main program, ImgMetrics, is built. These are the Analysis Codec, the Metric Base object, and the individual metrics.

To build the AnalysisCodec, open a command prompt and navigate to the AnalysisCodec directory. In this directory type the command "qmake". This will produce the system appropriate makefile for the Analysis Codec library. Once the makefile has been generated build the library according to your compilers instructions. For example, in Microsoft Visual C++ .Net version 2002, you would now type "nmake".

To build the Metric Base object, navigate to the MetricBase directory and perform the steps listed above.

The same procedure should be repeated in the individual metric directories to build these libraries. The metrics are located in subdirectories under the MetricSources directory. It is not necessary to build all of the metrics. Only those which you intend to use need to be built.

The ImgMetrics tool can now be built. Perform the steps listed above in the ImgMetrics directory to build the ImgMetrics tool. The resulting executable will be called ImgMetrics.exe. To build the console version of the tool perform these steps in the consoleApp directory. The steps preceding the makefile generation and compilation of the main tool are the same for the GUI and console versions of the tool. With the one

exception being that the console application does not need either the QT or QWT libraries.

2.3 GUI Version

This option will install a ready to run version of the GUI tool. The source files will not be included, the one exception being the template outlining the creation of new metrics. When the install is finished the following environment variables must be added to the system and then added to the path environment variable. These variables are:

Metricsdir – The location of the metric dlls.
Itools – The location of the ITools header files.
Codecs – The location of the codecs header files.
QTDIR – The location of the QT and QWT libraries, as well as the qmake utility.
ImgMetricsLibs – The location of the AnalysisCodec and Metric Base libraries.

2.4 Console Version

This option will install the console version of the tool. The source files will not be included. The console version does not require the graphical support provided by the QT and QWT libraries. Therefore the environment variables for these libraries need not be set with this installation. The environment variables that must be set are listed below.

metricsdir – The location of the metric dlls.
itools – The location of the ITools header files.
codecs – The location of the codecs header files.
ImgMetricsLibs – The location of the AnalysisCodec and Metric Base libraries.

3. Configuration

The only configuration issues involved are the setting of the environment variables listed in each of the installation sections above. The individual view windows may be positioned as the user sees fit.

4. Operation

This section will provide detail and instructions as to the operation of the ImgMetrics tool. There are two versions of the metric tool available, a GUI version and a console application.

4.1 Console Application

The console application is run from the command line by typing the command “consoleImgMetrics”. The program expects operational parameters to be supplied on the command line. There are two ways to accomplish this. The individual parameters can be supplied, or the name of an XML configuration file can be supplied. The individual parameters expected are listed below:

start – Frame to begin calculating.
numFrames – Number of frames over which to iterate.
vid – The name of the image sequence file.
vdec - The name of the video decoder to use for this image sequence.
gtr – The ground truth file name.
cal – The calibration file name.
output – The output file name.
metric – The name of a text file containing the metrics to be calculated, one per line.

4.2 GUI Application

There are three main tasks associated with the GUI version of the ImgMetrics tool. These are analysis file creation and editing, executing the analysis, and inspecting the execution results.

4.2.1 Analysis File Creation/Editing

There are two different types of items that can be added or deleted from an analysis file. These are image sequences and metrics. These items appear in the ImgMetrics GUI along the left hand side of the main window in an expandable list. The image sequences appear under the main heading Analysis, while the individual metrics are shown under the main heading Metrics. The window containing this list will be referred to throughout the rest of this document as the Project View. There is another window directly below the project view, this window is used to display the individual sequence parameters and shall be referred to as the Property View.

To add image sequences to the analysis select the Add menu on the menu bar. This is a drop down menu, when clicked three options will be presented. These are “Add Sequence”, “Add Sequences”, and “Add Metric”. We will discuss the “Add Metric” option a little later on.

If “Add Sequence” is selected a data entry form will be presented. The form can be seen in figure 1 below.

■ Add Sequence

Sequence Filename

Calibration Filename

Calibration Format

Codec Name

Frame Count

Frame Start

Groundtruth Filename

Groundtruth Format

Output Filename

Output Format

Figure 1. ImgMetrics Add Sequence Form

This form will allow the entry of all of the information required to create a new sequence on which to perform metric calculation. Where file names are required, the data can either be typed in or the buttons to the right of the text entry fields will present a navigable file selection dialog. After all of the fields have been filled in the user selects the add button. This will add the new sequence to the list of sequences. If cancel is selected, the data entered is discarded and no changes are made to the file.

If “Add Sequences” is selected a navigable file window will be presented. An example of this can be seen in figure 2 below.

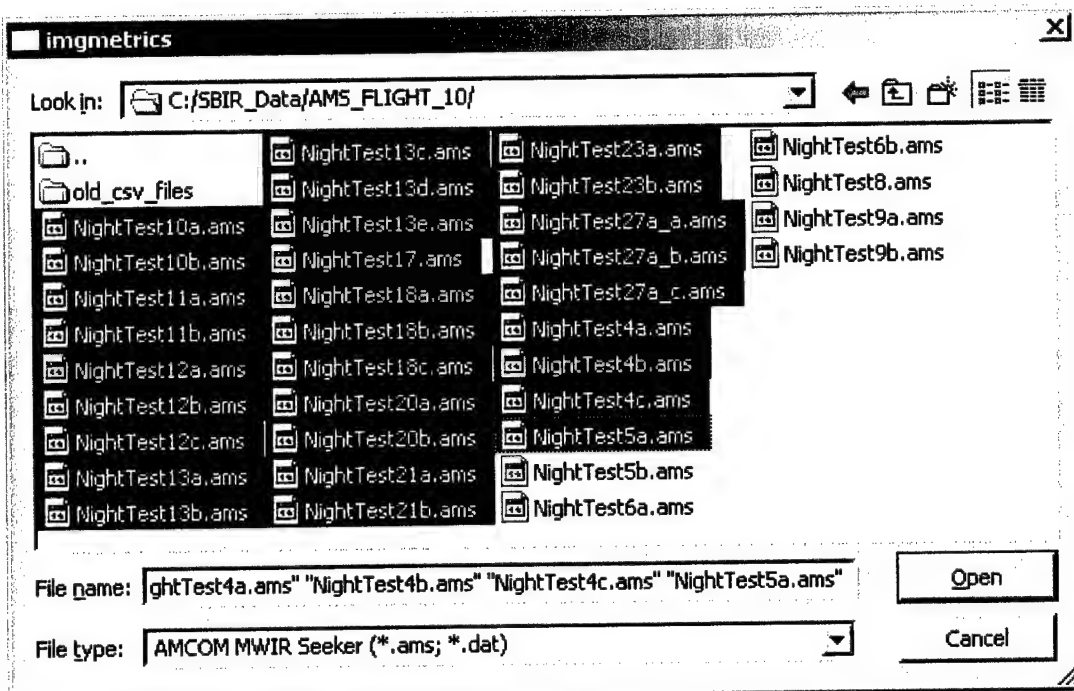


Figure 2. Add Sequences File Dialog

The file dialog will allow the selection of multiple files. The tool will fill out the rest of the data for the sequence based on the file type selected. If this method of addition is used all of the required files must be located in the same directory as the image sequences. Also, the calibration file must be named the same as the parent directory with a “.cal” extension. This method also sets the Frame Start and Frame Count parameters to 0. The program will determine the size of the image sequence during the metric run and perform the calculations over the entire sequence.

The sequence fields may be edited individually at any time. When an individual sequence is selected from the analysis list, the sequence parameter values are displayed in the Property View Window. This can be seen in figure 3.

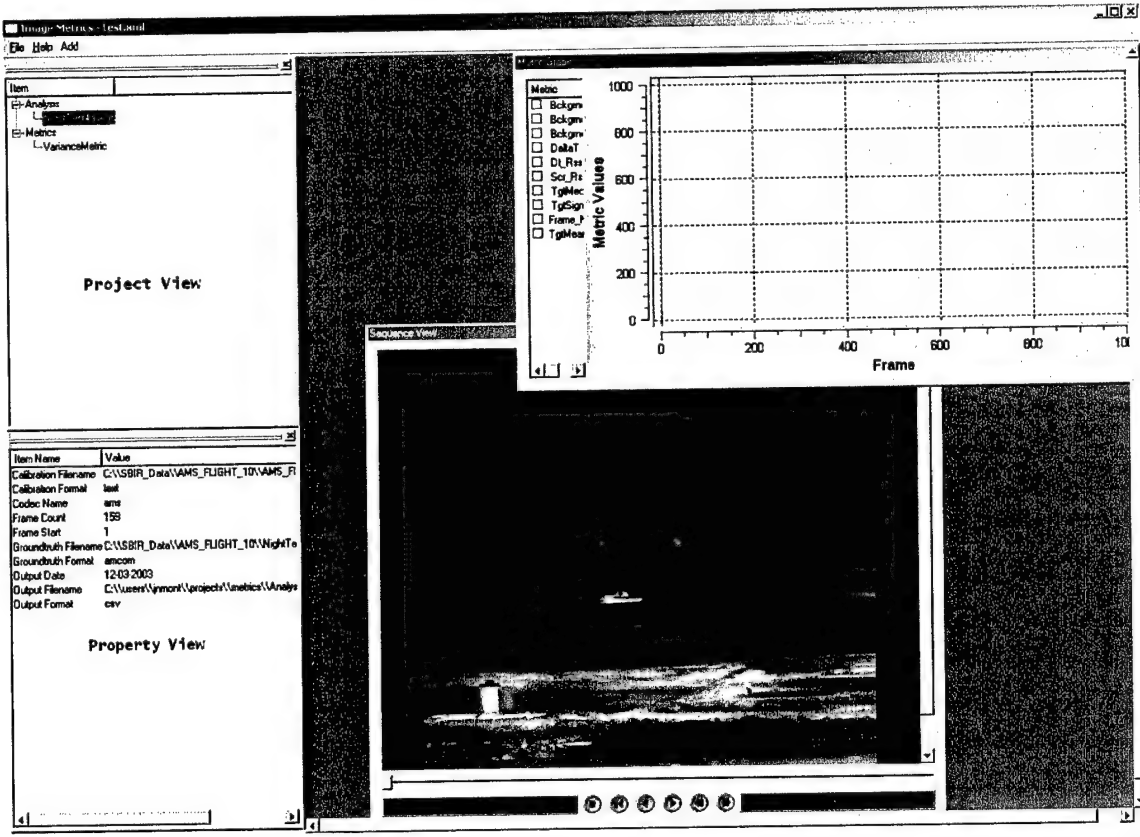


Figure 3. Project and Property Views

When the individual parameters are displayed in the Property View, they may be double clicked. This will produce an edit dialog for the property clicked allowing its value to be changed. The change can be accepted by clicking on the Accept button, or the changes can be discarded using the cancel button. An example of the edit property dialog is shown in figure 4.

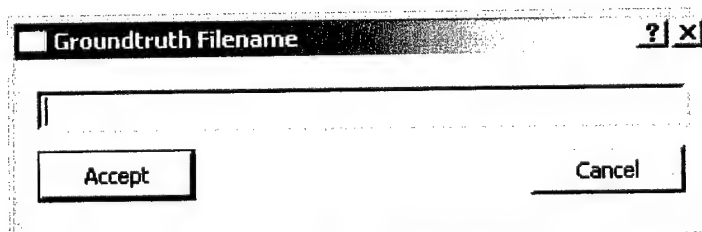


Figure 4. Property Edit Dialog

If "Add Metric" is selected the add metrics dialog will be presented as shown in figure 5.

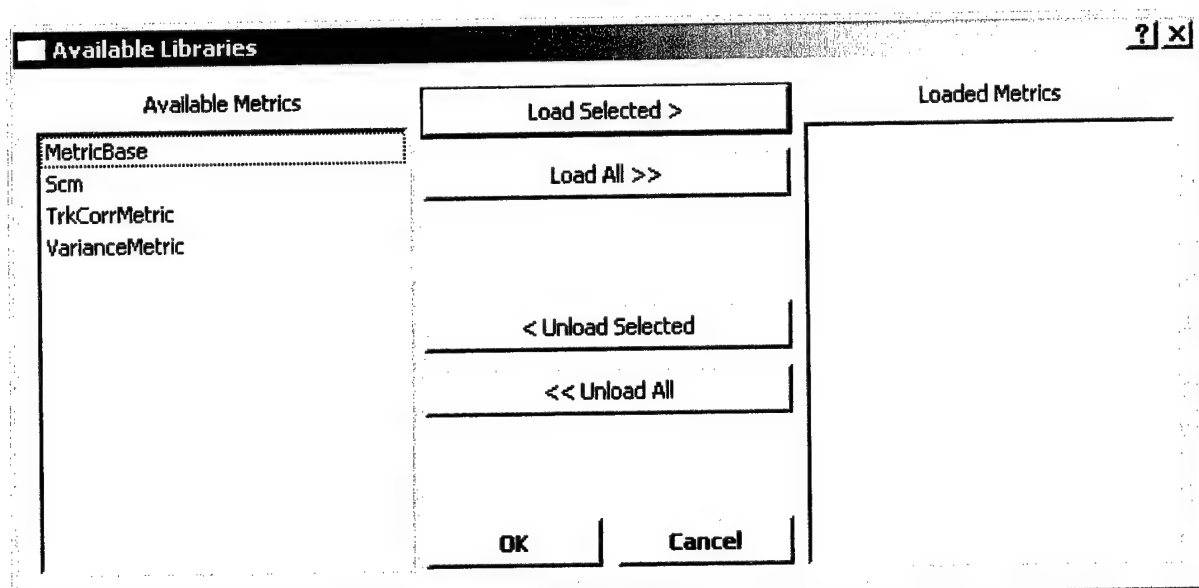


Figure 5. Add Metric Dialog

This option will allow the addition of metrics to be calculated. The list of available metric is populated by the metric dlls that are contained in the directory indicated by the METRICSDIR environment variable. To select the metrics click on the metric name in the available list and then click Load Selected. Load All will move all of the metrics listed in the Available section to the loaded section. Clicking OK will add the metric to the analysis. Cancel will discard the changes.

Deletion of either metric or sequences can be accomplished by right clicking on an item in the Project View. This will present a pop up menu with the delete option.

4.2.2 Executing the Analysis

To execute the analysis, select the Run Analysis option on the File menu. This option will calculate the metrics contained in the analysis for each frame of every sequence in the analysis. The results can be viewed at any time after the run is complete.

The tool will show a progress bar indicating the percentage complete for the current sequence. If the run contains more than one sequence, a new bar is presented for each sequence as it runs.

The main window remains active during the calculations. Sequences on which the run has completed may be viewed and the metric results inspected. If the analysis had been run previously, these results will be overwritten by the new run, unless the output file name is changed.

4.2.3 Inspecting the Execution Results

After an analysis run is complete, or having loaded a previously run file, the results may be analyzed using the ImgMetrics tool. The tool provides three view of the data resulting from a run. These views are presented in three separate windows. These windows will be called the Metric Graph, the Metric Data, and the Sequence View. Figure 6 shows the ImgMetrics tool displaying these views.

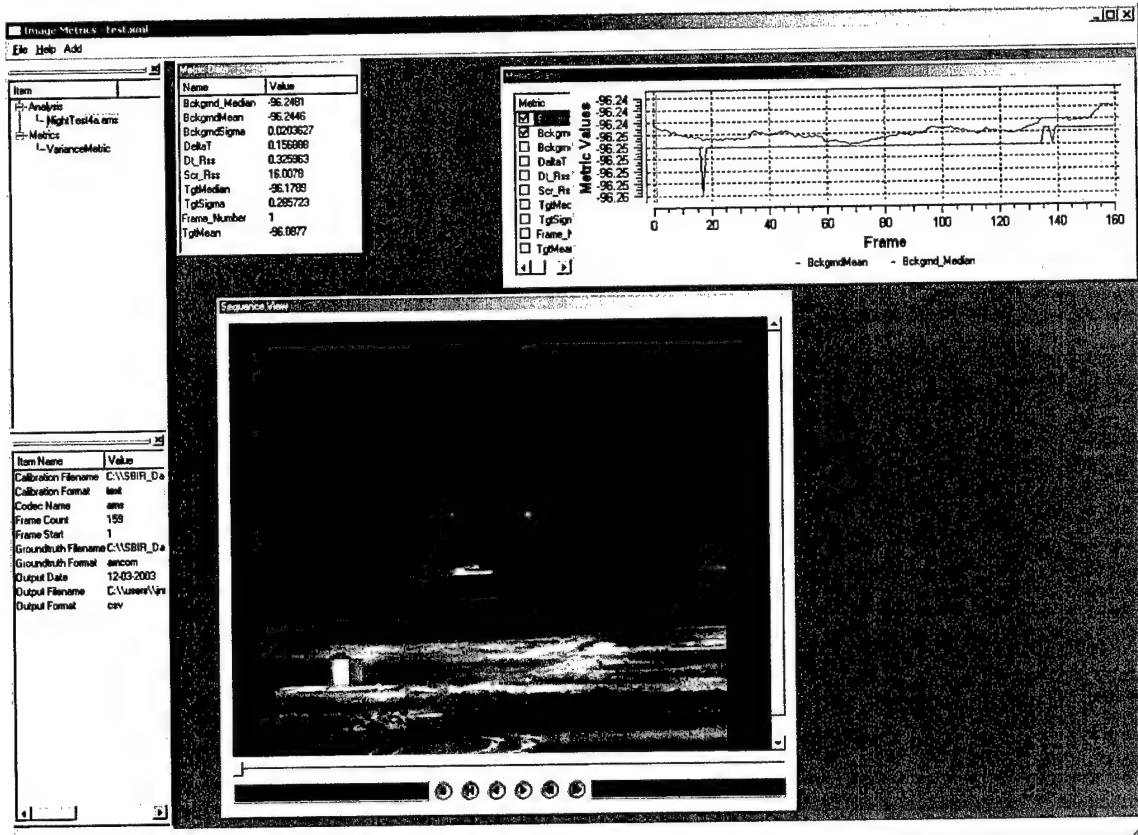


Figure 6. ImgMetrics Tool Analysis Windows

To begin viewing the results of an analysis run, select the desired image sequence from the list of sequences displayed in the Project View. When a sequence is selected, the sequence parameters will be displayed in the Property View, as discussed above. If the image sequence exists it will be displayed in the Sequence View window. If the analysis has already been run, and the output file exists, this data will populate the Metric Data window. The Graph View window will also present a list of metrics to be graphed.

The Metric Data view shows the specific values calculated for each metric in the analysis. These values are the calculation results for the frame currently displayed in the Sequence View window. Navigation through these values is accomplished using the VCR type control buttons in the Sequence View window.

The Sequence View window begins display with the first frame of the image sequence. From this point the sequence may be played, stopped, or stepped through in

forward or reverse. There is also a scroll bar to allow the sequence to be scrolled through. As an image plays, the Metric Data window will refresh with the currently displayed frame's metric values. If the analysis has not been run, but the sequence exists, it will be displayed. However no metric data will be displayed in the Metric Data window and the Graph window will not have any items to select for graphing.

The Graph View window will display plots of the metric data shown over the range of the image sequence. There is a pale yellow vertical bar displayed in the plot area indicating the location of the image frame currently displayed in the Sequence View window. Up to five metrics may be concurrently displayed in the graph area. Each metric will have a different colored line representing the values. There is a legend at the bottom of the Graph View indicating the color associations.

4.2.4 Other Operations

The ImgMetrics tool menu bar also provides for other standard functions generally expected in applications today. The file menu provides Save, Save As, Exit, New and Open operations. There is also a help menu which will display this document.

5. New Metric Creation

The ImgMetrics tool metric calculation capabilities are extendable through the addition of user defined metric calculations. These new metric may be built upon currently existing metrics, or be completely original. This section will outline the process for creating new metric libraries for use within the tool.

The different variations of the installation all provide a directory called MetricTemplate. This will be a subdirectory of the Metric Sources directory. This directory initially contains three files. These files are MetricTemplate.pro, MetricTemplate.cpp, and MetricTemplate.h. These files contain the starting point for creating your own metric library.

The first step in creating your own metric is to create a sub directory under the MetricSources directory. Once this is done, copy the three files named above to this directory. Detailed directions on the changes to be made to each of the three files follow.

5.1 MetricTemplate.pro

This file is to be used with the qmake utility. It contains all of the information qmake needs to generate the appropriate makefile for the current operating system. To configure this file for use with your metric it needs to be renamed. The new file name should match the name of the directory just created in the step above with the .pro extension. When this is done, edit the file and change all occurrences of "MetricTemplate" to the name of your new metric. Typically this will match the name

given to the .pro file. For example, if the .pro file were named MyMetric.pro, “MetricTemplate” would be changed to “MyMetric”. Save and close this file.

5.2 MetricTemplate.h

This file should also be renamed accordingly. Using the above example, it would be renamed to MyMetric.h. Open this file and change all occurrences of MetricTemplate to the name chosen for the new metric. Save and close this file.

5.3 MetricTemplate.cpp

Following the pattern illustrated above, rename this file to match the header file. Continuing to use the MyMetric example this file is renamed to MyMetric.cpp. The occurrences of MetricTemplate in this file should be changed to match the name used in the header file. When this is complete save and close this file. We are now ready to run qmake to create the makefile for the new metric.

5.4 Finishing Up

Up until this point the directions have been applicable to all target platforms. From this point forward the directions will be specific to a platform running Microsoft Windows and the Microsoft Visual C++ .Net version 2002 compiler.

To run qmake open a command window and navigate to the directory containing the new metric files. In the new directory type the command qmake if you wish to build the library from the command line. Alternatively the command may be entered as follows, “qmake -t vcapp”, this will create a project file with a “vcproj” extension for the new metric. This file may be opened using the C++ IDE.

The final step in the process is to implement the printHeader and calculate methods in the source files. The printHeader method should output a comma separated list of the metric values you will be calculating. There should be no new line contained in the list. The second method to be implemented is the calculate method. This is where the actual calculation of the metric is to be performed. The last thing calculate should do is output the result of the calculation, followed by a comma. Again, no new line should be inserted.

When the changes have been completed build the library by running nmake from the command line, or the library can be built inside the IDE using the build command. When the build command is finished the new library will be placed in the METRICDLLS directory and is now available to the ImgMetrics tool. The new library will appear in the Available Libraries list displayed by clicking the Add Metrics menu item in the ImgMetrics GUI. Good Luck and Have Fun!!

6. Metric Template Source

6.1 MetricTemplate.h

```

// Infrared Scene Metrics Program
// $Workfile::: MetricTemplate.h
//
// $Revision::: 1
// $Date::: 11/12/03 10:46a
// $Modtime::: 11/12/03 10:45a
// $Header::: MetricTemplate.h 1 11/12/03 10:46a
// $Source::: /cvsroot/irsm/MetricTemplate.h,v
// MetricTemplate is the "recipe" for creating your own metrics to use
// with the metric tool.
// All of the "MetricTemplate" keywords should be replaced with your
// class name.

#include "MetricBase.h"
#include <iostream>

<**
* Implementation of RectImgMetricBase for calculating the image
statistics.
* Calculates the scm.
*
* @1.0
* @scm.h
*/
// DLL specifiers...
#ifndef STATSMETRIC_BUILDDLL
    #define STATSMETRIC_DECLSPEC __declspec( dllexport )
    #define STATSMETRIC_EXPIMP
#endif defined STATSMETRIC_DLL
    #define STATSMETRIC_DECLSPEC __declspec( dllimport )
    #define STATSMETRIC_EXPIMP extern
#else
    #define STATSMETRIC_DECLSPEC
    #define STATSMETRIC_EXPIMP
#endif

class MetricTemplate : public RectImgMetricBase
{
public:
    typedef TImgMetricClass<RectImgMetricBase, MetricTemplate>
    MetaClass;
        static IImgMetricMetaClass* Class;
        MetricTemplate();
        ~MetricTemplate(){};

<**
* Calculate the metric for the given frame using the GroundTruth
* provided. The result is written to the file.

```

```

/*
* @param TImage The Image
* @param RectangularGroundTruth The groundtruth
* @param OStream The output file stream
*/
    void printHeader(std::ostream&);

/**
* calculate the metric for the given frame using the GroundTruth
* provided. The result is written to the file.
*
* @param TImage The Image
* @param RectangularGroundTruth The groundtruth
* @param OStream The output file stream
*/
    void
calculate(TImage<float> &, RectangularGroundTruth &, std::ostream &);

}; //End MetricTemplate

//EOF

```

6.2 MetricTemplate.cpp

```

//~~~~~
// Infrared Scene Metrics Program
// $workfile:: MetricTemplate.cpp
// $Revision:: 1
// $Date:: 11/12/03 10:46a
// $Modtime:: 11/12/03 10:45a
//~~~~~

// This is the "recipe" for creating your own metrics to be used with
// the metric tool. All of
// the "MetricTemplate" keywords should be replaced with the name of
// your class. The printhead
// method gets called once at object creation to put the metric header
// in the output file. The calculate
// method gets called for each frame of data in the image sequence.
// The metric calculation code goes here.
// Private methods can also be added to provide modularity in metrics
// requiring complex or detailed
// calculations.

#include "MetricTemplate.h"
#include "video/VideoDecoder.h"
#include "cpputil/cstring.h"
#include "cpputil/TSubArray.h"
#include "cpputil/TScalarArray.h"
#include "numerics/StatsAlgo.h"
#include "eo_ir/RectGroundTruth.h"
#include "eo_ir/Calibration.h"

#include <iostream>
#include <cstdlib>
#include <algorithm>

```

```

#include <stack>

using namespace std;
using namespace util;

ImgMetricMetaClass* MetricTemplate::Class =
MetricTemplate::MetaClass::Instance();

MetricTemplate::MetricTemplate()
: RectImgMetricBase()
{
    std::cout << "MetricTemplate construct" << std::endl;
}// end constructor ~~~~~

// Print the headers to the output file
void MetricTemplate::printHeader(std::ostream& output)
{
// TODO: Put the print header code for the metric here.
    output << "MetricTemplate header line goes here" << std::endl;;
}//End of printHeader ~~~~~

// Calcualte the metrics.
void MetricTemplate::calculate(TImage<float>& imageFrame,
                               RectangularGroundTruth& gt,
                               std::ostream& output)
{
// TODO: The metric calculation code goes here.
    std::cout << "MetricTemplate example code, put metric calculation
code here." << std::endl;
}//End calculate ~~~~~

//EOF

```

6.3 Sample XML File

```

<?xml version="1.0" encoding="UTF-8"?>
<analysis>
    <sequences>
        <sequence format="ams" start_frame="1" num_frames="159">
            <path>C:\\SBIR_Data\\AMS_FLIGHT_10\\NightTest4a.ams</path>
                <calibration format="text">
            </calibration>
                <ground-truth format="amcom">
            </ground-truth>
                <output format="csv" date="12-03-2003">
                    <path>C:\\users\\jnmont\\projects\\metrics\\AnalysisCodecTst\\jnmt
_Stats.csv</path>
                </output>
            </sequence>
        </sequences>
    </analysis>

```

```
        </output>
    </sequence>
</sequences>
<metrics>
    <metric>VarianceMetric</metric>
</metrics>
</analysis>
```